Climate change and migration: the case of Africa*

Bruno Conte†

July 2024

Abstract

How will future climate change affect rural economies like sub-Saharan Africa (SSA) in terms of migration and welfare? How can policymakers enhance SSA's capacity to adapt to this process? I answer these questions with a quantitative framework that, coupled with rich spatial data and forecasts for the future climate, estimates millions of climate migrants and unequal welfare losses across SSA. Investigating migration and trade policies as mitigating tools, I find a trade-off associated with the former: reducing SSA migration barriers reduces aggregate welfare losses at the cost of more climate migration and high regional inequality. Reducing tariffs attenuates this cost.

Keywords: Climate change, migration, economic geography.
JEL Codes: O15, Q54, R12.

*I am indebted to my advisors Hannes Mueller and Dávid Nagy for their constant support, guidance, and patience. I am also thankful to Gabriel Ahlfeldt, Clare Balboni, Paula Bustos, Donald Davis, Klaus Desmet, Albrecht Glitz, Remi Jedwab, Gabriel Kreindler, David Lagakos, Joan Monràs, Ishan Nath, Heitor Pellegrina, Giacomo Ponzetto, Esteban Rossi-Hansberg, Silvia Sarpietro, Sebastian Sotelo, Jaume Ventura, Giulio Zanella, Yanos Zylberberg, and various referees for useful comments and rich discussions along different stages of this project. Audiences at numerous seminars and confereces provided valuable feedback, to which I am also grateful. Julie Albigot and Mayu Suzuki provided excellent research assistance. All errors are my own.

†Universitat Pompeu Fabra, Barcelona School of Economics, and CESifo (bruno.conte@upf.edu).

1 Introduction

One of the most concerning potential consequences of climate change is population displacement, recently coined as the *Great Climate Migration* (Lustgarten, 2020). Subsistence rural economies, like the sub-Saharan African (SSA henceforth) countries, lie at the center of this issue. They are agriculture-dependent economies whose populations are expected to increase remarkably during the next decades (United Nations and Social Affairs, 2019). Understanding how these rural economies would adjust to a climate-changing world, with potentially different crop yields, is crucial for identifying how this growing population will reallocate geographically.

Assessing the potential decisions of SSA economic agents when adapting to climate change is challenging. Changing agricultural yields could lead farmers to switch production towards alternative crops (but remain in the agricultural sector). Alternatively, they could leave agriculture, potentially moving geographically. Trade frictions would determine how much specialization between agriculture and non-agriculture is feasible. Migration barriers would discipline the capacity of affected individuals to reallocate geographically, potentially limiting sectoral reallocation. Understanding how these forces (production switching, trade, and migration) respond to climate change is key to evaluating its impact on the economy.

In this paper, I develop a spatial model that accounts for these forces and can be used to quantify how their response to climate change translates into migration and welfare losses. I link the model to a unique spatial dataset that I assemble, covering 42 countries of SSA. Simulating the model for a future scenario by the end of the century, I estimate the aggregate and distributional impacts of climate change in terms of migration flows, welfare losses, and sectoral and spatial reallocation of production. I also study the mitigating power of real-world migration and trade policies, finding a novel trade-off associated with the former, which the latter attenuates.

My analysis begins with motivational evidence of the exposure of SSA agriculture to future climate change, the potential margins of adaptation, and underlying frictions. In terms of climate shocks, I document heterogeneous expected impacts across SSA's geography and, within locations, across crops. Hence, in terms of adaptation margins, local producers could respond to this uneven shock by switching production across crops and sectors. Importantly, I show that trade could have a key role in this process, but subject to trade barriers in SSA. Migration could also be crucial: I document a positive relationship between past changes in the climate and past internal and international migration flows, though limited by geographical mobility barriers.

Informed by this evidence, I develop a multi-sector spatial model that accommodates these mechanisms and frictions in general equilibrium. In the model, trade

and migration between locations are costly. In each location, farmers produce goods from multiple agricultural sectors (crops) and firms produce non-agricultural goods. Differences in sectoral total factor productivities and market access across locations generate trade, shaping the spatial pattern of sectoral specialization. Relative sectoral prices and real income determine sectoral expenditure shares, generating endogenous structural transformation through substitution and income effects.

My framework takes the perspective of subnational locations, so that trade and migration happen within and across countries in SSA. The intensity of the spatial frictions depends primarily on the distance between locations over the transportation network. However, they are also determined by country-level institutional factors. In particular, frictions for international trade are subject to tariffs. Likewise, international migration is subject to an additional mobility cost related to barriers to foreign migrants at the destination country. Integrating these realistic features of SSA trade and migration policies into my framework allows me to investigate their role in the resulting climate change effects and the effectiveness of alternative policy schemes.

To quantify the model, I assemble a high-resolution spatial dataset on, among others, population, transportation infrastructure, international trade, crop prices, internal and international migration, and agricultural production and suitability in SSA. Following Costinot et al. (2016), I model climate change as a shock to the suitability for growing crops. In practice, I draw on the GAEZ (IIASA and FAO, 2012) estimates of crop-specific potential yields for several grain crops in recent, past, and future (under IPCC's business-as-usual climate change scenario) periods. These potential yields reflect only local natural characteristics (e.g. topographic and climatic) and thus provide a measure of geographical natural advantages for growing a specific crop.

I link the data to my model in two steps. First, I measure several elements and fundamentals of my model directly from the data. Then, I quantify the remaining fundamentals and parameters, like sectoral productivities, amenities, migration costs, and trade frictions, by embedding standard quantification methods for spatial models into a GMM framework. The richness of my data is a crucial input in this step. For instance, I carefully separate the role of tariffs and geographical distances when determining trade frictions by exploiting, respectively, variation from international trade flows and the spatial distribution of prices. Likewise, I quantify mobility barriers with empirical variation from both international and internal migration flows.

Importantly, I quantify trade costs with an innovative approach that exploits second moments of local prices. Compared to the standard practice of using spatial price wedges (e.g., Donaldson, 2018; Atkin and Donaldson, 2015), my method has the advantage of requiring more accessible data: local prices rather than bilateral (origin-destination) prices. Methodologically, that is an important innovation, as it expands

the range of empirical applications in data-scarce contexts like developing economies.

With the quantified model in hand, I perform a backcasting exercise that validates it. Using past crop suitabilities, I simulate the model back in time to 1975 and contrast the results with observable data. The model predicts well the grid cell-level changes in population between 1975 and 2000, reassuring its capacity to provide similar numbers for the future. An additional overidentification test shows that the model captures closely the degree of specialization in agriculture across countries.

My main counterfactual exercise consists of simulating a climate-changed SSA by the end of the century. I retrieve GAEZ's estimates for crop suitabilities in 2080 with climate change and simulate the model with them, keeping all other fundamentals unchanged. The results show that climate change displaces about 22 million individuals in SSA. Most of the climate migrants move out of the Western Sahel and DR Congo, regions severely hit by climate change, into nearby countries like South Africa or Tanzania. Damaged countries also experience large internal migration flows, and overall the population in country capitals increases. Importantly, the welfare effects, measured as changes in real income per capita, are small in aggregate terms. However, they are very heterogeneous across space: the 5th and 95th percentiles of the welfare changes across countries are -15 and 3 percent, respectively, and some countries experience losses of up to -33 percent. Importantly, welfare results are similar if accounting also for utility losses from migration costs, congestion, and other aspects.

Analogously, climate change does not affect SSA aggregate sectoral employment but does so in distributional terms. The median country increases agricultural employment by about 1 percentage point, and the distribution of sectoral employment changes is fairly skewed. As in Nath (2023), this happens because crops are subsistence goods. Thus, affected economies respond to the reduced crop yields by allocating more labor to that sector. Nonetheless, this effect is spatially heterogeneous, and the direction of sectoral specialization roughly follows the relative changes in sectoral productivity (i.e. affected countries specialize out of agriculture, and the opposite for the least damaged), but constrained by spatial frictions (i.e., migration and trade).

Next, I investigate the mitigating role of reducing these frictions with real-world migration and trade policies. For that, I design a policy experiment that infers the climate change effects in a hypothetical scenario where migration and trade frictions in SSA drop to the European Union (EU) levels. In practice, I build a similarly rich spatial dataset for the EU and, with the same quantification procedure, retrieve the values of the parameters that reflect migration and trade policies in place in the EU. With those in hand, I perform simulations that assume the adoption of these policies, separately and combined, by SSA.

The quantified EU policy parameters are informative about the strictness of SSA

policy and how to interpret my policy experiments. The estimated EU tariffs are 3 times lower than SSA, and the country-level distribution of mobility barriers is substantially less skewed. Hence, the EU migration policy changes mobility barriers unevenly, as it reduces the barriers of the strictest SSA countries by larger magnitudes vis-à-vis the less strict countries. That differs from usual the approach in related work that evaluate the role of these frictions with stylized experiments (e.g., by shutting down migration or homogeneously increasing trade costs by an ad-hoc value).

Starting with migration policy, I find that reducing migration barriers to EU levels increases total climate migration to 34 million individuals and reduces aggregate welfare losses by about half. That happens because lower mobility barriers boost the push aspect of climate change, reallocating labor out of unproductive rural regions. However, these aggregate gains hide an underlying cost. While the policy permits many individuals to be better off by migrating, those incapable of doing so remain as worse off as before, and the distribution of welfare changes across countries remains wide and skewed. Thus, this experiment uncovers a trade-off associated with climate change mitigation with migration policy: it can reduce aggregate losses at the expense of more climate migration and high regional inequality.

Subsequently, I assess the role of trade policy alone. Reducing tariffs to EU levels reduces climate migration, as it increases the capacity to adapt by changing specialization rather than migrating. In terms of welfare, aggregate losses decrease moderately, but disparities across countries decline substantially. Again, the channel is the higher scope for sectoral specialization in this setting: lower trade barriers permit agents to adapt by switching production out of agriculture. Extreme welfare losses attenuate, and the distribution of country-level welfare changes narrows substantially (the worst-off country experiences losses of -8 percent vis-à-vis -33 percent in the baseline). Hence, trade policy is a powerful mitigating tool that moderates climate migration and addresses the inequalities of welfare losses of climate change.

The last exercise combines both policies and shows that trade openness attenuates the trade-off associated with migration policy alone. There is a reduction in aggregate losses, as in the migration experiment. However, climate migration and inequalities in the welfare effects also decrease. The policy mix increases the allocation efficiency of factors across sectors and space, fostering a climate-driven process of structural change (i.e., a relative increase in non-agricultural employment). This last result has important policy implications: by combining both tools, SSA policymakers could take advantage of the changes in the climate and allow the economy to structurally change, through trade and migration, in a less unequal manner.

I close my investigation with simulations centered on mechanisms, extensions, and robustness checks. For instance, I show that the capacity of producers to reallocate

production across crops is a crucial margin of adaptation. Ignoring this margin overestimates the productivity and welfare losses of climate change by not considering that crop yields are differently affected within locations. I also extend my framework by allowing trade and migration with the rest of the world. Migration and welfare losses grow, but not as much if increasing SSA's integration with the global economy. I also check the sensitivity of my results to assumptions on the evolution of fertility, productivity growth, alternative climate damages, and future climate scenarios.

This paper contributes to a growing literature that, pioneered by Desmet and Rossi-Hansberg (2015, 2023), evaluates the spatial consequences of climate change and the role of spatial frictions. My work enriches this field in two ways. First, rather than focusing on the global economy (Desmet et al., 2021; Cruz, 2023) or the US (Rudik et al., 2021; Bilal and Rossi-Hansberg, 2023), I carefully zoom into SSA, a low-income context where climate impacts and migration are pressing issues (Rigaud et al., 2018). Second, while this literature usually investigates the role of frictions with informative but stylized exercises (e.g., reducing trade or migration frictions by an ad-hoc value), I evaluate the effectiveness of spatial policies with experiments that have tangible counterparts in reality (i.e., if SSA adopts the EU's integration policy).

Hence, my policy recommendations complement those from this field. I stress the mitigating potentials of policies that target regional integration within SSA, adding to the evidence of the gains from integrating developing economies with the global economy through migration (Benveniste et al., 2020; Burzyński et al., 2022; Cruz and Rossi-Hansberg, 2024) and trade (Conte et al., 2021; Nath, 2023). While echoing some of the individual takeaways from these studies, my two central findings on (i) the inequality trade-off associated with migration policy and (ii) the attenuating role of trade policy are, to my knowledge, new to this literature.

These results are not simply a consequence of my geographical choice, but instead of my innovative conceptual and empirical approaches to the climate migration issue in SSA. Conceptually, I embed real-world policy in my framework by letting spatial frictions in SSA depend not only on geography, but also on quantifiable institutional features that my policy experiments exploit. Empirically, I uncover the rich structure of these spatial frictions thanks to my unique continental-scale dataset and the new quantification method that I propose. These innovations (and the novel welfare inequality trade-offs that they uncover) are my main contributions to this field.

My results also relate to the literature on the inequality of climate change effects. Because climate damages depend on costly adaptation, this literature usually finds unequal effects associated with exposure to extreme climate along several dimensions, such as age, race, income, or location. Examples include the mortality effects of temperatures (Carleton et al., 2022), damages from pollution exposure (Currie et al.,

2023; Colmer et al., 2021), firm performance and climate extremes (Jia et al., 2022; Castro-Vincenzi et al., 2024), and urban damages from coastal flooding (Desmet et al., 2021; Hsiao, 2024). In my paper, the unequal effects of climate change (and policy) also play a central role, but with a focus on how welfare effects differ across space.

I also contribute to the literature on the welfare benefits of reducing migration barriers in developing settings. This literature documents that relaxing these barriers improves welfare through several mechanisms, such as risk sharing (Bryan et al., 2014; Morten, 2019; Meghir et al., 2022), insurance (Lagakos et al., 2023), and improved spatial sorting (Bryan and Morten, 2019; Imbert et al., 2023). Others investigate how the benefits of migration policy interact with trade and comparative advantage (Morten and Oliveira, 2024; Pellegrina and Sotelo, 2024). My contribution is to show that these welfare gains (and the power of integrating migration and trade policies) also hold in the context of adaptation to climate change.

Finally, my paper speaks to the literature at the intersection of trade, development, and the environment. This flourishing field establishes the importance of market integration for development (Donaldson, 2018; Asturias et al., 2019; Sotelo, 2020; Pellegrina, 2022; Nagy, 2023; Farrokhi and Pellegrina, 2023), inequality (Atkin et al., 2021), environmental outcomes (Shapiro, 2016, 2021; Hsiao, 2022; Dominguez-Iino, 2023; Farrokhi et al., 2024), climate change impacts (Costinot et al., 2016; Nath, 2023; Porteous, 2024; Farrokhi and Lashkaripour, 2024), and others. While my trade policy results corroborate many findings from this literature, they also convey the novel takeaway of how trade openness attenuates the welfare inequality trade-off associated with migration policy. Moreover, my novel method for quantifying trade frictions – which has the advantage of requiring more accessible data than standard methods – is a methodological contribution to this field.

2 Data sources

I collect and aggregate several sources of geographical data within $1^\circ \times 1^\circ$ grid cells (about 100 km^2 at the equator), the empirical unit of observation. The set of cells covering 42 countries of SSA contains 2,007 cells. The data sources, collection, and aggregation follow below; see Appendix A for details.

GDP. Grid cell-level data on GDP per capita in US$ PPP (2000) comes from the Global Gridded Geographically Based Economic Data v4 (G-Econ, Nordhaus et al., 2006).

Population. The G-Econ database also provides the population count at the grid cell-level for 1990 and 2000, which is complemented with grid cell-level 1975 population data from the Global Human Settlement Project (GHSP, Florczyk et al., 2019). Finally,

country-level projections for the future population at the end of the century were taken from United Nations and Social Affairs (2019).

Agricultural suitability. I construct a spatial and time-varying dataset of crop-specific suitabilities using the Food and Agriculture Organization's Global Agro-Ecological Zones database (GAEZ, IIASA and FAO, 2012). This data is generated by an agronomic model that combines geographic characteristics (e.g. soil, elevation, etc.) with yearly climatic conditions to produce high-resolution estimates of potential yields for different crops and periods.[1] I collect and aggregate the potential yields for the six main subsistence-type crops for 1975, 2000, and 2080.[2,3]

Agricultural production. Grid cell-level crop production comes from two sources: grid cell-level production data (in tonnes) for 2000 from GAEZ and country-level crop production (in current US$) for 2000-2010 from FAO-STAT. I convert current US$ to US$ PPP using their ratio on the G-Econ data.

Crop prices. I retrieve spatially disaggregated crop price data from the Vulnerability Assessment and Mapping program of the World Food Programme (WFP-VAM), which has been monitoring crop prices in more than 900 markets across SSA since the early 1990s. I focus on prices for maize, millet, sorghum, and rice – the crops with higher temporal and spatial coverage. Figure 1 Panel A shows the wide spatial coverage within and across countries of this data, as well as a rich within-market coverage of prices for different crops (i.e. many markets with data for more than one crop).

Transportation network. I build up a network connecting all grid cells of SSA by combining the Global Roads Open Access Data Set (gROADS, CIESIN, 2013) with the friction surface from the Accessibility to Cities project (Weiss et al., 2018).

Bilateral trade. I extract bilateral crop trade flows (in current US$, scaled to PPP as above) between SSA country pairs from the International Trade and Production Database (ITPD-E, Borchert et al., 2021). It is a benchmark source of trade data due to its large geographical, sectoral, and temporal (2000 to 2016) coverage.

Internal and international migration flows. I obtain bilateral gross migration flows between SSA countries from Abel and Cohen (2019)'s database (a comprehensive source of migration data that covers about 200 countries and 25 years). Moreover, I built a matrix of internal (i.e. within countries) migration at the grid cell pair-level from census data (from IPUMS, 2020) by aggregating individual-level migration data

[1] These potential yields refer to the yield that a certain cell would obtain, on average, if its surface was fully devoted to a specific crop.

[2] The 2080 yields refer to a climate-changed world under the business-as-usual scenario RCP 8.5.

[3] To focus on subsistence agriculture, I consider only the main staple crops produced and consumed in the region: cassava, maize, millet, rice, sorghum, and wheat (see Table D.2). They account for 80% of the agricultural production, as of 2000, and 50% of the caloric intake in SSA (Porteous, 2019).

Figure 1: Spatial coverage of crop prices and internal (within-country) migration data

Panel A: Location of WFP markets. *Panel B:* Subnational regions with migration data.

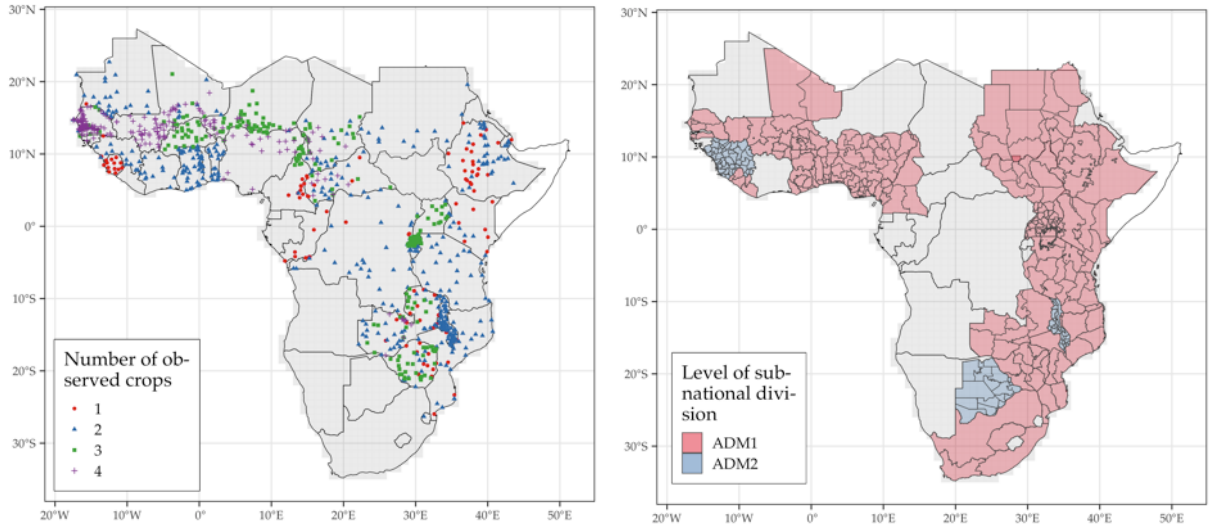

Notes: Panel A shows the locations (markets) with crop price data from the WFP-VAM project. Panel B shows the subnational locations with within-country migration data from IPUMS (2020).

at the subnational level for 24 countries and 40 years (since the 1970s to the early 21st century). Figure 1 Panel B shows the high coverage and granularity of this data, with migration between regional (ADM1) and provincial (ADM2) units.

3 Motivating facts

This section documents three facts about the potential impact of climate change in SSA. It establishes that (i) these effects are expected to be strong and heterogeneous and, as such, (ii) potentially determinant in the future organization of the SSA economy and (iii) future migration flows. Overall, these facts provide empirical support for the channels I embed in the model.

Fact 1: Climate change is expected to bring about substantial and spatially heterogeneous changes in agricultural suitability in SSA.

I use the GAEZ estimates of agro-climatic potential yields for 2000 and 2080 to show the expected degree of severity and heterogeneity in climate change's impact.[4] I define ΔA_i^k as the changes in the yields of crop k (in tonnes/ha) in location (i.e. grid cell) i between the two periods, and ΔA_i as the average change within locations.

Panel A of Figure 2 illustrates the high level of heterogeneity in the average climate change shock to agricultural yields. In terms of levels, several locations will become

[4]The 2080 GAEZ forecasts are calculated assuming a hypothetical scenario for the future evolution of the world's climate. Appendix A describes how I chose the scenario from which to draw the data in order that the results refer to the Representative Concentration Pathway (RCP) 8.5.

Figure 2: Expected impact of climate change on average crop yields (left) and the standard deviation of crop-yield changes (right) in SSA between 2000 and 2080

Panel A: Change in average crop suitability.

Panel B: Location-level standard deviation.

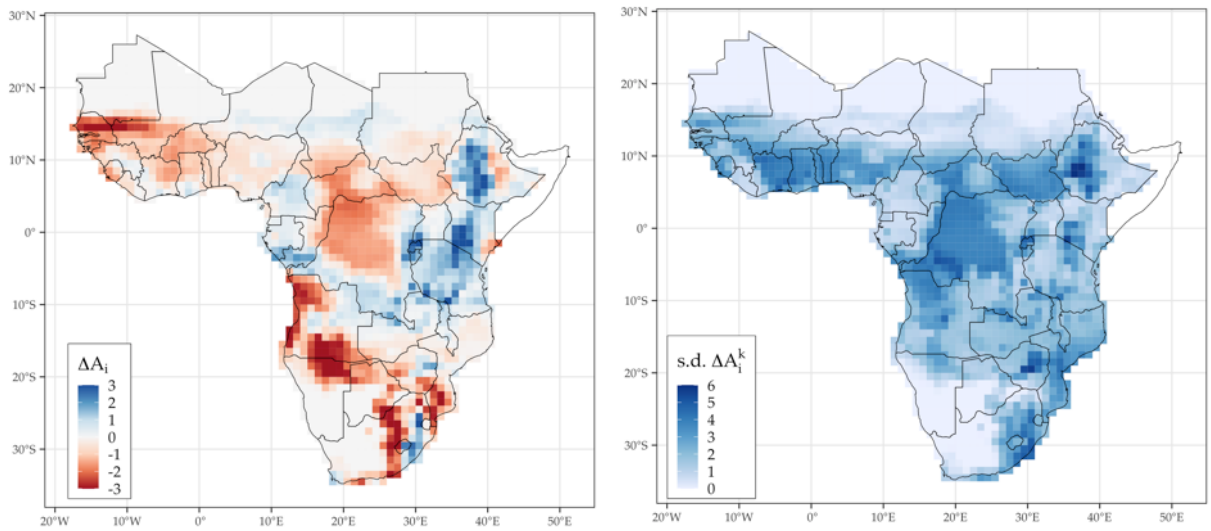

Notes: Panel A shows the level changes in average potential yields between 2000 and 2080. Panel B shows the standard deviation of the crop-level yield changes within cells. See Section 2 and Appendix A for details, and Figure B.6 for Panel A in relative changes.

less suitable for agriculture, with average yields declining by 3 tonnes/ha (50 percent of average yields) or more. However, other locations will become more suitable and to a similar extent. This finding contradicts a general view of climate change as a spatially homogeneous shock.

To illustrate the heterogeneity across crops, Panel B of Figure 2 documents the dispersion of climate change effects at the cell level (in standard deviations of ΔA_i^k). The changes in yields are not homogenous across crops, differentially shifting the relative ranking of crop suitabilities within cells. Hence, climate change will affect agricultural comparative advantages heterogeneously across both space and crops.

Thus, adjusting crop choices is a potential coping margin for affected farmers in SSA. However, the extent to which such Ricardian production adjustments can take place in SSA depends on the strength of these natural comparative advantages in shaping effective agricultural production. The next empirical fact provides evidence that such a mechanism indeed exists and emphasizes the importance of embedding it in my theoretical framework.

Fact 2: Natural crop suitability closely explains the patterns of crop specialization across SSA, as well as crop trade between countries (but subject to frictions).

Figure 3 Panel A documents a positive correlation between observed production and the GAEZ yields in 2000. It plots the linear fit of effective crop production on average crop yields at the country level, both in logs and net of crop and country fixed ef-

fects.[5] The strong, positive correlation (elasticity of 0.73) is evidence of specialization in production, with countries producing the crops that they are more suitable for.[6]

Furthermore, Panel A documents a weaker degree of specialization in trade: the slope of bilateral trade on exporter-importer relative yields is about 40 percent lower.[7] Notably, this pattern remains if controlling for the distance between exporter-importer capitals (a component of trade costs; see Appendix D.1), suggesting that other resistance elements (e.g., tariffs) could be the reason for the weaker specialization in trade.

Hence, to align with these empirical patterns, my model will take the perspective of subnational locations (and countries) that specialize in (and trade, but costly) crops based on comparative advantage. As such, it will consider how climate change, in general equilibrium, will reshuffle production and trade in SSA in the next decades.

Fact 3: Changes in crop suitability positively correlate with past internal and international migration flows in SSA.

Panels B and C of Figure 3 show that changes in crop suitabilities between 1975 and 2000 explain migration choices, within and across countries, in SSA. For that, they plot the linear fit of bilateral migration flows on the change in the relative yields between subnational locations (i.e., regions or provinces) or countries.[8] A positive relationship is correlational evidence of relative yields as a push factor of migration over time, with larger bilateral flows for the pairs whose destination-origin relative yields increased.

This is the case for both internal and international migration. As shown in Table D.1, this association is somehow weak on average, but stronger for location pairs (subnational regions or countries) that are geographically closer: controlling for bilateral distances increases the estimated slopes for both types of migration flows. This shows that migration costs, like geographical distance, limited the capacity of agents migrating to locations that became relatively better off in the past decades. Hence, my model will incorporate these mobility barriers in general equilibrium, limiting the capacity of migration as an adaptation response to future climate change.

[5] Importantly, the country-level production data is retrieved from national statistics, and not aggregated from the FAO spatial data. Hence, using these two independent data sources prevents a mechanical correlation between production and suitability data.

[6] Appendix D.1 discusses more formally these correlations, documents the associated regression results, and documents additional facts, e.g., evidence for within-country specialization in production.

[7] The trade slope refers to the linear fit of bilateral crop trade on exporter-importer relative crop yields, in logs, and net of importer-exporter and crop fixed effects.

[8] The relative yield changes refer to the percentual changes, between 2000 and 1975, in the relative average yields between location pairs. Moreover, the migration flows refer to thousands of migrants between origin and destination per thousand population at the origin in 1975 (which is equivalent to controlling for the initial population at origin). Note that these results are not causal, but correlational; see Appendix D.1 for details.

Figure 3: Comparative advantage and the organization of the SSA economy: relationship between crop yields (changes) and effective production, trade, and migration

Panel A: Country-level crop production and trade (in logs).

Panel B: Bilateral internal migration flows.

Panel C: Bilateral international migration flows.

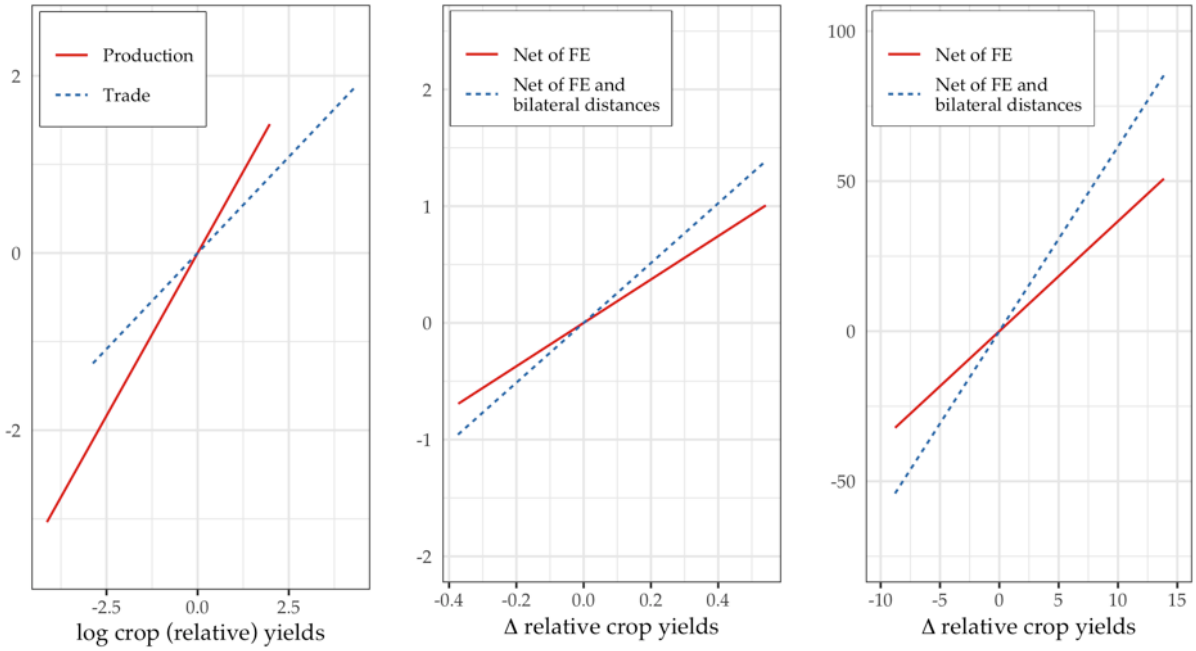

Notes: Panel A plots, with the solid line, the correlation between GAEZ potential yields and country-level effective production from FAOSTAT. The dashed line plots the correlation between country-pair relative GAEZ potential yields and bilateral trade flows from ITPD-E. Panel B plots the correlation between internal (within-country) migration and changes in relative potential yields over time (and if controlling for bilateral distances). Panel C plots analogous correlations to B but for international migration (between countries). All the correlations shown are net of fixed effects that make cross-country (and cross-crop) relationships comparable; see appendix D.1 for details.

4 Model

This section presents a static quantitative spatial model that quantifies the general equilibrium impacts of future climate change. It provides a tractable framework to account for the role of geographical heterogeneity along several dimensions (i.e. sectoral productivities, market access, and migration barriers, among others) in determining the spatial distribution of economic activity and population.[9]

4.1 Environment

The economy S is composed by N locations, denoted by i, j, or s. Each i belongs to a country $c(i) \in \{1, ..., C\}$, has a surface $H_i \in \{H_i\}_{i \in S} \equiv \mathcal{H}$, and is initially populated by $L_i^0 \in \{L_i^0\}_{i \in S} \equiv \mathcal{L}$ of workers who supply their labor inelastically. There are K sectors $k \in \{1, ..., K\}$ in the economy: $K - 1$ crops and a non-agricultural composite K sector.

[9] Refer to Appendix B for further details and derivations of the model.

Locations can produce a horizontally differentiated variety ω of each sector's goods. Each location has a sector-specific fundamental productivity $A_i^k \in \mathcal{A} = \{A_1^1, ..., A_N^K\}$ that partially drives the degree of sectoral comparative advantage across space. Moreover, workers residing in i enjoy an amenity value $u_i \in \{u_i\}_{i \in S} \equiv \mathcal{U}$.

Goods and labor units are mobile in S, subject to frictions. In particular, $\mathcal{T} = \{\tau_{ij}\}_{i,j \in S}$ is the bilateral trade friction matrix where $\tau_{ij} = \tau_{ji} \geq 1$ is the iceberg cost of trading betwen i and j. Frictions to migration depend on an analogous mobility cost $\bar{m}_{ij} \in \mathcal{M}$ and on an idiosyncratic taste shock to the migration choices of agents.

The geography of the economy is $\mathcal{G}(S) = \{\mathcal{L}, \mathcal{H}, \mathcal{A}, \mathcal{U}, \mathcal{T}, \mathcal{M}\}$: the set of spatial fundamentals that interact with the economic forces of the economy and determine the spatial distribution of the economic activity, explained next.

Technology and Market Structure. In every i, a continuum of firms produces an ω variety of sector k goods with labor $L_i^k(\omega)$ and land $H_i^k(\omega)$ in:

$$q_i^k(\omega) = z_i^k(\omega) \times L_i^k(\omega)^{\alpha_k} H_i^k(\omega)^{1-\alpha_k}, \text{ where} \tag{1}$$

$z_i^k(\omega)$ is a Hicks-neutral productivity shifter that firms draw independently from:

$$z_i^k(\omega) \sim F_i^k(\omega) = e^{-\omega^{-\xi_k} \times \left(b_i^k A_i^k\right)}. \tag{2}$$

F_i^k's shape parameter ξ_k determines the dispersion of firms' productivity draws (hence, their ex-post heterogeneity) around the scale parameter $\left(b_i^k A_i^k\right)$. Thus, they depend on A_i^k (i.e., i's fundamental characteristics) and b_i^k, a location-sector efficiency shifter that represents other determinants of firms' productivity (e.g. technology).

The output can be locally consumed or traded with other locations in a perfectly competitive, full information framework. Thus, the final price of the sector k variety ω produced in i and shipped to j is:

$$p_{ij}^k(\omega) = \left(\bar{c}^k w_i^{\alpha_k} r_i^{1-\alpha_k} / z_i^k(\omega)\right) \times \tau_{ij}, \tag{3}$$

where $\bar{c}^k$ is a constant and w_i and r_i are factor prices (wages and land rents).

Preferences. Each location i is initially populated by a continuum of workers who decide where to live and how much to consume. In particular, a worker n initially living in location i who decides to migrate to j enjoys

$$U_{ij}(n) = C_j \times \bar{m}_{ij}^{-1} \times \varepsilon_j(n), \tag{4}$$

where C_j is the utility obtained from consumption in j, $\bar{m}_{ij}$ is the mobility cost of migrating to j, and $\varepsilon_j(n)$ is a destination taste shock that disciplines workers' (ex-

post) heterogeneous taste with respect to their preferred destination.

Consumption choice. Workers in a location j decide how much to consume of all possible ω varieties from all K sectors goods, $c_j^k(\omega)$. Their preferences feature love for varieties, which is modeled using a sectoral tier with CES $\eta_k > 1$:

$$C_j^k = \left(\int c_j^k(\omega)^{\frac{\eta_k - 1}{\eta_k}} d\omega \right)^{\frac{\eta_k}{\eta_k - 1}}. \tag{5}$$

Workers at j enjoy per capita income $v_j = w_j + r_j H_j / L_j$. Following Eaton and Kortum (2002), the share of j's spending on sector k goods is:

$$\lambda_{ij}^k = b_i^k A_i^k \left(\Gamma^k \bar{c}^k w_i^{\alpha_k} r_i^{1-\alpha_k} \tau_{ij} / P_j^k \right)^{-\xi_k}, \text{ where} \tag{6}$$

$$P_j^k = \Gamma^k \left(\sum_{i \in \mathcal{S}} b_i^k A_i^k \left(\bar{c}^k w_i^{\alpha_k} r_i^{1-\alpha_k} \tau_{ij} \right)^{-\xi_k} \right)^{-1/\xi_k} \tag{7}$$

is the price index of sector k at j. Thus, workers expend a larger share on the cheapest suppliers (i.e., with the lowest price vis-à-vis sectoral price index P_j^k). ξ_k determines the extent to which this occurs, being the sectoral trade elasticity in the economy.

Worker choices across the $K-1$ crops also feature love for varieties. All crop C_j^k composites are aggregated into the following agricultural CES tier:

$$C_j^a = \left(\sum_{k \neq K} \left(C_j^k \right)^{\frac{\gamma_a - 1}{\gamma_a}} \right)^{\frac{\gamma_a}{\gamma_a - 1}}. \tag{8}$$

$\gamma_a > 1$ is the CES between crops which drives their degree of substitutability. Hence, j's share of expenditure on crop k relative to total crop expenditure is:

$$\Xi_j^k = \left(P_j^k / P_j^a \right)^{1-\gamma_a}, \text{ where} \tag{9}$$

$$P_j^a = \left(\sum_{k \neq K} \left(P_j^k \right)^{1-\gamma_a} \right)^{\frac{1}{1-\gamma_a}} \tag{10}$$

is the price index of the aggregate agricultural sector a. Therefore, workers substitute crops based on their relative prices. Larger values of γ_a imply more consumption of the locally cheapest crop and a stronger degree of specialization in crop consumption across locations.

Finally, the consumption choice between agricultural and non-agricultural goods is modeled with a further nonhomothetic CES tier in the spirit of Comin et al. (2021).

In particular, the utility from consuming goods, C_j, is implicitly determined from:

$$\sum_{k\in\{a,K\}} \left(\Omega^k\right)^{1/\sigma} \left(C_j\right)^{\epsilon_k/\sigma} \left(C_j^k\right)^{(\sigma-1)/\sigma} = 1, \tag{11}$$

where $\sigma > 0$ is the CES between the a and K aggregate sectors, ϵ_k is their nonhomothetic elasticity of substitution, and Ω_k are sectoral preference shifters. Utility maximization implies that total consumption equals real income, $C_j = v_j/P_j$, and that aggregate price indexes and expenditure shares at j are respectively determined as:

$$P_j = \left(\sum_{k\in\{a,K\}} \left(\Omega^k \left(P_j^k\right)^{1-\sigma}\right)^{\frac{1-\sigma}{\epsilon_k}} \times \left(\mu_j^k v_j^{1-\sigma}\right)^{\frac{\epsilon_k-(1-\sigma)}{\epsilon_k}}\right)^{\frac{1}{1-\sigma}}, \text{ and} \tag{12}$$

$$\begin{aligned}\mu_j^k &= P_j^k C_j^k / v_j \\ &= \Omega^k \times \underbrace{\left(P_j^k/P_j\right)^{1-\sigma}}_{\text{substitution}} \times \underbrace{\left(v_j/P_j\right)^{\epsilon_k-(1-\sigma)}}_{\text{nonhomotheticity}} \quad \forall k \in \{a,K\}.\end{aligned} \tag{13}$$

Equation (13) shows that workers' choices between agricultural and non-agricultural goods are more complex than within agriculture. The reasons are two: first, it contains a substitution component analogous to eq. (9) that nevertheless permits a lower degree of substitutability between sectors ($\sigma < 1$). That makes it possible for changes in sectoral expenditures to be relatively lower (in magnitude) than the changes in relative prices. Second, it features a nonhomothetic component that maps changes in real income onto changes in sectoral expenditure shares – essentially, an income effect. The elasticities ϵ_k determine this relation: if $\epsilon_k < 1-\sigma$, then sector k goods are a necessity whose expenditure decreases with income (and the opposite if $\epsilon_k > 1-\sigma$). Note that if $\epsilon_k = 1-\sigma$ for all k, then the nonhomothetic component vanishes and eqs. (12) and (13) become isomorphic to eqs. (9) and (10).[10]

In equilibrium, j's per capita demand for sector k goods produced in i is $\lambda_{ij}^k \Xi_j^k \mu_j^a v_j$

[10]Such a demand structure is required in order to account for the necessity (subsistence) aspect of agricultural goods when endogenizing sectoral shifts from agriculture to non-agriculture (i.e. structural change). This is what Gollin et al. (2007) refer to as the food problem and what Nath (2023) shows to be a limitation of structural change as a response to climate change. I discuss this further in Section 4.2.

for crops and $\lambda_{ij}^K \mu_j^K v_j$ for the K^{th} sector. Hence, the total bilateral expenditure X_{ij} is:

$$\begin{aligned} X_{ij} &= \sum_{k \in \mathcal{K}} X_{ij}^k = \sum_{k \neq K} \lambda_{ij}^k \Xi_j^k \mu_i^a v_j L_j + \lambda_{ij}^K \mu_j^K v_j L_j \\ &= \sum_{k \neq K} b_i^k A_i^k \left(\Gamma^k \bar{c}^k w_i^{\alpha_k} r_i^{1-\alpha_k} \tau_{ij} / P_j^k \right)^{-\xi_k} \left(\frac{P_j^k}{P_j^a} \right)^{1-\gamma_a} \Omega^a \left(\frac{P_j^a}{P_j} \right)^{1-\sigma} \left(\frac{v_j}{P_j} \right)^{\epsilon_a - (1-\sigma)} v_j L_j + \\ &+ b_i^K A_i^K \left(\Gamma^K \bar{c}^K w_i^{\alpha_K} r_i^{1-\alpha_K} \tau_{ij} / P_j^K \right)^{-\xi_K} \Omega^K \left(\frac{P_j^K}{P_j} \right)^{1-\sigma} \left(\frac{v_j}{P_j} \right)^{\epsilon_K - (1-\sigma)} v_j L_j. \end{aligned} \tag{14}$$

Location choice. Workers choose where to live in order to maximize utility. In particular, worker n initially living in i chooses a destination j in order to solve:

$$\max_j \quad U_{ij}(n) = \left(v_j / P_j \right) \times \bar{m}_{ij}^{-1} \times \varepsilon_j(n). \tag{15}$$

Therefore, workers will prefer locations with higher real income, although subject to the bilateral migration cost $\bar{m}_{ij}$ and the destination taste shock $\varepsilon_j(n)$. Formally, the former is modeled as

$$\bar{m}_{ij} = m_{ij} \times m_{c(j)} \text{ if } c(i) \neq c(j), \text{ and } \bar{m}_{ij} = m_{ij} \text{ otherwise,} \tag{16}$$

where m_{ij} and $m_{c(j)} \geq 1$. Thus, mobility costs depend on m_{ij} (which accounts for bilateral characteristics like distance) and potentially $m_{c(j)}$. The latter matters only if the location choice requires workers to switch countries. Hence, it captures country-specific characteristics of destination j in terms of national barriers to foreigners.

I assume that the taste shock is drawn independently from an extreme-value distribution with shape parameter $\theta > 0$ and scale parameter $u_j (L_j / H_j)^{-\beta}$:

$$\varepsilon_j \sim G_j(z) = e^{-z^{-\theta} \times u_j (L_j / H_j)^{-\beta}}. \tag{17}$$

The parameter θ drives workers' heterogeneity with respect to their location tastes (and, to some extent, the dispersion forces in the economy). A higher θ makes agents more homogeneous and their location decisions more dependent on real income v_j / P_j. That drives down the dispersion forces in the economy. In contrast, a lower θ implies greater heterogeneity among agents who are more likely to draw higher values of taste shocks for every location. In that case, dispersion forces increase. Moreover, the scale parameter $u_j (L_j / H_j)^{-\beta}$ determines the average of the preference draws; u_j stands for the fundamental amenity of destination j; and $\beta > 0$ determines the extent to which population density diminishes quality of life.

Analogously to eq. (2), the distributional assumption on taste preferences allows

for a closed-form solution to the share of workers initially in i migrating to j:

$$\Pi_{ij} = \mathbb{P}\Big(W_j(v) \geq \max\{W_s(v)\}_{s\neq j}\Big) = \frac{(v_j/P_j)^{\theta}\bar{m}_{ij}^{-\theta}u_j(L_j/H_j)^{-\beta}}{\sum_{s\in S}(v_s/P_s)^{\theta}\bar{m}_{is}^{-\theta}u_s(L_s/H_s)^{-\beta}}. \tag{18}$$

Therefore, the total number of workers that choose to live in destination j is:

$$L_j = \sum_{i\in S}\Pi_{ij} \times L_i^0. \tag{19}$$

This is an intuitive result: locations with higher real income (v_j/P_j) and/or density-adjusted amenities $u_j(L_j/H_j)^{-\beta}$ will have a higher population in equilibrium. The magnitude of this effect is partially driven by θ, which is the elasticity of the location choice with respect to real income and to bilateral migration costs.

Spatial equilibrium. Given the geography $\mathcal{G}(S)$ and the exogenous parameters $\Theta \equiv \{\Omega_k, \eta_k, \gamma_a, \epsilon_k, \alpha_k, \xi_k, \sigma, \theta, \beta\}$, a spatial equilibrium is a vector of factor prices and labor allocations $\{w_j, r_j, L_j\}_{j\in S}$ such that eqs. (7), (10), (12) to (14) and (19) hold, and markets for goods clear. Formally, market clearing requires trade-balacing, such that each j's income equals total exports to and total imports from all locations $i \in S$:[11]

$$w_jL_j + r_jH_j = \sum_{i\in\mathcal{S}}X_{ji} = \sum_{i\in\mathcal{S}}X_{ij}. \tag{20}$$

4.2 Illustration and discussion of the underlying mechanisms

I illustrate how changes in the fundamentals shape the geographical distribution of economic activity and population by representing it as a line with a discrete number of locations. By doing so, I emphasize the effect of the model's underlying mechanisms on the agent's mobility decisions in response to a climate shock to the economy.

The locations $i \in \{1, ..., N\}$ are distributed over a line and are homogeneous with respect to amenities, efficiency shifters, and initial population ($u_i = u$, $b_i^k = b$, and $L_i^0 = l\ \forall i, k$). The economy is composed of two countries, where the ten left-most locations stand for country 1. I initially set $K = 2$, so that the agricultural a sector consists of one crop only. I assume that the distribution of sectoral fundamental productivities is increasing in the right-most locations and that every location is more productive in the K^{th} sector. I also set bilateral trade and mobility frictions to be proportional to the bilateral distances and make it costly to migrate to country 2. In terms of preferences, I assume that the agricultural crop is a necessity good and the

[11] Appendix B.3 documents the non-linear system of $7 \times N$ equations that characterize the spatial equilibrium, the iterative algorithm used to solve it, and aspects related to its existence and uniqueness.

Figure 4: Equilibrium values of $\{L_i^1, L_i^2\}_{i \in S}$ for an economy represented on a line

Panel A: Migration barriers, sectoral specialization, and CΔ.

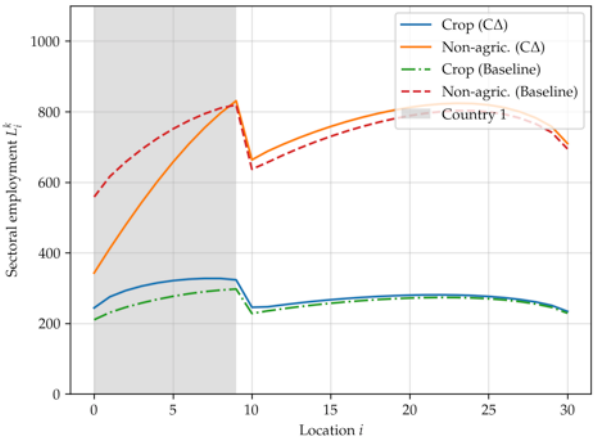

Panel B: CΔ, the food problem, and the role of trade frictions.

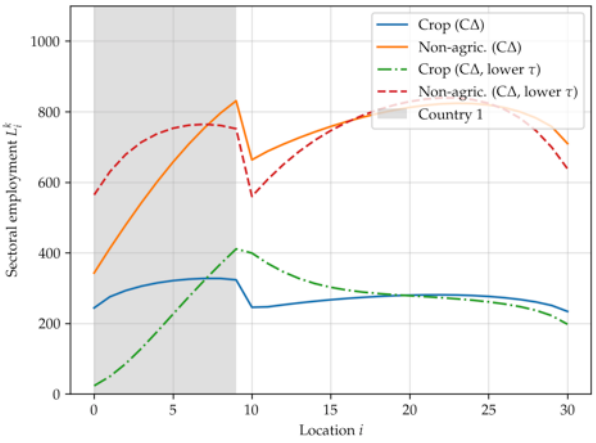

Panel C: CΔ and migration barriers.

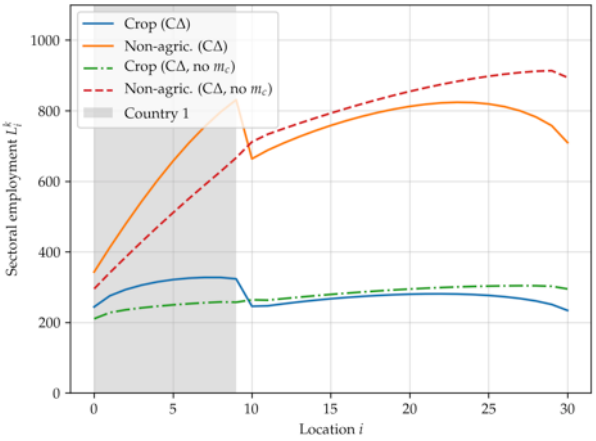

Panel D: CΔ and crop switching.

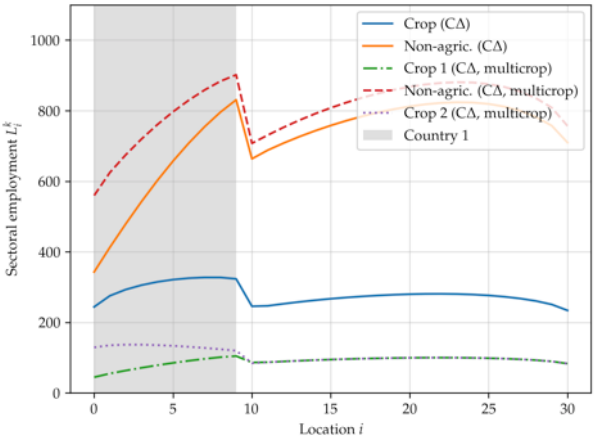

Notes: Equilibrium labor allocations for the model described in Section 4.2. Panel A describes the equilibrium of the baseline and climate change simulations (country 1 becomes less suitable for crops). Panel B, C, and D plot the results of the climate change scenario with, respectively, lower trade frictions (a reduction in τ), no migration barriers between countries ($m_c = 1$ for all c) and multiple crops ($K = 3$). See Appendix B.5 for details and a graphical representation of the fundamentals.

opposite for the K^{th} sector. For simplicity, I disregard land $\mathcal{H}$.[12]

Panel A of Figure 4 plots the equilibrium distributions of $\{L_i^k\}$ as dashed lines (baseline). Overall, the economy produces more non-agricultural goods, which is the most productive sector. In distributional terms, the rightmost locations in each country have a higher level of economic activity and a larger population. The discontinuity at the country boundaries (i = 10) illustrates the role of country migration barriers (i.e. $m_2 > 1$). There is a higher population density on country 1's side due to the inability of workers to cross into country 2, where productivities and real wages are higher.

Subsequently, I simulate a climate shock by reducing country 1's crop productiv-

[12] That is, $\alpha_k = 1 \; \forall k$, $\epsilon_a < 1 - \sigma$ (and the opposite for $k = K = 2$), $m_1 = 1$, $m_2 = 1.5$, $\tau_{ij} = m_{ij} = e^{\tau \times |i-j|}$, and $A_i^k = a_k \times i$, where $\tau = 0.05$ and $a_2 > a_1$. See Appendix B.5 for details.

ities even further. The result is shown in Panel A of Figure 4 using solid lines (CΔ). Country 1 changes its patterns of sectoral specialization by increasing its relative employment in agriculture. This is driven by the necessity aspect of agricultural goods. Climate change reduces crop productivity in country 1, which reacts by increasing agricultural employment so to produce the needed quantity of crops. This reduces real income in that country, increasing its share of expenditure on crops. Country 2, if anything, gets benefitted. Its population and non-agricultural employment increase due to the climate migrants from country 1.

This simple exercise illustrates the limitations of structural transformation as a response to climate change. As rightly argued by Nath (2023), economies will switch production out of affected sectors only if capable of importing subsistence goods from unaffected regions. He refers to this as the food problem, inspired by previous studies of structural change and development (Gollin et al., 2007; Herrendorf et al., 2014). Panel B of Figure 4 provides further quantitative evidence of how this mechanism works in my model. When facing lower trade frictions, country 1 switches production out of agriculture, since it can now outsource crops from the nearest locations in country 2 (which shifts its production towards agriculture).

The novelty of my framework lies in the addition of two dimensions that further interact with the mentioned adaptation mechanisms. The first is migration barriers, whose role is illustrated in Panel C of Figure 4 (the climate change scenario without country migration barriers, i.e. $m_c = 1$ for all c). The results are intuitive: instead of reacting to the food problem, workers in country 1 migrate to country 2. Overall, workers enjoy higher real wages and spend lower income shares on agricultural goods, making climate change less of a problem. Thus, migration can have a welfare-improving role as a response to climate change. It permits individuals to move out of unproductive rural regions, allowing for a more efficient sectoral spatial sorting of workers. This echoes the insights obtained from research on spatial structural change (Eckert and Peters, 2022) and on the gains from lowering migration barriers in rural economies (Bryan and Morten, 2019; Pellegrina and Sotelo, 2024; Lagakos et al., 2023). This is a key, novel aspect that I account for: I quantify the distribution of $\{m_c\}_c$ across SSA and investigate their mitigating role in policy experiments.

The second additional dimension is the multi-crop aspect of the agricultural sector. Crops are partial substitutes as subsistence, and Section 3 shows that climate change is expected to alter their yields heterogeneously within locations. Thus, a potential response of farmers in affected locations would be to switch production towards less-affected crops. The role of this margin is shown in Panel D of Figure 4. Dashed lines represent the outcomes of a simulation with two crops, where only crop 1 is affected in country 1. As a result, locations in that country switch production towards

(unaffected) crop 2. This increases non-agricultural employment, real wages and welfare. Country 2 remains qualitatively unaffected, and overall the economy is better off relative to the one-crop scenario.

5 Bringing the model to the SSA data

I quantify the model to match SSA data by the early 21st century. To do so, I define the economy S as the geography of SSA, leaving aside interactions with the rest of the world.[13] Then, I use a mix of quantification methods to map Θ and $\mathcal{G}(S)$ to observable features of SSA. Tables 1 and 2 document the methods and sources used, and Section 5.5 the overidentification tests that validate the calibrated model.[14]

5.1 Parameters from the literature

I draw the values for $\{\eta_k, \gamma_a, \epsilon_k, \alpha_k, \xi_k, \sigma, \theta, \beta\}$ from the related literature. I set the lower-tier CES as $\eta_k = 5.4$ for crops and $\eta_K = 4$ (as in Costinot et al., 2016; Desmet et al., 2018, respectively), and the mid-tier CES as $\gamma_a = 2.5$ as in Sotelo (2020). As for the upper-tier nonhomothetic CES, I follow Comin et al. (2021) and set $\sigma = 0.26$, $\epsilon_a = 0.2$, and $\epsilon_K = 1$. Therefore, agricultural goods in my framework are a necessity, as opposed to non-agricultural K goods. I obtain the factor shares $\alpha_k = 0.39$ and $\alpha_K = 0.58$ from Fajgelbaum and Redding (2022) and the trade elasticities $\xi_k = 5.66$ and $\xi_K = 6.63$ from Pellegrina (2022). Finally, I set $\theta = 3$ and $\beta = 0.32$ following Morten and Oliveira (2024) and Desmet et al. (2018), respectively. Appendix B.8 further discusses the implications of these parameter choices.

5.2 Transportation and trade networks

I follow the related literature (e.g. Allen, 2014; Donaldson, 2018; Pellegrina, 2022) by assuming that trade frictions are proportional to the travel distance between locations:

$$\tau_{ij} = \text{distance}(i,j)^{\delta} \times \tau_{ij}^{F}, \tag{21}$$

where $\text{distance}(i,j)$ is the shortest distance between the location pair (in kilometers) and $\tau_{ij}^{F} \geq 1$ is an additional tariff-like trade friction. That is, $\tau_{ij}^{F} > 1$ only if $c(i) \neq c(j)$.

I retrieve $\text{distance}(i,j)$ for all location pairs by feeding the road network and friction surface data to a pathfinding algorithm that calculates the shortest routes and

[13] My baseline setting refrains from migration and trade with the rest of the world because about 75% of international migrants from SSA by the early 21st century moved within the continent. However, I extend my setting by adding these interactions with the rest of the world in Section 6.4.

[14] Appendix B.6 discusses the data used, data quality issues, and the numerical algorithms.

Table 1: Preference and technology parameters borrowed from the related literature

Parameters	Description	Source
Panel A: Demand parameters		
$\eta_k = 5.4$	Lower-tier CES ($k \neq K$, crops)	Costinot et al. (2016)
$\eta_K = 4$	Lower-tier CES (non-agriculture)	Desmet et al. (2018)
$\gamma_a = 2.5$	Mid-tier CES (across crops)	Sotelo (2020)
$\sigma = 0.26$	Upper-tier CES	Comin et al. (2021)
$\epsilon_a = 0.2$	Non-homothetic CES (agriculture)	Comin et al. (2021)
$\epsilon_K = 1$	Non-homothetic CES (non-agriculture)	Comin et al. (2021)
Panel B: Supply parameters		
$\xi_k = 5.66$	Sectoral trade elasticity ($k \neq K$, crops)	Pellegrina (2022)
$\xi_K = 6.63$	Sectoral trade elasticity (non-agriculture)	Pellegrina (2022)
$\alpha^k = 0.39$	Crop labor share ($k \neq K$)	Fajgelbaum and Redding (2022)
$\alpha^K = 0.58$	Non-agricultural labor share	Fajgelbaum and Redding (2022)
Panel C: Location choice parameters		
$\theta = 3$	Migration elasticity $\in [2, 4]$	Morten and Oliveira (2024)
$\beta = 0.32$	Congestion to population density	Desmet et al. (2018)

respective distances between all neighboring cells. Then, I use the Dijkstra algorithm to calculate the shortest distance between all pairs. Finally, I map these distances onto $\mathcal{T}$ with a GMM that estimates $\delta = 0.17$ and $\tau_{ij}^F = 6.75$. This last step is done simultaneously with the calibration of other fundamentals, as explained in Section 5.3.

Figure 5 illustrates subsamples of the quantified $\mathcal{T}$. It shows the complexity of the trade network, which replicates well the existing transportation infrastructure both within and across countries. As expected, trade frictions increase with distance. Moreover, the discontinuity of the distance gradient shows the additional cost of international trade captured by τ_{ij}^F.

5.3 Productivities, sectoral shifters, land endowments, and trade costs

The set of fundamentals and parameters $\{\mathcal{H}, \mathcal{A}, b_i^k, \Omega_k, \tau_{ij}^F, \delta\}_{i,j,k}$ are quantified as follows. First, I set $\mathcal{H}$ as each cell's land area in square kilometers. Subsequently, I follow Costinot et al. (2016) and use the agro-climatic yields from GAEZ as the fundamental productivities of crops $\{A_i^k\}_{i \in S, k \neq K}$.[15] The underlying rationale is that the GAEZ data provides potential yields and is thus informative about the productivity variation across location-crops that is driven exclusively by differences in natural character-

[15] To be consistent with the SSA rural context in 2000, I use the agro-climate potential yields calculated for rain-fed agriculture with low usage of modern inputs. See Appendix A for details.

Figure 5: Estimated trade network for SSA – Western and Eastern Africa

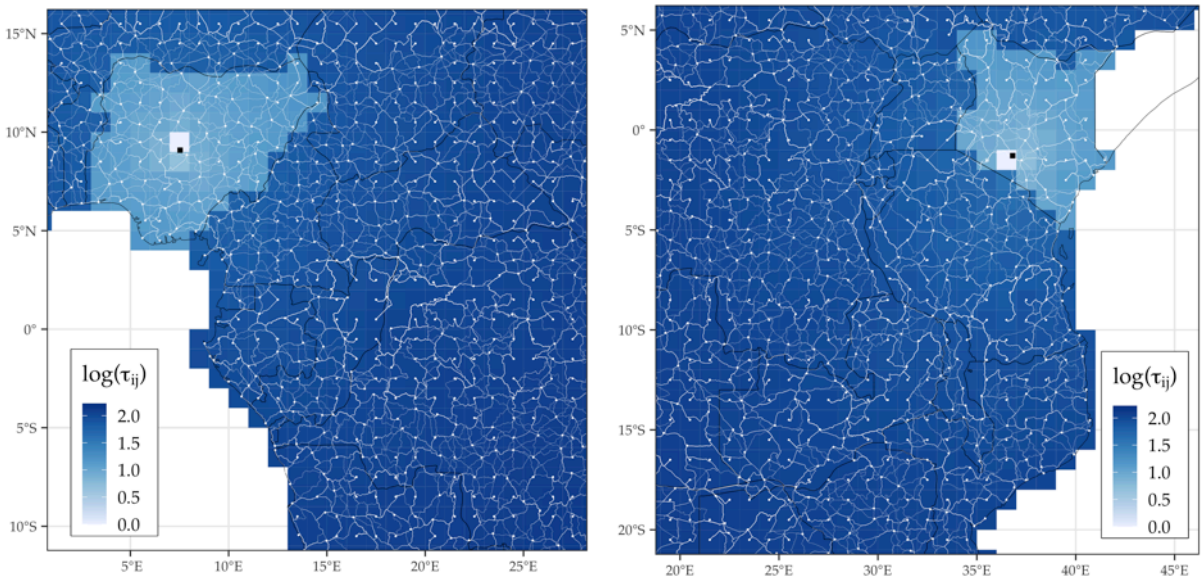

Notes: Notes: Estimated trade network for Western Africa (left) and Eastern Africa (right). The network is built by finding the shortest path between all neighboring cells over the road infrastructure. τ_{ij} represents the estimated iceberg trade costs with respect to the capital of Nigeria (left) and the capital of Kenya (right), both represented by a black dot. See Section 5.2 for details.

istics, including the climate. The variation in effective producvity across locations, conditional on the former, is embedded in $\{b_i^k\}_{i,k}$.

To quantify the remaining elements $\mathbf{t} \equiv \{\tau_{ij}^F, \delta\}$ and $\mathbf{T} \equiv \{\{A_i^K\}_i, \{b_i^k\}_{i,k}, \{\Omega_a, \Omega_K\}\}$, I implement a two-stage procedure. In the first stage (inner loop), I guess values for $\mathbf{t}$ and quantify $\mathbf{T}$ by inverting the general equilibrium conditions of the model. Then, the second stage (outer loop) estimates $\hat{\mathbf{t}}$ with a GMM that targets model-generated moments to their data counterparts conditional on the first stage. In what follows, I concisely describe this two-stage approach, leaving further details to Appendix B.6.

Model inversion (inner loop). This step calibrates $\mathbf{T}$ by inverting the spatial equilibrium so that the model reproduces, in general equilibrium, the spatial distribution of GDP, the spatial distribution of sectoral production, and the relative a and K aggregate expenditure shares. Following Farrokhi and Pellegrina (2023), I represent the solution of this inner loop, conditional on a guess for $\mathbf{t}$, as $z(\mathbf{T}; \mathbf{t}) = 0$.

Importantly, the model inversion identifies the product $\{b_i^K A_i^K\}_i$ (since its two elements cannot be separated), and pins down $\{b_i^k\}_{k \neq K}$ in relative terms within locations. Therefore, the latter is identified using within-crop variation in observed production across locations, conditional on the fundamental productivities of $\mathcal{A}$. The former, conditional on the latter, is identified using spatial variation in GDP.

Estimation (outer loop). This step estimates $\mathbf{t}$ with a GMM that exploits moments

related to international trade flows and prices. Specifically, I design the first moment $m_1 = \sum_c \sum_{c'} \sum_{i \in c} \sum_{j \in c'} \sum_k X_{ij}^k$, that is, the aggregate exports between all country pairs in SSA. It provides variation to identify $\tau_{ij}^F = \tau^F$ given the (intuitive) decreasing relationship between tariffs and international trade flows in the economy.[16]

Then, I take an innovative approach that identifies δ using spatial variation in crop prices. Rather than using bilateral price wedges, as in the literature, I read my crop price data as sectoral prices P_i^k and use its dispersion to identify δ with $m_2 \equiv \text{standard deviation}\left(P_i^k\right)$.[17] Intuitively, the identification relies on the positive relationship between trade frictions and price dispersion: the lowest the former, the more homogeneous are price indexes across space (hence, less dispersion). Appendices B.6 and B.7 elaborate on identification aspects and discuss data-related aspects, such as the mapping between time-varying prices with my static framework.

My approach is innovative for two reasons. First, it pins down the differential role of geography (δ) and tariffs (τ^F) when determining trade costs, thus allowing for experiments along these dimensions. Second, and most importantly, it quantifies bilateral trade costs using only local prices, a much more accessible type of data vis-à-vis the usual approach in the literature (which requires origin-destination prices).[18]

For the estimation, I define $\mathbf{m} = [m_1, m_2]$ and $g(\mathbf{t}) = \left[\mathbf{m}(\mathbf{t}) - \mathbf{m}^{\text{data}}\right]$ and solve for $\hat{\mathbf{t}}$ which, based on $\mathbb{E}\left[g(\mathbf{t})\right] = 0$, satisfies:

$$\hat{\mathbf{t}} = \arg \min_{\mathbf{t}} g(\mathbf{t}) W g(\mathbf{t})' \text{ subject to } z(\mathbf{T}; \mathbf{t}) = 0,$$

where W is the weighting matrix. The estimates $\hat{\mathbf{t}} = \{6.75, 0.17\}$ (with bootstrapped standard errors of $\{0.38, 0.01\}$) have meaningful economic implications. First, $\hat{\tau}^F = 6.75$ suggests barriers for international trade in SSA that are substantially larger than developed economies (such as $\tau^F = 2.3$ for the US from Antras et al., 2024). Second, my δ estimate is about half of what Moneke (2020) estimates using only Ethiopian data. That stresses the importance of using cross-country data for continental-scale applications like mine. Assuming a higher δ would underestimate $\hat{\tau}^F$.[19]

[16] In practice, m_1 is aggregated over the set of country-pair-crop combinations covered by the ITPD-E trade data. In fact, the data sparsity (in terms of observed trade flows for SSA by the early 2000s) is the main reason behind the modeling of $\tau_{ij} = \tau^F$, that is, a common tariff for all country pairs in SSA.

[17] I take this approach because the WFP-VAM data do not specify the location of production of the crops. Hence, it should not be interpreted as bilateral prices (as in, for instance, Donaldson, 2018), but rather as local crop prices in different locations in SSA (i.e., crop prices indexes as in Equation (7)).

[18] Specifically, the literature pins down trade frictions with spatial price wedges: price differences of goods produced in a common origin but sold in different destinations. Implementing that requires origin-destination price data (e.g., prices of Malian rice sold in multiple locations, like Senegal, Niger, and so on). Instead, my approach requires only local prices, regardless of their origin. This is a relatively much more accessible type of data, especially for developing economies and in contexts of high spatial granularity (i.e., where one needs price information within and between countries).

[19] My estimated trade costs lie also within other estimates that use different functional formats (e.g.,

Table 2: Quantified fundamentals and parameters, data sources, and matched moments

	Subset	Description	Data source/Moment matched
$\mathcal{L}$	-	SSA's initial population	Population data in 2000 and 1990
$\{b_i^k\}_{i\in S}$	-	Productivity shifters	Matched to location-sector production data
$\{\Omega_k\}_{a,K}$	$\Omega_a = 1$ Ω_K =0.19	Sectoral preference shifters	Matched to aggregate sectoral expenditure
$\mathcal{H}$	-	Land endowments	Grid cell land areas
$\mathcal{A}$	$\{A_i^k\}_{i\in S,k\neq K}$	Agricultural productivities	GAEZ data
	$\{A_i^K\}_{i\in S}$	Non-agricultural productivities	Matched to GDP data
$\mathcal{U}$	-	Amenities	Matched to population data
$\mathcal{T}$	dist(i,j)	Bilateral travel distance	Transportation data
	δ =0.17 (0.01)	Distance elasticity of τ	Matched to spatial dispersion of sectoral prices
	τ_{ij}^F =6.75 (0.38)	Tariff-like trade friction	Matched to aggregate trade flows
$\mathcal{M}$	dist(i,j)	Bilateral travel distance	Transportation data
	ϕ =0.41 (0.02)	Distance elasticity of m_{ij}	Matched to total internal migration (from census data)
	$\{m_c\}_{c=1}^C$	Country migration barriers	Matched to country migration data (from bilateral flows)

Notes: Values in parenthesis stand for bootstraped standard errors; refer to Appendix B.6 for details.

5.4 Migration frictions and amenities

As with τ_{ij}, I set the bilateral component of migration frictions to be proportional to distance, i.e. $m_{ij} = \text{distance}(i,j)^{\phi}$. Thus, the remaining elements to be quantified are $\{\phi, m_c, u_i\}_{i,c}$, which are solved for with an analogous two-stage procedure.

Inner loop. It uses the quantified elements in Section 5.3 to solve for prices and real income in the economy. Then, starting with a guess for ϕ, it inverts the spatial equilibrium for $\{m_c\}_c$ and $\{u_i\}_i$ such that the model replicates, respectively, the gross

Donaldson, 2018; Pellegrina, 2022, for India and Brazil, respectively); see Appendix B.9 for details.

migration flows at the country level and the spatial distribution of the population.[20] The separate identification of $\{m_c\}_c$ and $\{u_i\}_i$ is possible because they are additively separable in the denominator of eq. (18). That provides within-country variation in terms of potential origins from which the migration cost is or is not scaled by $\{m_c\}_c$, and allows for a separate identification conditional on $\{u_i\}_i$.[21] The latter, conditional on the former, is identified with spatial variation in population.[22]

Outer loop. It consists of a similar GMM that estimates $\hat{\phi} = 0.41$ (with bootstrapped standard errors of 0.02) by matching the total internal migration observed in the census data.[23] It conveys evidence of large mobility barriers in SSA: the resulting (median) $\{m_{ij}\}_{i,j}$ is about 20 percent higher than the estimates for Indonesia (from Bryan and Morten, 2019), and three and four times larger than those for Brazil and the US (respectively from Morten and Oliveira, 2024; Allen and Donaldson, 2022).[24]

5.5 Validating the model

Before using the quantified model to simulate the future, I first check the reasonability of the quantified fundamentals. They align well with the mechanisms in the model. I find high non-agricultural productivities in highly productive locations, high migration barriers in countries with (relative) little migration, high amenities in denser locations with (relative) low real income, and preference shifters that match the SSA context (and are close to estimates from related studies; see Appendix B.10 for details).

Next, I test the capacity of the model to replicate observed moments with a backcasting exercise that solves for the spatial equilibrium in 1975 using the GAEZ agricultural productivities and population endowments in that year. The result illustrates how well the model replicates the population changes in SSA between 1975 and 2000 using the observed changes in the climate during that period.[25]

[20] Importantly, the international migration data from Abel and Cohen (2019) provides cross-country gross flows between 1990 (the earliest year available) and 2000. Thus, my estimation requires a measure of the initial population in 2000, i.e. $\{L_i^0\}_i$. I calculate it by scaling the distribution of the population in 1990 to the levels of SSA population in 2000, while accounting for the observed natural population growth rates (fertility minus mortality) across countries during the period. Intuitively, this represents the population distribution in SSA if there had been no mobility during that period.

[21] Intuitively, the additive separation holds because, for each destination, there are several origins of migrants, some of them being in other countries and others not.

[22] Therefore, amenities stand as a structural residual of my model that rationalize all location choices observed in the data that cannot be explained by differences in real wages and migration frictions.

[23] To be consistent other data, I use internal migration flows between 1990 and the early 2000s.

[24] As with trade costs, the estimates from these sources are not directly comparable to my $\hat{\phi}$ due to different functional formats and/or units (e.g., travel time rather than distance). Appendix B.9 discusses their equivalence in detail and the reasons for (and benefits of) my specification.

[25] The data source for the 1975 population (GHSP) differs from that used in the calibration (G-Econ). I check their compatibility using the correlation between them for the population in 2000 (available in both datasets) at the grid-cell and country level. Furthermore, in order to have an initial population for

Figure 6: Validation of the calibrated model in levels and differences

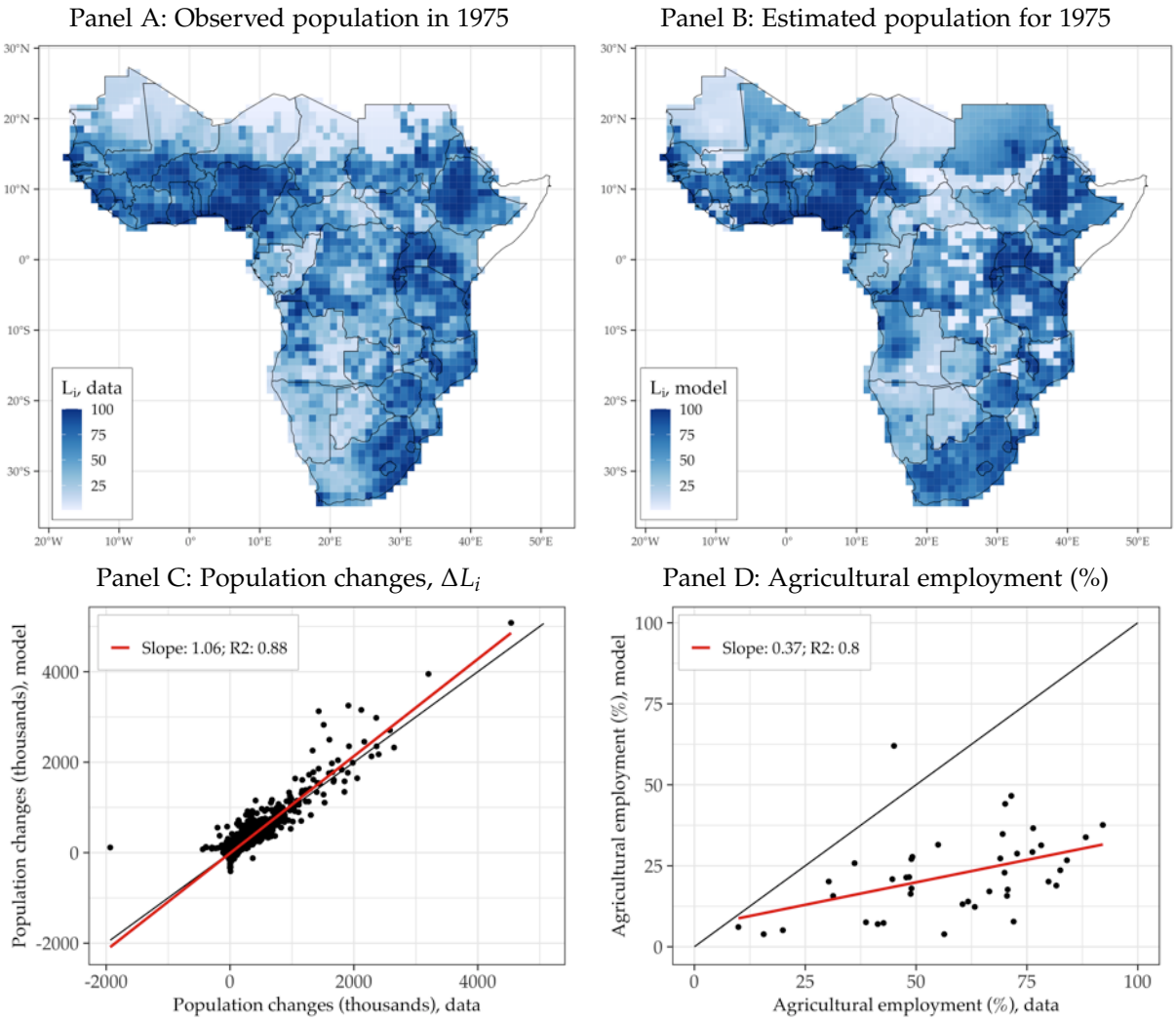

Notes: Panels A shows the observed 1975 population distribution in SSA while Panel B shows the distribution produced by the model. The values are shown in percentiles, where 1 (100) stands for the bottom (top) percentile of each sample. Panel C plots the model fit in terms of population change (between 1975 and 2000, in thousands) while Panel D plots the model fit for country-level agricultural employment in 2000 (in percentage points).

Panels A and B of Figure 6 report the results in levels. The model closely replicates the spatial distribution of the population in 1975 both within and across countries. Moreover, Panel C shows that the results closely fit the population changes between 1975 and 2000, with a slope and R^2 very close to one. Importantly, the major change in this backcasting exercise is on the agricultural suitabilities, i.e. $\{A_i^k\}_{i,k\neq K}$. According to the GAEZ estimates, about 75 percent of the locations in SSA experienced a decline in crop yields between 2000 and 1975. Thus, the fact that using this variation in the model can explain the changes in population during the period confirms the model's

solving the model for 1975 – i.e. $\{L_i^0\}_i$ – I project the 2000 population distribution onto the 1975 levels. Appendix B.11 discusses that in detail.

capacity to provide reliable forecasts of the future using the GAEZ estimates.[26,27]

As an additional overidentification test, Panel D compares country-level agricultural employment shares (for all crops) generated by the model for 2000 against World Bank data. The model closely replicates the ranking of countries with respect to agricultural employment shares, though underestimating their levels. In aggregate, the model predicts about a 24 percent share of employment in agriculture as compared to 59 percent in the data. The main reason for this discrepancy is that I include only a subset of the crops produced in SSA.

6 Climate change and migration: the 2080 forecast

I quantify potential climate migration in SSA by performing a series of counterfactual simulations. The benchmark exercise consists of solving for the spatial equilibrium in 2080 with and without climate change. By comparing the two, I quantify the impact of climate change on population reallocation, welfare losses, and other outcomes. Subsequently, I study how policy attenuates these effects with an experiment that hypothetically assumes that SSA adopts the migration and trade policies of the EU. I conclude with additional discussions, extensions, and robustness checks.

6.1 Benchmark counterfactual

I solve for the spatial equilibrium in 2080 by inserting the 2080 forecasts of the initial population $\mathcal{L}$ and crop productivities $\mathcal{A}$ into the calibrated model. The former is obtained by scaling the observed population of 2000 using the estimates of country-level population increase from the Population Prospects of United Nations and Social Affairs (2019) for 2080.[28] The latter, in contrast, is taken directly from the GAEZ data. For the climate change simulations, I use the estimates of potential crop productivities in 2080 based on the business-as-usual scenario.[29] The simulations with no climate

[26] A complementary explanation for the good fit in this exercise is path dependence (i.e. the densest locations in 1975 are also the densest in 2000). That is, in a context of high mobility frictions, such as in SSA, the geography of the economy needs extreme shocks to its fundamentals in order to generate dramatic changes in this kind of counterfactual. As shown in Figure B.6, the changes between 1975 and 2000 are not as dramatic as the ones expected by 2080.

[27] However, the model performs less precisely for outmigration predictions because of amenities outliers in the Sahel regions (where very little income but somehow dense population is interpreted in the model inversion as high-amenities).

[28] These estimates project the observed country-level natural rates of population growth (fertility minus mortality without migration) at the beginning of the 21st century onto subsequent years. Hence, I assume that fertility is exogenous. Section 6.4 shows how the results change if fertility is endogenized.

[29] Specifically, I draw the GAEZ data that assumes the business-as-usual future scenario, that is, the Representative Concentration Pathway (RCP) 8.5; see Appendix A for details.

change assume no changes in $\mathcal{A}$ and thus capture only the increase in population $\mathcal{L}$.[30]

I quantify climate migration, ΔL_i, using the differences between the equilibrium populations of the two simulations – with and without climate change. Hence, it measures migration pressure in each location i net of the potential migration inflows and outflows. Similarly, I infer the changes in sectoral specialization from the differences in non-agricultural employment ΔL_i^K (in percentage points) and the welfare changes from the percentage change in real income per capita, $\Delta v_i / P_i$.[31]

Figure 7 shows the results on a map. At the country level, Panel A shows large climate migration flows – on the order of a million individuals or more – from Western Sahelian countries like Mauritania and Mali to nearby countries (e.g. Niger, Ivory Coast, and Burkina Faso) and from DR Congo and other South African countries to Tanzania and South Africa. Panel B, which presents grid-cell-level results, shows a high degree of within-country heterogeneity. Countries experiencing large migration outflows, such as Senegal and DR Congo, also experience a high level of internal migration. There are large movements from their central locations, which are highly affected by climate change, to their relatively less affected south(western) locations. Overall, countries heterogeneously hit by climate change experience large internal migration flows and large population increases in their capitals.[32]

Panels C to F show the results in terms of structural change and real income per capita. The countries that benefit from climate change, such as Tanzania, Rwanda, and Uganda, specialize into agriculture (Panel C). This occurs because such an increase in comparative advantage transforms them into the new agricultural powerhouses of SSA. As a consequence, their real income increase (Panel E), which attracts migrants from nearby countries, such as DR Congo and Mozambique. Panel D and F illustrate the richness of these results in terms of within-country heterogeneity. Even within countries that benefit from climate change, there is substantial variation in terms of sectoral specialization and welfare effects.

Nevertheless, some countries forcedly shift towards agriculture in a non-welfare-improving way. Western African countries like Guinea and Sierra Leone are an example: compared to the no climate change scenario, they need to produce higher crop quantities to supply food domestically and to nearby countries that, being much more affected by climate change, specialize out of agriculture (e.g. Senegal). This shows that the necessity aspect of crops limits the Western African economies to adapt to cli-

[30] Note that the spatial distribution of outcomes in the no-climate-change simulations differs from the observed distribution for 2000 due to dispersion forces driven by θ and β.

[31] I extend this welfare measure by also accounting for utility losses from migration costs, congestion, and other aspects, in Section 6.3.

[32] See Table D.3 for details. Note that the large estimated increase in the populations of capital cities is consistent with the findings in the empirical literature on the high urbanization rates associated with climate change (e.g. Henderson et al., 2017; Peri and Sasahara, 2019; Castells-Quintana et al., 2021).

Figure 7: Counterfactual results for a climate-changed SSA in 2080

Panel A: Climate migration - country level

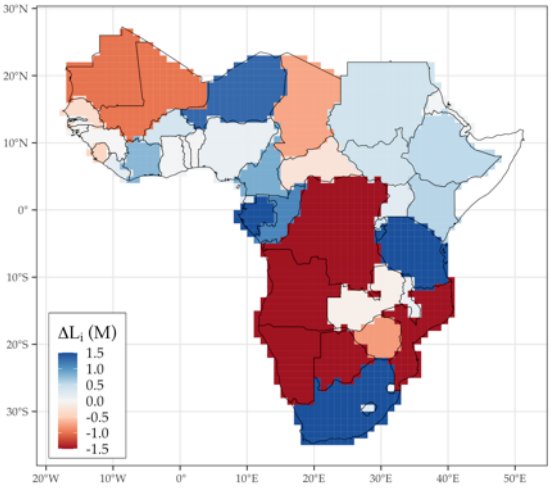

Panel B: Climate migration - grid cell level

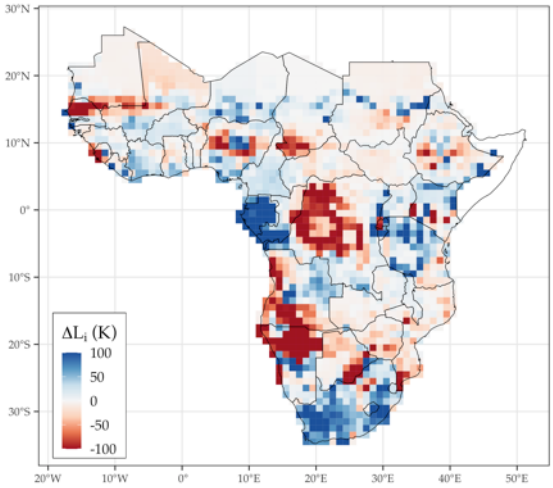

Panel C: Non-agric. employment - country level

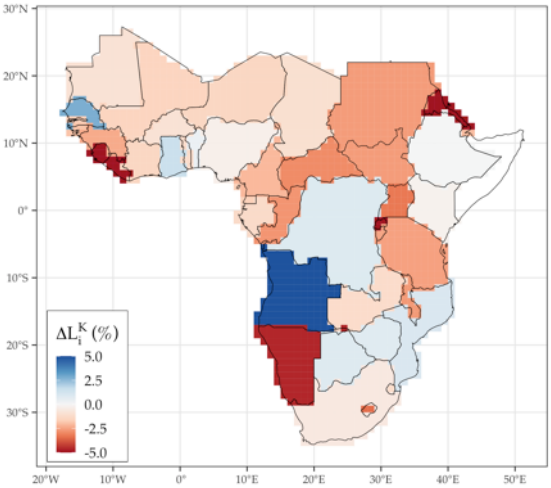

Panel D: Non-agric. employment - grid cell level

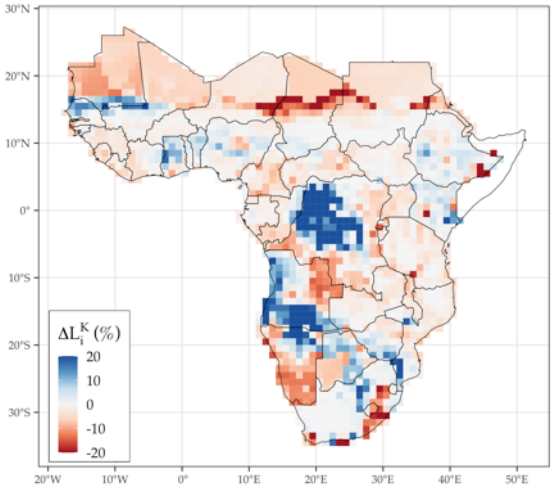

Panel E: Real GDP pc - country level

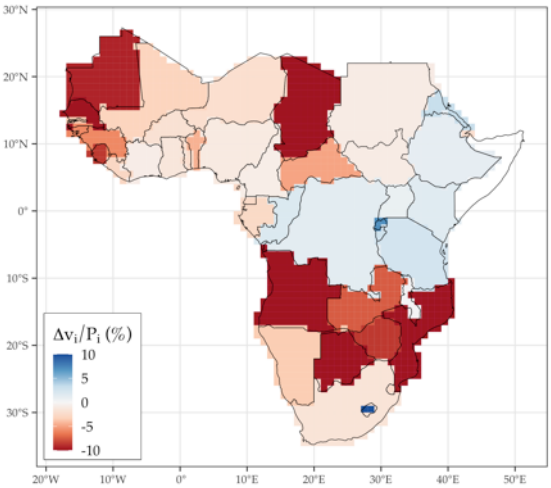

Panel F: Real GDP pc - grid cell level

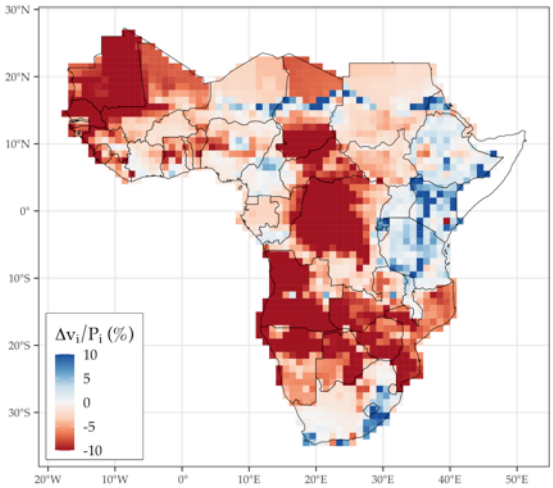

Notes: Panel A and B plot the results of climate migration in thousands of individuals. Panel C and D describe the results in terms of non-agricultural employment, in percentage points. Panel E and F present the welfare results in terms of percentage changes in real GDP per capita.

mate change (through structural change) and forces them into a climate change-driven poverty trap. Interestingly, the opposite holds for DR Congo. Climate change pushes individuals from its poorest regions either abroad or to its more productive south. As it stands among the poorest SSA countries in the no climate change scenario, such a productivity-improving reallocation slightly increases real income in relative terms.

In aggregate, the estimated climate migration flows in SSA total about 22 million individuals (Panel A of Table 3 column 1). This is much lower than Rigaud et al. (2018)'s estimates of 90 million climate migrants in SSA by 2050. This discrepancy is explained by the migration frictions that I account for and estimate using actual migration data. As shown later in Section 6.4, removing them increases my climate migration estimates to 80 million individuals, surprisingly close to these studies.[33]

Table 3 also shows that climate change barely affects aggregate welfare. However, this seemingly null effect hides a large degree of heterogeneity. At the country level, the 5^{th} and 95^{th} percentiles of welfare changes are about -15 percent and 3 percent, respectively (Panel B). Thus, climate change will lead to unequal consequences across SSA, generating a few winners and many losers (see Figure 7 Panel E). This final outcome depends on several mechanisms that interact with each other, such as migration barriers and the heterogeneous forces driving sectoral specialization and structural change. I investigate the welfare importance of these mechanisms, and the potential mitigating role of trade and migration policies, in Section 6.2.

Furthermore, climate change hardly affects aggregate sectoral employment. In distributional terms, however, this effect is also heterogeneous and negatively skewed: the 5^{th} and 95^{th} percentiles of the country-level changes in non-agricultural employment are about -5 percentage points and 1.5 percentage points, respectively, and the median country experiences a decrease in non-agricultural employment of about 1 percentage point. This happens because, with climate change, more labor needs to be employed in agriculture to produce the necessary quantity of crops (making these countries poorer and increasing their agricultural expenditure share).[34]

[33]This pattern is with consistent related findings that show that large mobility frictions in developing economies may have an inhibiting effect on future climate migration and thus may exacerbate welfare losses (e.g. Peri and Sasahara, 2019; Benveniste et al., 2020; Burzyński et al., 2022).

[34]This result is consistent with related findings in the literature. For instance, Nath (2023) estimates an increase in the global agricultural expenditure shares of about 4 percentage points, whereas Cruz (2023) estimates an increase in global agricultural employment of about 2 percent. The main channel explaining the differences in magnitude between those estimates and my own (0.82) is the multi-crop feature of my framework. By not taking into consideration the potential production reallocation within agriculture (i.e. across crops), the consumption specialization effect of climate change is overestimated.

Table 3: Aggregate and disaggregate results of the climate change counterfactuals

	(1) Baseline	(2) EU mig. barriers	(3) EU trade frictions	(4) EU trade + mig. barriers
Panel A - Aggregate effects:				
Climate migration[1]	22.32	34.00	9.18	20.46
Δ Real income pc (%)	-1.76	-1.01	-1.31	-1.41
ΔL_i^K (non–agric. employment, %)	-0.82	-0.54	-0.84	-0.76
Panel B - Country-level effects:				
Median Δ population[1]	0.06	0	0.01	-0.05
5th/95th deciles	[-2.8; 2.76]	[-4.18; 2.14]	[-0.9; 1.13]	[-2.69; 2.46]
Median Δ Real income pc (%)	-2.15	-1.68	-2.29	-2.37
5th/95th deciles	[-14.62; 3.27]	[-11.32; 4.69]	[-6.32; 3.69]	[-5.64; 3.35]
Median ΔL_i^K (%)	-1.42	-1.02	-0.11	-0.11
5th/95th deciles	[-5.36; 1.55]	[-4.03; 3.42]	[-5.32; 1.2]	[-3.04; 1.11]
Panel C - Welfare effects:[2]				
Δ Aggregate Welfare (%)	1.16	1.18	-2.12	-3.32
Median Δ Welfare (%)	-1.27	-0.54	-2.18	-2.85
5th/95th deciles	[-9.89; 0.95]	[-7.65; 1.81]	[-4.41; -0.41]	[-3.83; -0.07]

Notes: Column 1 presents to the baseline results, while columns 2 to 4 present the results of policy experiments in which frictions are equated to EU levels: in column 2, SSA adopts the migration policy of the EU; in column 3 it adopts the same level of tariffs as the EU, and in column 4 it combines both policies. [1]Climate migration in million individuals. [2]Results if using the alternative welfare measure of Equation (22). Aggregate stands for changes in all SSA, as in Panel A. Median and percentiles stand for the country-level distributional effects, as in Panel B.

6.2 Policy experiment - SSA as frictionless as the EU

One of the key takeaways from related literature is the magnifying role that spatial frictions have on welfare losses from climate change (Desmet et al., 2021; Conte et al., 2021; Bilal and Rossi-Hansberg, 2023; Cruz and Rossi-Hansberg, 2024). These studies show that relaxing these frictions increases the scope for economic adaptation through several margins, like sectoral specialization and migration. Yet, their findings reflect experiments on extreme scenarios (e.g., shutting down migration completely or homogeneously reducing frictions across the entire economy by an arbitrary value). Hence, while informative about the role of the underlying mechanisms, their results somehow lack realism if one thinks of policies to be implemented in the real world.[35]

I overcome this limitation with a realistic set of policy experiments that quantify

[35]Two exceptions are Nath (2023), who conducts policy experiments related to trade openess by reducing trade barriers to the bottom decile of the worldwide distribution, and Bryan and Morten (2019), whose experiments reduce mobility barriers in Indonesia to US levels.

Figure 8: Estimated trade and migration frictions in the European Union

Panel A: Tariff-like trade frictions τ_{ij}^F in the EU

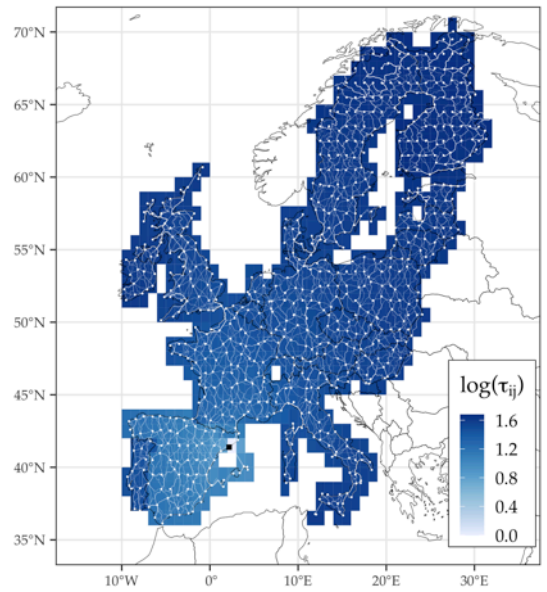

Panel B: Country migration barriers $\{m_c\}_c$ (in logs)

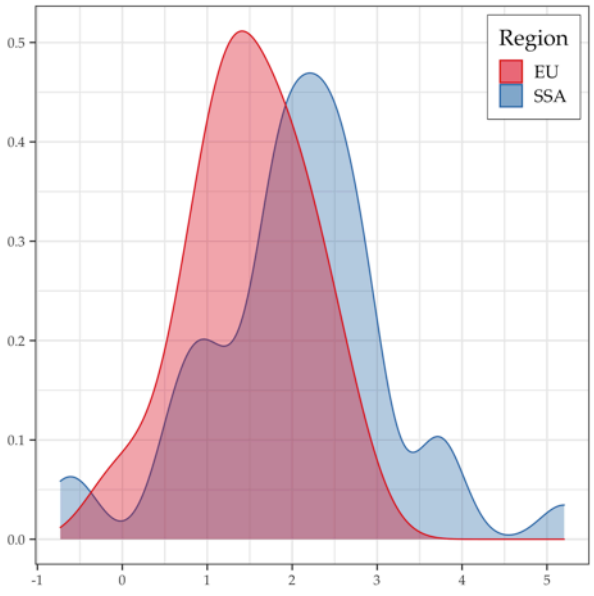

Notes: Panel A presents trade frictions in the EU as was done for SSA in Figure 5 (in this context, trade frictions are relative to Barcelona (Spain), represented by the black dot). Panel B plots the distribution of country migration barriers $\{m_c\}_c$ (in logs, x-axis) in SSA and the EU.

climate change effects in the hypothetical scenario where SSA migration and trade frictions drop to EU levels. Doing so requires quantifying migration and trade frictions in the EU within the structure of my model. I do that by mapping the country migration barriers $\{m_c\}_c$ and tariffs τ_{ij}^F onto EU migration and trade policies. Focusing on these parameters is particularly convenient because they reflect the institutional characteristics of the EU in terms of trade and migration policies. In other words, they are more tangible and realistic, as policy tools, than the elasticity parameters ϕ or δ.

In practice, I quantify $\{m_c\}_c$ and τ_{ij}^F by bringing the model to the EU data using the procedure described in Section 5.[36] The estimated EU frictions are substantially lower than those in the SSA. For trade, I estimate $\tau_{ij}^F = 2.60$, which is about a third of SSA's and remarkably close to estimates for the US ($\tau^F = 2.3$ from Antras et al., 2024). Figure 8 shows that: the discontinuity in bilateral frictions for cross-country trade is barely visible. It also shows that the estimated EU country migration barriers are much less stringent. The average $\{m_c\}_c$ is 63 percent lower than in the SSA case, and its distribution is shifted far more to the left (Panel B).

Armed with that, I perform counterfactual simulations that replace the migration

[36]This requires data for the same period and therefore the estimated values for the EU are also for 2000. Importantly, I focus on isolating the variation in the observed trade and migration flows within the EU. Thus, the values of the preference parameters and the bilateral elasticities δ and ϕ remain as described in Table 2. See Appendix B.12 for details.

and trade barriers with the EU values.[37] Table 3 Column 2 shows the results for migration policy only.[38] In this setting, aggregate climate migration flows increase by about 12 million individuals (52 percent), and aggregate welfare losses drop by half. The mechanism behind these welfare gains is the interaction between migration and sectoral specialization forces. Facing reduced mobility barriers, workers in affected areas can migrate to farther away, more productive regions, improving the efficiency of the SSA economy in terms of sectoral comparative advantage. In the climate change scenario, this means that agricultural production reallocates to the climate-change-benefitted regions, while non-agricultural production moves to the most developed countries in SSA. This efficiency gain increases real income in SSA and reduces the demand for agricultural goods and employment in that sector. Thus, migration allows SSA to benefit from the push aspect of climate change by permitting individuals to move out of unproductive rural regions and allowing the economy to go through a welfare-improving process of structural transformation.

Table 3 Panel B provides quantitative evidence of this result. The distribution of non-agricultural employment changes across countries shifts rightwards with lower mobility frictions, thus confirming that more countries specialize out of agriculture in this scenario. As such, my results corroborate the well-established potential of reducing migration barriers in rural economies (e.g., Bryan et al., 2014; Bryan and Morten, 2019; Lagakos et al., 2023), but in the context of adaptation to climate change.

Importantly, these aggregate gains hide a persistent inequality across countries: the country-level distribution of welfare changes remains as wide as in the baseline. That is, migration policy reduces aggregate welfare losses from climate change, but individuals left behind in the most affected regions remain as worse off as before. That happens because the policy does not imply that all individuals in affected regions can migrate away and, because of high trade frictions, they cannot adapt by locally changing production out of agriculture.[39] Hence, reducing migration barriers to EU levels poses a trade-off: it moderates aggregate welfare losses at the cost of high migration flows and regional inequality. Figure 9 Panel A documents this inequality aspect visually (and Panel B shows the same pattern if using alternative welfare measures, discussed in Section 6.3).

Next, I investigate the potential of trade policy to attenuate this trade-off. Reduc-

[37] These exercises reduce migration and/or trade frictions to the EU levels in the simulations with and without climate change. Thus, the comparison of the two isolates the climate change effect and shows how they compare with the baseline in the absence of these barriers. Section 6.3 discusses this further by disentangling level and relative effects of these policy experiments.

[38] I match the EU $\{m_c\}_c$ values to the SSA countries by deciles (i.e. scaling the barriers of the SSA countries to the value of their respective decile in the EU distribution). See Appendix B.12 for details.

[39] Note that this policy experiment unevenly changes migration barriers across countries (reducing barriers more for the strictest countries) but does not remove them completely.

Figure 9: Welfare effects of climate change for the baseline and different EU policies

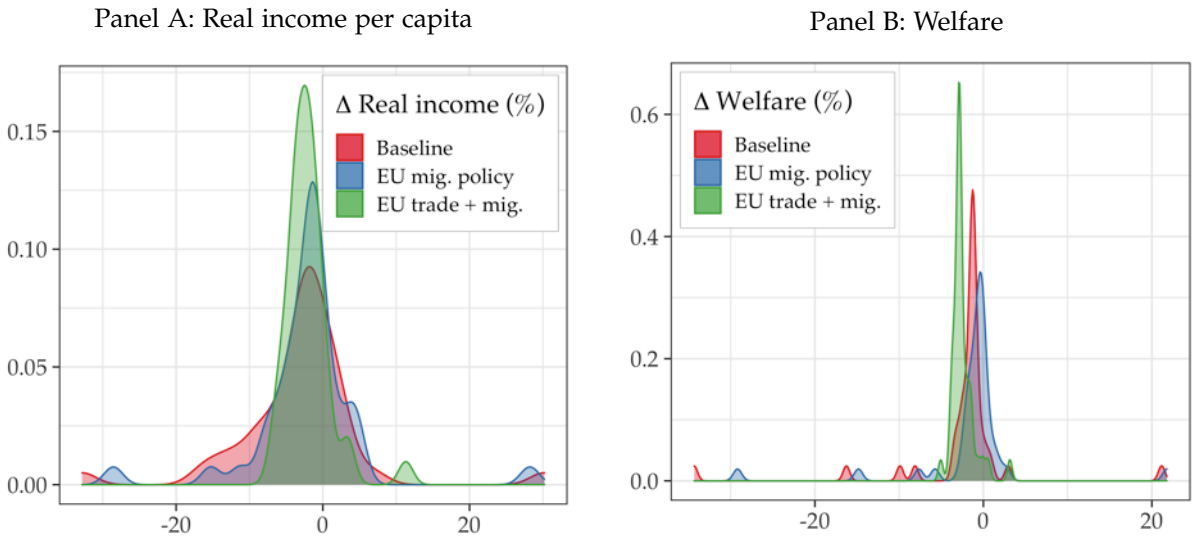

Notes: Panel A and B plot the country-level distributions of welfare in three different policy scenarios for SSA: baseline, EU migration policy, and EU trade and migration policy. Panel A refers to the baseline welfare measure (real income per capita). Panel B refers to an alternative welfare measure that also account for mobility barriers and congestion (see Section 6.3).

ing tariffs to EU levels halves aggregate climate migration and moderately reduces welfare losses (column 3). More importantly, it narrows the country-level distribution of welfare changes (Panel B). The underlying channel is the higher adaptive capacity through sectoral specialization, as seen in the rightward shift in the distribution of non-agricultural employment changes (i.e., the median sectoral employment changes centers at zero). Being able to adapt by switching out of agriculture reduces the need for migrating from affected areas and attenuates inequality on the climate change impacts. Thus, trade policy can be a powerful tool for a policymaker interested in reducing migration flows while attenuating the distributional impacts of climate change.

The implementation of both policies (column 4) provides combined results. In this setting, climate migration not only does not increase, but actually decreases (by about 9 percent). More importantly, while not as efficient when reducing aggregate losses, it drastically attenuates the inequality aspect of the baseline and migration policy settings. The distribution of welfare changes narrows, and the mass of countries experiencing substantial welfare losses drastically reduces (Figure 9). The policy relevance of this result cannot be overstated: by combining both tools, a policymaker can take advantage of climate change by enabling SSA to structurally change and adapt, through trade and migration, more efficiently and less unequally.

6.3 Alternative welfare measures

My main results use real income per capita (v_j/P_j) as the welfare measure. The advantage of this approach is to show the climate change impacts on spatial disparities in income, a pressing aspect in developing economies like SSA. However, it misses other components of utility considered in Equation (4), such as utility losses from costly migration and congestion and benefits from amenities. I account for those components with the alternative welfare measure

$$W_R = \sum_{j \in R} \omega_j \left(\sum_{i \in S} (v_j/P_j)^{\theta} \bar{m}_{ij}^{-\theta} u_j (L_j/H_j)^{-\beta} \right)^{1/\theta}, \tag{22}$$

where $\omega_j \equiv L_j / \sum_{j \in R} L_j$. Hence, W_R measures the per-capita-weighted average of the ex-ante expected welfare across all j locations of region R.

Starting with the baseline results of Table 3 Column 1, Panel C shows qualitatively similar results: small aggregate welfare changes and a highly dispersed and right-skewed distribution of country-level welfare changes. That is, few countries are better off at the expense of many worse-off countries. Importantly, the distributional welfare effects across different policy experiments (Columns 2 to 4) convey the same takeaways on the effects of (and trade-offs behind) migration and trade policies. Figure 9 Panel B provides further evidence of that, showing that, as before, trade policy attenuates the unequal climate change welfare effects in migration policy experiment.

However, a few aspects of the aggregate welfare effects need further discussion. The first is that, under the baseline counterfactual, climate change increases aggregate welfare. How can a spatially unequal shock that reduces aggregate income (Panel A) increase aggregate welfare? The answer lies in the high spatial correlation between positive climate change shocks and fundamental amenities and available land. Climate change pushes, in relative terms, more migrants towards locations with high amenities and abundant land (i.e., less congested), increasing aggregate welfare vis-à-vis the scenario without climate change. The same holds for the EU migration policy experiment (Column 2). Even though, it is worth stressing again that these small gains reflect a handful of better-off countries, while most of SSA is worse off.

A second intriguing aspect of Panel C relates to the role of trade policy: in columns 3 and 4, aggregate welfare losses increase in magnitude. This can suggest that relaxing trade barriers makes SSA worse off, which is not the case. To show that, Table 4 documents aggregate welfare in levels for different climate scenarios and policy schemes. Panel A shows that, with the EU trade policy, aggreagate welfare is about 70 larger than the baseline economy in the two scenarios (with and without climate change). Hence, what Table 3 Panel C shows is that their difference widens, and negatively so.

Table 4: Level and relative climate change effects in different counterfactuals

	(1) With climate change	(2) No climate change	(3) Climate change effect (%)
Panel A - Welfare W_R:			
Baseline	1.01	1.00	1.16
EU mig. policy	0.88	0.87	1.18
EU trade policy	1.65	1.69	-2.12
Both policies	1.84	1.90	-3.32
No mig. barriers ($\bar{m}_{ij} = 1$)	5.34	5.39	-0.89
Panel B - Real income per capita v_j/P_j:			
Baseline	0.98	1.00	-1.76
EU mig. policy	1.18	1.19	-1.01
EU trade policy	1.35	1.36	-1.31
Both policies	1.63	1.65	-1.41
No mig. barriers ($\bar{m}_{ij} = 1$)	1.32	1.32	-0.66

Notes: Columns 1 and 2 document the aggregate welfare and real income in levels normalized to the baseline, no climate change scenario. Column 3 refers to the percentage difference between 1 and 2.

The reason for this counterintuitive finding is congestion externalities. Because many benefitted regions are land-abundant, climate change pushes more individuals to less congested areas, reducing the utility losses from congestion. Reduced trade barriers attenuate this mechanism, as there are fewer incentives to adapt through migration. Because congestion is an externality that agents do not account for, they migrate less to these less congested areas. In other words, while lower trade barriers increase welfare, it does less so with climate change because of higher congestion.

The third intriguing finding relates to the level effects of migration policy alone. Panel A shows that, in that setting, aggregate welfare in SSA is about 12 percent lower than the baseline. How can a policy that reduces frictions (thus, utility penalties from migrating) diminish aggregate welfare? Again, the channel is congestion externalities. As Figure 8 Panel B shows, the EU migration policy exercise unevenly changes mobility borders, reducing the relative country barriers more drastically in the strictest countries. Hence, in both climate change scenarios, there is more population in these countries. This magnifies congestion, reducing aggregate welfare.

Importantly, this outcome depends on how much the congestion forces outweight the welfare gains from reduced mobility barriers. To illustrate that, Table 4 also documents the results for a (irrealistic) scenario without these barriers (i.e. $\bar{m}_{ij} = 1 \; \forall \; i, j$). Here, we see that the gains from having no utility penalties from migration vastly outweights congestion externalities, drastically increasing aggregate welfare. Finally,

Table 4 shows that combined policies always welfare dominate trade or migration policies separately implemented. Real income and welfare are both higher, corroborating the main policy recommendations from Section 6.2 in favor of an integrated approach that implements both policies.

6.4 Underlying channels, extensions, and robustness checks

In what follows, I check the robustness (or discuss the importance) of the previous results in several dimensions: the role of crop switching as an adptation mechanism, the addition of the rest of the world, the migration barriers, the climate change data used in the simulations, and various model's assumptions. Table 5 shows the main results and Appendix C provides further details.

Crop switching. To investigate the importance of the multi-crop feature of my framework, I perform a counterfactual exercise where I reduce γ_a by a half (i.e. where subsititution between crops in lower, and thus there is less room for crop switching). Table 5 Panel A shows that this setting magnifies the climate change effects: aggregate climate migration, welfare losses, and agricultural employment increase. This is explained by the heterogeneity of the expected crop yield changes within locations (Figure 2). Affected producers can, in a multi-crop setting, reallocate agricultural production to the less-affected crop (and less so if crops are not substitutes). Hence, disregarding crop switching (as in, for instance, Nath, 2023; Cruz, 2023) overestimates the impact of climate change on agricultural productivity, amplifying incentives to migrate and the necessity for the economy to allocate, on aggregate, more labor into agriculture. Thus, accounting for this margin is key in correctly predicting the impact of climate change on subsistence rural economies like those in SSA.

Country migration barriers. I also check the sensitivity of my baseline results to potential changes in country barriers over time. There are two reasons for that. First, the time frame of migration choices in my setting is of about a decade, whereas the time interval of my counterfactuals is of almost a century (during which agents could become less sensitive to the decade-specific migration barriers). Second, restrictive countries could become even stricter to foreign migrants over time. I account for these two potential patterns by increasing or decreasing $\{m_c\}_c$ (results in Table 5 Panel B).[40] The results change as expected. I also check how the results change in the complete absence of bilateral barriers ($\bar{m}_{ij} = 1$) and estimate similar values to related studies that disregard these barriers (e.g., 90 million migrants from Rigaud et al., 2018).

[40] In particular, I alter the distribution of country barriers with $(m_c)^\iota$, where ι is 1.25 (0.75) in the increasing (decreasing) case. I choose the monotonic transformation (instead of scaling them up or down) because the barriers $\{m_c\}_c$ matter in the location choice (Equation (18)) up-to-scale.

Rest of the world. I introduce trade and migration with the rest of the world (ROW) by augmenting my setting with an additional R representative location.[41] Table 5 Panel C documents the aggreate results of several climate change simulations under this setting.[42] Starting with an analogous baseline exercise but with the ROW, I find that the interaction with the ROW increases remarkably climate migration and welfare losses from climate change. That happens because now SSA increases crop imports from the ROW and switches specialization as a response to the agricultural losses. In fact, the changes in aggregate and median non-agricultural employment are close to zero, and most of migrations sort into non-agricultural regions.

Moreover, removing mobility barriers with the ROW ($m_R = 1$) decreases aggregate migration within SSA, but increases flows towards the ROW (documented in Table C.1). Welfare losses remarkably diminish in this setting. Moreover, removing tariffs between SSA and the ROW (τ^R) amplifies the capacity of crop imports as adaptation (as in Nath, 2023). In this setting, there are major migration flows to highly productive regions (and countries) in non-agriculture that acquire crops through imports and specialize in non-agriculture. In fact, almost all SSA countries have now higher non-agricultural employment, as seen in the changes in non-agricultural employment. Combining both policies magnifies these effects and remarkably attenuate the climate change effects in SSA. That is, opennes to the rest of the world is an additional tool for SSA policymakers when addressing these future effects.

Homothetic preferences. I also show that the nonhomotheticity feature of the preferences for agricultural goods and non-agricultural goods is a key driver of climate change's welfare consequences. Table 5 Panel D shows the results of a counterfactual that assumes homothetic preferences (see Appendix C.2 for details). There is almost no aggregate climate migration in this framework, and the welfare losses are dramatically centered around zero. This occurs because, by disregarding the subsistence aspect of agricultural goods, agents replace agricultural goods with non-agricultural goods. This intensifies the patterns of sectoral specialization (i.e. more production and consumption of non-agricultural goods takes place in the most affected regions), increasing non-agricultural employment on aggregate and distributional terms.

Endogenous fertility. I perform a simple exercise that illustrates how the results change if fertility is allowed to be endogenous to climate change. To do so, I adjust the estimates for population growth taken from the Population Prospects of United Nations and Social Affairs (2019) using a damage function that depends on the average

[41] I introduce R as a representative location whose fundamentals and observed economic outcomes are aggregates of the ROW (e.g., land endowments, population, income, migration flows). Appendix C.1 elaborates on that and documents the quantification method for this setting.

[42] The climate migration reported in Table 5 stand only for migration within SSA. Table C.1 documents detailed results in this setting, such as migration to the ROW and distributional effects.

Table 5: Robustness of the benchmark results with respect to trade and migration frictions, model assumptions, and climate change scenarios

	(1) Climate migration (million individuals)	(2) Δ Real income per capita (%)	(3) Δ Non–agricultural employment (%)
Baseline results	22.32 [0.06]	-1.76 [-2.15]	-0.82 [-1.42]
Panel A: Role of crop switching			
Less crop switching (lower γ_a)	27.36 [0.02]	-1.88 [-2.94]	-1.04 [-1.62]
Panel B: Robustness to country barriers			
Higher country barriers m_c	16.93 [0.04]	-2.07 [-2.2]	-0.88 [-1.52]
Lower country barriers m_c	27.85 [0.03]	-1.54 [-2]	-0.7 [-1.23]
No migration costs ($\bar{m}_{ij} = 1$)	79.95 [-0.16]	-0.66 [-0.93]	-1.28 [-0.56]
Panel C: Adding the rest of the world (ROW)			
Baseline with ROW	123.48 [0.31]	-19.05 [-18.49]	-0.09 [-0.01]
ROW + no m_R barriers	111.08 [-1.13]	-4.76 [-3.75]	-0.14 [-0.01]
ROW + no tariffs τ_R	87.8 [0.22]	-1.37 [-1.91]	2.46 [0.45]
ROW + no m_R and τ_R	89.3 [-0.1]	-0.78 [-1.19]	2.53 [0.38]
Panel D: Robustness to model assumptions			
Homothetic preferences	1.78 [0]	-0.21 [-0.29]	0.68 [0.49]
Endogenous fertility	21.6 [0.05]	-1.75 [-2.14]	-0.82 [-1.42]
Non-agricultural prod. growth	22.23 [0.06]	-2 [-2.26]	-0.87 [-1.54]
Modern inputs in agriculture	20.95 [0.07]	-1.95 [-1.93]	-0.83 [-1.47]
Panel E: Robustness to CΔ damages or scenarios			
CΔ damages to non-agriculture	22.2 [0.06]	-1.76 [-2.15]	-0.81 [-1.42]
CΔ damages to amenities	22.31 [0.06]	-1.75 [-2.15]	-0.81 [-1.42]
RCP 4.5 CΔ scenario	10.27 [0.01]	-0.94 [-0.66]	-0.37 [-0.59]

Notes: Each panel presents the aggregate climate change effects in terms of climate migration, real income per capita changes, and sectoral employment changes. Square brackets document median effects. Panel A refers to a simulation that assumes lower room for crop switching. Panel B documents the results of various simulations assuming different evolution of migration barriers. Panel C describe the results of an extension that accounts for trade and migration with the rest of the world (ROW). Panel D refers to simulations (separately) assuming homothetic preferences between agriculture and non-agriculture, endogenous fertility, and productivity growth. Panel E shows the results of simulation that assume additional types of climate damages or a less severe climate change scenario.

change in potential crop yields.[43] This reduces the initial population $\mathcal{L}$ assumed in the counterfactuals for 2080, particularly in the most affected countries. Table 5 Panel D shows that the baseline results are unresponsive to this dimension: aggregate climate

[43]In particular, I assume that the rate of net population growth changes by 50 percent of the change in average potential yield in each location. Appendix C.3 provides further details and documents additional results with alternative scaling rules. Importantly, I adopt this approach for simplicity, rather than the more realistic approaches in the literature (Delventhal et al., 2024; Cruz and Rossi-Hansberg, 2024), due to the static feature of my model.

migration and related effects remain around the same magnitude.

Economic growth. I also allow the non-agricultural sector to grow by increasing sector K's TFP over time (using each i's average country growth in the first decades of the century). Panel D shows that the results remain qualitatively robust to this extension. This happens because the quantified $\{b_i^K A_i^K\}_i$ has remarkable spatial differences in levels. Thus, even if accounting for uneven growth across countries, the results remain unaffected.[44] Likewise, I allow for productivity growth in agriculture with information from GAEZ. I retrieve the increase in crop suitabilities $\{A_i^k\}_{i,k\neq K}$ if moving from production techinique from subisistence methods (the baseline) to high usage of modern inputs (see Figure A.1). For the same reason as in the non-agricultural sector, that does not affect profoundly the spatial distribution of these fundamentals, and so the aggregate results under this scenario.

Climate damage to non-agriculture. My baseline counterfactual assumes no effects of climate change on the non-agricultural sector. The advantage of that is isolating the consequences of the effects on agriculture, the most relevant push factor of migration for subsistence rural economies like SSA. However, I also check how the results change if allowing the K^{th} sector to be also affected. To do that, I scale the quantified productivities of that sector by the equivalent sectoral damage function from Conte et al. (2021).[45] Table 5 Panel E shows that the baseline results remain unchanged if so, for the same reason if allowing for economic growth (see footnote 44).

Climate damage on amenities. Analogously, the baseline counterfactuals assume that amenities $\{u_i\}_i$ remain constant and unaffected by climate change. I relax this assumption using the damage function of temperature on amenities by Cruz and Rossi-Hansberg (2024).[46] The baseline results remain robust (Table 5 Panel E) due to the large spatial dispersion of the quantified amenities.[47]

Assumption of climate change scenario. I also check the sensitivity of the results to the severity of the underlying climate change scenario, by switching to the RCP 4.5 scenario (which assumes that carbon emissions will peak by mid-century and decrease thereafter). I simulate the model with the suitability data for this scenario (Table 5 Panel C). As expected, all climate change effects are attenuated in this setting.

[44] Specifically, the observed real income differences (in levels) across SSA are remarkably high, yielding level $\{b_i^K A_i^K\}_i$ differences across locations in the order of thousands or more. Hence, allowing for uneven, country-level growth does not affect drastically its distribution, which explains the little sensitivity of my results to this extension. Appendix C.4 discusses that in detail.

[45] The damage function depends on the deviations from the optimal temperature for the non-agricultural sector. Thus, to conduct this experiment, I also use the forecasts of temperature for 2080 from Conte et al. (2021) and match them to the locations of SSA. See Appendix C.5 for details.

[46] I use their estimated $\Lambda^b(T_i)$ damage function for the global economy; see Appendix C.6 for details.

[47] Analogously to the above (footnote 44), this is due to the large observed real income differences across space that map into large level differences in $\{u_i\}_i$ across locations. See Appendix C.6 for details.

Endogenous climate and dynamics. The static nature of my model excludes, naturally, dynamic mechanisms such as climate-economy feedback (as in Cruz and Rossi-Hansberg, 2024) and forward-looking agents (like Balboni, 2021; Kleinman et al., 2023). The reason for the former is that Africa emits about 3 percent of global emissions, which makes it reasonable to assume exogenous climate change. The reason for the latter are data and tractability constraints. First, the GAEZ data provides estimates for specific points in time, rather than a time-varying function to feed a dynamic setting. Besides, and more importantly, characterizing transition dynamics in my highly ganular, multisector ($K = 7$ and $N > 2000$) setting augmented with forward looking agents would not be feasible with the standard "dynamic hat algebra" approach (Caliendo et al., 2019), and would require ignoring second-order effects (as in Bilal and Rossi-Hansberg, 2023; Bilal, 2023), which might not be ideal in the SSA setting.

Sectoral frictions and home bias. Because of data limitations, my framework refrains from additional frictions to sectoral reallocation of factors and home biased preferences. If accounting for them, my results would be magnified. For instance, if allowing for frictions on sectoral reallocation of labor (as in Cruz, 2023) or land (as in Chen et al., 2023), the climate change effects on the food-problem and welfare losses would be further magnified. The same would hold if allowing preferences to be home biased, because trade attenuates to a large extent the welfare losses that I identify.

7 Conclusion

The main message of this paper is that climate change must not lead to bad outcomes if rural economies like SSA can adapt to it. If mobility barriers can be reduced, climate change can encourage the shift of population out of poor, low-productivity rural locations and set off a process of structural change. Openness to trade determines the aggregate and distributional welfare effects of this process, by allowing affected economies to switch production to less-affected sectors. The interaction of these – and other – mechanisms in general equilibrium is complex and interconnected. I model that with a transparent framework that I develop and connect to SSA data.

I identify that a high degree of frictions in SSA that inhibit the welfare-improving process just described. My estimates suggest sizeable welfare losses and migration flows in many orders of magnitude smaller than reduced-form estimates from the literature. However, a policy experiment shows that, by becoming as frictionless as the EU, SSA adaptation to climate change would moderate welfare losses both in aggregate and distributional terms. My climate migration estimates when relaxing migration frictions approach those from other studies that disregard these barriers.

My results deliver important contributions to the literature and the policy debates.

I connect the findings from the literature on the gains from incentivizing migration in developing economies with those from the literature on the importance of sectoral specialization and trade in adapting to climate change. I also deliver a policy-relevant message on the potential role of real-world trade and migration policies in adapting to climate change.

References

Abel, Guy J and Joel E Cohen, "Bilateral international migration flow estimates for 200 countries," *Scientific data*, 2019, *6* (1), 1–13.

Allen, Treb, "Information frictions in trade," *Econometrica*, 2014, *82* (6), 2041–2083.

_ **and Costas Arkolakis**, "Trade and the Topography of the Spatial Economy," *The Quarterly Journal of Economics*, 2014, *129* (3), 1085–1140.

_ **and Dave Donaldson**, "Persistence and path dependence in the spatial economy," 2022.

Antras, Pol, Teresa Fort, Agustín Gutiérrez, and Felix Tintelnot, "Trade Policy and Global Sourcing: A Rationale for Tariff Escalation," *Journal of Political Economy Macroeconomics, vol 2, no. 1, pp. 1-44.*, 2024. revise and resubmit, Journal of Political Economy Macroeconomics.

Asturias, Jose, Manuel García-Santana, and Roberto Ramos, "Competition and the welfare gains from transportation infrastructure: Evidence from the Golden Quadrilateral of India," *Journal of the European Economic Association*, 2019, *17* (6), 1881–1940.

Atkin, David and Dave Donaldson, "Who's getting globalized? The size and implications of intra-national trade costs," Technical Report, National Bureau of Economic Research 2015.

_ **, Arnaud Costinot, and Masao Fukui**, "Globalization and the Ladder of Development: Pushed to the Top or Held at the Bottom?," Technical Report, National Bureau of Economic Research 2021.

Balboni, Clare Alexandra, "In Harm's Way? Infrastructure Investments and the Persistence of Coastal Cities," 2021.

Benveniste, Hélène, Michael Oppenheimer, and Marc Fleurbaey, "Effect of border policy on exposure and vulnerability to climate change," *Proceedings of the National Academy of Sciences*, 2020, *117* (43), 26692–26702.

Bernard, Andrew B, Jonathan Eaton, J Bradford Jensen, and Samuel Kortum, "Plants and productivity in international trade," *American economic review*, 2003, *93* (4), 1268–1290.

Bilal, Adrien, "Solving heterogeneous agent models with the master equation," Technical Report, National Bureau of Economic Research 2023.

_ **and Esteban Rossi-Hansberg**, "Anticipating Climate Change Across the United States," Working Paper 31323, National Bureau of Economic Research June 2023.

Borchert, Ingo, Mario Larch, Serge Shikher, and Yoto V Yotov, "The international trade and production database for estimation (ITPD-E)," *International Economics*, 2021, *166*, 140–166.

Bryan, Gharad and Melanie Morten, "The aggregate productivity effects of internal migration: Evidence from Indonesia," *Journal of Political Economy*, 2019, *127* (5), 2229–2268.

_ **, Shyamal Chowdhury, and Ahmed Mushfiq Mobarak**, "Underinvestment in a profitable technology: The case of seasonal migration in Bangladesh," *Econometrica*, 2014, *82* (5), 1671–1748.

Burzyński, Michał, Christoph Deuster, Frédéric Docquier, and Jaime De Melo, "Climate Change, Inequality, and Human Migration," *Journal of the European Economic Association*, 2022, *20* (3), 1145–1197.

Caliendo, Lorenzo, Maximiliano Dvorkin, and Fernando Parro, "Trade and labor market dynamics: General equilibrium analysis of the china trade shock," *Econometrica*, 2019, *87* (3), 741–835.

Carleton, Tamma, Amir Jina, Michael Delgado, Michael Greenstone, Trevor Houser, Solomon Hsiang, Andrew Hultgren, Robert E Kopp, Kelly E McCusker, Ishan Nath et al., "Valuing the global mortality consequences of climate change accounting for adaptation costs and benefits," *The Quarterly Journal of Economics*, 2022, *137* (4), 2037–2105.

Castells-Quintana, David, Melanie Krause, and Thomas KJ McDermott, "The urbanising force of global warming: the role of climate change in the spatial distribution of population," *Journal of Economic Geography*, 2021, *21* (4), 531–556.

Castro-Vincenzi, Juanma, Gaurav Khanna, Nicolas Morales, and Nitya Pandalai-Nayar, "Weathering the Storm: Supply Chains and Climate Risk," Technical Report, National Bureau of Economic Research 2024.

Chen, Chaoran, Diego Restuccia, and Raül Santaeulàlia-Llopis, "Land misallocation and productivity," *American Economic Journal: Macroeconomics*, 2023, *15* (2), 441–465.

CIESIN, "Global roads open access data set, version 1 (gROADSv1)," *Palisades, NY: NASA Socioeconomic Data and Applications Center (SEDAC)*, 2013.

Colmer, Jonathan, Dajun Lin, Siying Liu, and Jay Shimshack, "Why are pollution damages lower in developed countries? Insights from high-Income, high-particulate matter Hong Kong," *Journal of Health Economics*, 2021, *79*, 102511.

Comin, Diego, Danial Lashkari, and Martí Mestieri, "Structural change with long-run income and price effects," *Econometrica*, 2021, *89* (1), 311–374.

Conte, Bruno, Klaus Desmet, Dávid Krisztián Nagy, and Esteban Rossi-Hansberg, "Local sectoral specialization in a warming world," *Journal of Economic Geography*, 2021, *21* (4), 493–530.

Costinot, Arnaud, Dave Donaldson, and Cory Smith, "Evolving comparative advantage and the impact of climate change in agricultural markets: Evidence from 1.7 million fields around the world," *Journal of Political Economy*, 2016, *124* (1), 205–248.

Cruz, Jose Luis, "Global Warming and Labor Market Reallocation," 2023.

Cruz, José-Luis and Esteban Rossi-Hansberg, "The economic geography of global warming," *Review of Economic Studies*, 2024, *91* (2), 899–939.

Currie, Janet, John Voorheis, and Reed Walker, "What caused racial disparities in particulate exposure to fall? New evidence from the Clean Air Act and satellite-based measures of air quality," *American Economic Review*, 2023, *113* (1), 71–97.

Delventhal, Matthew J, Jesús Fernández-Villaverde, and Nezih Guner, "Demographic transitions across time and space," Technical Report 2024.

Desmet, Klaus and Esteban Rossi-Hansberg, "On the spatial economic impact of global warming," *Journal of Urban Economics*, 2015, *88*, 16–37.

_ and _ , "Climate Change Economics over Time and Space," 2023.

_ , Dávid Krisztián Nagy, and Esteban Rossi-Hansberg, "The geography of development," *Journal of Political Economy*, 2018, *126* (3), 903–983.

_ , Robert E. Kopp, Scott A. Kulp, Dávid Krisztián Nagy, Michael Oppenheimer, Esteban Rossi-Hansberg, and Benjamin H. Strauss, "Evaluating the Economic Cost of Coastal Flooding," *American Economic Journal: Macroeconomics*, April 2021, *13* (2), 444–86.

Dominguez-Iino, Tomas, "Efficiency and redistribution in environmental policy: An equilibrium analysis of agricultural supply chains," 2023.

Donaldson, Dave, "Railroads of the Raj: Estimating the impact of transportation infrastructure," *American Economic Review*, 2018, *108* (4-5), 899–934.

Eaton, Jonathan and Samuel Kortum, "Technology, geography, and trade," *Econometrica*, 2002, *70* (5), 1741–1779.

Eckert, Fabian and Michael Peters, "Spatial structural change," Technical Report, National Bureau of Economic Research 2022.

Fajgelbaum, Pablo and Stephen J Redding, "Trade, Structural Transformation, and Development: Evidence from Argentina 1869–1914," *Journal of Political Economy*, 2022, *130* (5), 1249–1318.

Farrokhi, Farid and Ahmad Lashkaripour, "Can trade policy mitigate climate change," *Unpublished Working Paper*, 2024.

_ **and Heitor S Pellegrina**, "Trade, technology, and agricultural productivity," *Journal of Political Economy*, 2023, *131* (9), 2509–2555.

_ **, Elliot Kang, Heitor S Pellegrina, and Sebastian Sotelo**, "Deforestation: A global and dynamic perspective," Technical Report 2024.

Florczyk, AJ, C Corbane, D Ehrlich, S Freire, T Kemper, L Maffenini, M Melchiorri, M Pesaresi, P Politis, M Schiavina et al., "GHSL Data Package 2019," *Luxembourg. EUR*, 2019, *29788*.

Gollin, Douglas, Stephen L Parente, and Richard Rogerson, "The food problem and the evolution of international income levels," *Journal of Monetary Economics*, 2007, *54* (4), 1230–1255.

Henderson, J Vernon, Adam Storeygard, and Uwe Deichmann, "Has climate change driven urbanization in Africa?," *Journal of development economics*, 2017, *124*, 60–82.

Herrendorf, Berthold, Richard Rogerson, and Akos Valentinyi, "Growth and structural transformation," *Handbook of economic growth*, 2014, *2*, 855–941.

Hsiao, Allan, "Coordination and Commitment in International Climate Action: Evidence from Palm Oil," Technical Report 2022.

_ , "Sea Level Rise and Urban Inequality," *AEA Papers and Proceedings*, 2024. Forthcoming.

IIASA and FAO, "Global Agro-Ecological Zones (GAEZ v3. 0)," 2012.

Imbert, Clément, Joan Monras, Marlon Seror, and Yanos Zylberberg, "Floating population: migration with (out) family and the spatial distribution of economic activity," 2023.

IPCC, "IPCC Special Report," 2000.

_ , *Managing the risks of extreme events and disasters to advance climate change adaptation: special report of the intergovernmental panel on climate change*, Cambridge University Press, 2012.

IPUMS, "Integrated Public Use Microdata Series, International: Version 7.3 [dataset]," Technical Report, Minnesota Population Center, Minneapolis, MN: IPUMS 2020.

Jia, Ruixue, Xiao Ma, and Victoria Wenxin Xie, "Expecting floods: Firm entry, employment, and aggregate implications," Technical Report, National Bureau of Economic Research 2022.

Kleinman, Benny, Ernest Liu, and Stephen J Redding, "Dynamic spatial general equilibrium," *Econometrica*, 2023, *91* (2), 385–424.

Lagakos, David, Ahmed Mushfiq Mobarak, and Michael E Waugh, "The welfare effects of encouraging rural–urban migration," *Econometrica*, 2023, *91* (3), 803–837.

Lustgarten, Abrahm, "The Great Climate Migration Has Begun," *The New York Times*, Jun 2020.

Meghir, Costas, A Mushfiq Mobarak, Corina Mommaerts, and Melanie Morten, "Migration and informal insurance: Evidence from a randomized controlled trial and a structural model," *The Review of Economic Studies*, 2022, *89* (1), 452–480.

Moneke, Niclas, "Can big push infrastructure unlock development? evidence from ethiopia," *STEG Theme*, 2020, *3*, 14–15.

Morten, Melanie, "Temporary migration and endogenous risk sharing in village India," *Journal of Political Economy*, 2019, *127* (1), 1–46.

_ **and Jaqueline Oliveira**, "The Effects of Roads on Trade and Migration: Evidence from a Planned Capital City," *American Economic Journal: Applied Economics*, 2024. Forthcoming.

Nagy, Dávid Krisztián, "Hinterlands, city formation and growth: Evidence from the US westward expansion," *Review of Economic Studies*, 2023, *90* (6), 3238–3281.

Nath, Ishan B, "The Food Problem and the Aggregate Productivity Consequences of Climate Change," Technical Report 2023.

Nordhaus, William, Qazi Azam, David Corderi, Kyle Hood, Nadejda Makarova Victor, Mukhtar Mohammed, Alexandra Miltner, and Jyldyz Weiss, "The G-Econ database on gridded output: methods and data," *Yale University, New Haven*, 2006, *6*.

of Economic United Nations, Department and Population Division Social Affairs, "World Population Prospects 2019: Highlights," 2019.

Pellegrina, Heitor S, "Trade, productivity, and the spatial organization of agriculture: Evidence from Brazil," *Journal of Development Economics*, 2022, p. 102816.

_ **and Sebastian Sotelo**, "Migration, Specialization, and Trade: Evidence from Brazil's March to the West," *Journal of Political Economy*, 2024. Forthcoming.

Peri, Giovanni and Akira Sasahara, "The impact of global warming on rural-Urban migrations: Evidence from global big data," Technical Report, National Bureau of Economic Research 2019.

Porteous, Obie, "High trade costs and their consequences: An estimated dynamic model of African agricultural storage and trade," *American Economic Journal: Applied Economics*, 2019, *11* (4), 327–66.

_ , "Agricultural Trade and Adaptation to Climate Change in Sub-Saharan Africa," Technical Report 2024.

Rigaud, KK, B Jones, J Bergmann, V Clement, K Ober, J Schewe, S Adamo, B McCusker, S Heuser, and A Midgley, "Groundswell: Preparing for Internal Climate Migration (Washington, DC: World Bank)," 2018.

Rudik, Ivan, Gary Lyn, Weiliang Tan, and Ariel Ortiz-Bobea, "The Economic Effects of Climate Change in Dynamic Spatial Equilibrium," 2021.

Shapiro, Joseph S, "Trade costs, CO2, and the environment," *American Economic Journal: Economic Policy*, 2016, *8* (4), 220–254.

_ , "The environmental bias of trade policy," *The Quarterly Journal of Economics*, 2021, *136* (2), 831–886.

Sotelo, Sebastian, "Domestic trade frictions and agriculture," *Journal of Political Economy*, 2020, *128* (7), 2690–2738.

Veronese, N and H Tyrman, "MEDSTATII: Asymmetry in Foreign Trade Statistics in Mediterranean Partner Countries," Technical Report, Eurostat Methodologies Working Papers 2009.

Weiss, D, A Nelson, HS Gibson, W Temperley, S Peedell, A Lieber, M Hancher, E Poyart, S Belchior, N Fullman et al., "A global map of travel time to cities to assess inequalities in accessibility in 2015," *Nature*, 2018, *553* (7688), 333.

Appendix

Appendix A provides more details about the data sources mentioned in Section 2 and other data sources not mentioned therein. Appendix B documents theoretical derivations that support the main results of Section 4. Appendix C describe alternative models used in the robustness. Appendix D contains additional figures and tables.

A Data Appendix

Table A.1 below documents all data sources used and their temporal coverage. Next, I provide further detail on the data choices and aggregation.

Table A.1: Main data sources

Type of data	Coverage	Source
GDP and Population	2000	G-Econ Project v4.0 (Nordhaus et al., 2006)
Population	1975, 2000	Global Human Settlements Project (Florczyk et al., 2019)
Population projections	2021 – 2100	United Nations and Social Affairs (2019)
Agric. Productivities	1960–2000	GAEZ v3.0 (IIASA and FAO, 2012)
Climate Δ projections	2020, 2050, 2080	GAEZ v3.0 (IIASA and FAO, 2012)
Transportation data	2000	gROADS project (CIESIN, 2013)
Friction transportation surface	2000	Accessibility to Cities' project (Weiss et al., 2018)
Bilateral crop international trade	1995–2005	ITPD-E (Borchert et al., 2021)
Bilateral international migration	1990–2000	Abel and Cohen (2019)
Bilateral internal migration	1970–2015	Census data from IPUMS (2020)
Crop prices	1990–2015	VAM project, World Food Program

GAEZ agro-climatic yields. The GAEZ's database provides estimates of agricultural potential yields for several crops, in different time periods, and for different degrees of technology usage in agriculture. As my interest in subsistence agriculture setup of SSA, I aim at building a time varying dataset of potential yields over the entire subcontinent, for several crops, at low usage of modern inputs: with rainfed water access, labor intensive techniques, and no application of of nutrients, no use of chemicals for pest and disease control and minimum conservation measures.

A challenge, however, is that the time varying potential yields from GAEZ are available only for high usage of modern inputs (based on improved high yielding varieties, fully mechanized with low labor intensity techniques, and usage of optimum applications of nutrients and chemical pest, disease and weed control). The estimates for different input levels are only available for the long-run estimates (averages between 1960-1990).

Figure A.1: Yield gains from adoption of high inputs in agriculture vis-à-vis low inputs for selected crops.

Panel A: High input gains for rice

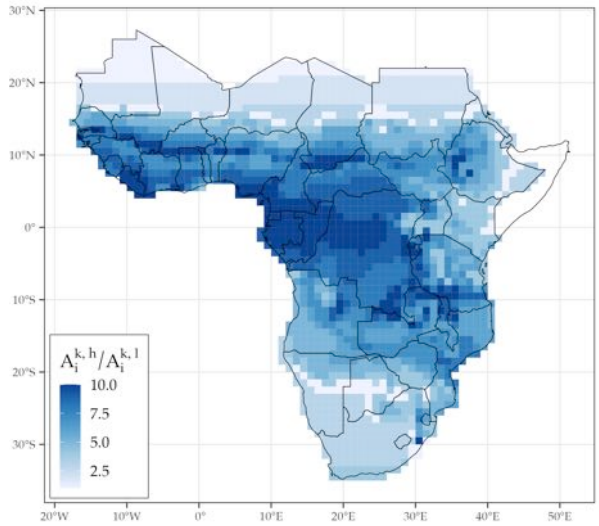

Panel B: High input gains for sorghum

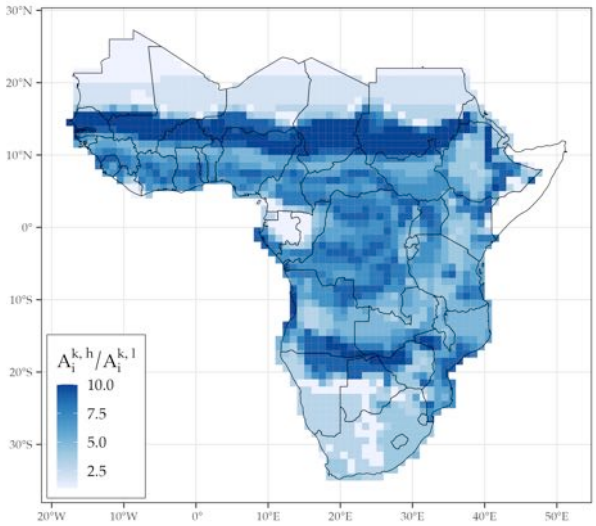

Notes: Panels A and B show the ratio of high/low input usage yields for growing two selected crops according to GAEZ long-run estimates. The values are shown in deciles; 1 (10) stands for the bottom (top) decile of each sample.

Therefore, to obtain a time varying dataset of the agro-climatic yields at low input usage, I first use the long-run values to calculate the GAEZ-implied ratio between high inputs $(A_i^{k,h})$ / low inputs $(A_i^{k,l})$ yields for each crop. This procedures reveals how the gains from adopting higher input levels differ across locations and crops – Figure A.1 illustrates the results for two selected crops in deciles. I use the calculated ratios to scale down the time varying estimates for high inputs that I collect.

Armed with the location-crop technology scales, I collect the time varying estimates of agro-climatic yields for high input usage. For the estimates in the past, retrieve those for 1971-1975 and 1996-2000. I average out the 5 years' blocks so to avoid year-specific outliers. The reason is to capture long term changes, which could be contaminated if a certain year faces unusual climate conditions.

The yield estimates for future periods require another parametrical selection: the underlying scenario for which the data is produced and with which climatic (general circulation) model (GCM) the data is produced. As carefully discussed by Costinot et al. (2016), the GAEZ v3.0 database provides such estimates produced with four main GCM, and for several future scenarios. The latter is of key importance: it contains the underlying assumption on how the global carbon emissions are going to evolve in the future so to produce the changes in the climate.

I choose the scenario A1 from the GAEZ database, which is the baseline scenario of Costinot et al. (2016) that matches closely the current standard of severe evolution

Figure A.2: Equivalence between long and longer-run estimates of radiative forcing (proportional to carbon emissions) between SRES and RCP scenarios.

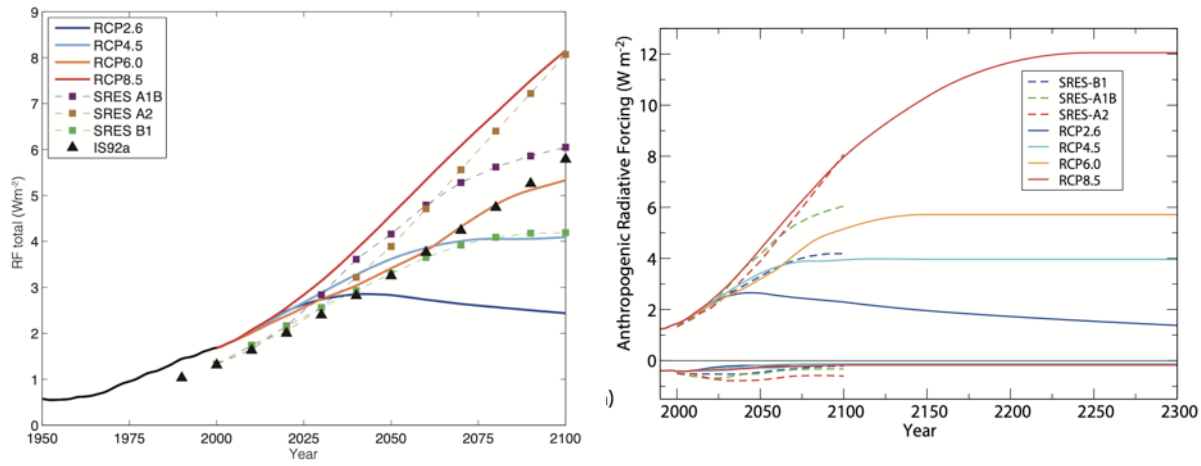

Source: IPCC (2012), chapter 1, Figure 1.15 (left) and Chapter 12, Figure 12.3 (right).

of the global climate for the future: the RCP 8.5.[48] This scenario assumes a steady increase in carbon stocks in the atmosphere througout the 21st and 22nd centuries, becoming stable by mid-23rd century. A milder scenario that I use for my robustness checks is the B1, which is similar to the nowadays-standard RCP 4.5. It assumes that the global stock of carbon will peak by late 21st century, becoming stable thereafter.

Agricultural production data. To build a dataset for agricultural production at the location-crop level for 2000, I combine the GAEZ data of production (in tonnes) with the FAOSTAT agricultural production data (country-crop level) and World Bank country GDP data (both in current US$). First, I use the GAEZ data at the cell-crop level to calculate the share that each cell is observed to produce, of each crop, over its country's total production. Second, I obtain with the FAOSTAT and WB data the share of each country crop production for the years of 2000 to 2010. I average out such shares and multiply them by the country GDP implied by the G-Econ data, so that the unit is consistent with the monetary unit of the model (US$ PPP). Finally, I multiply the country-crop PPP values by the location-crop shares. For very few locations, the outcome exceeds their total GDP: I then trim the value by 99.99% of its GDP.

Crop price data. The Vulnerability and Assessment Program from the WFP (WFP-VAM) has been collecting prices at various markets (locations within cities) across the developing world since the early 1990s at the monthly basis; I retrieved the prices for all SSA markets from the earliest dates to early 2019. When doing so, I focus on

[48]The GAEZ v3.0 forecasts are based on the Special Report on Emission Scenarios (SRES; see IPCC, 2000). The SRE Scenarios were later updated by IPCC as the RCP scenarios, which are now the standards in the climate community (IPCC, 2012). Figure A.2 illustrates the equivalence between the SRES and RCP scenarios.

Table A.2: Summary statistics of the WFP-VAM price data

	Obs.	Mean	St. Dev.	Min	Pctl(25)	Median	Pctl(75)	Max
All Sample								
Year	173,101	2,012.006	4.578	1,992	2,009	2,013	2,016	2,019
Maize	173,101	0.376	0.484	0	0	0	1	1
Millet	173,101	0.216	0.411	0	0	0	0	1
Sorghum	173,101	0.218	0.413	0	0	0	0	1
Rice	173,101	0.191	0.393	0	0	0	0	1
Market-Crop								
Lenght of Series	2,516	68.800	60.627	1	20.8	53	107	329
Min(Year)	2,516	2,010.331	4.824	1,992	2,007	2,011	2,014	2,018
Max(Year)	2,516	2,016.914	2.070	2,006	2,016	2,018	2,018	2,019
Average crop price (USD)	2,516	0.437	0.243	0.035	0.284	0.377	0.541	2.244
Market								
# Crops	978	2.573	0.940	1	2	2	3	4
Country								
Number of Markets	31	31.548	23.511	1	13.5	25	46	87

maize, millet, sorghum, and rice (the set of crops with the largest temporal and spatial coverage). I geocode each market with Google Maps to subsequently link them to the grid cells by overlaying the former on the latter. Figure 1 shows the wide spatial coverage of the WFP-VAM data for SSA.

Besides, Table A.2 documents summary statitics. The whole data consists of about 173 thousand data points, of which about 37 percent of maize prices (and about 20 percent of the other crops). The data contain about 2,500 market-crop series, on average covering 5 years (68 months) during the 2010s (on average, starting at 2011 and ending at 2018). The data provides crop prices for 978 markets (for about 2 crops, on average) across 31 countries. On average, countries have about 30 markets surveyed.

ITPD-E international trade data. The trade data used in this paper is obtained from the ITPD-E database (Borchert et al., 2021). I collect all available bilateral trade flows, in current US$, for all country-crops combinations of my study. Consistent with good practice with trade data, I collect import flows rather than exports.[49] Then, I transform the trade data to monetary unit of my study (US$ PPP from G-Econ) as follows. First, I calculate the share of trade flows, at the importer-exporter-crop-year levels, over the GDP of of the importing country in each year, in current values. Next, I average out the shares over the 2000-2010 period, so to avoid outliers in the year of

[49]The reson for that is the usual discrepancy between total import and exports at the country-pair-product level. While import flows are registered between country of production and final country of shipment, export data usually register intermediate countries on the trade chain as final destination, biasing the trade flows (Veronese and Tyrman, 2009).

Table A.3: Census waves for SSA countries available from IPUMS

Country	1960s	1970s	1980s	1990s	2000s	2010s
Benin		1979		1992	2002	2010
Botswana			1981	1991	2001	2011
Burkina Faso			1985	1996	2006	
Cameroon		1976	1987		2005	
Ethiopia			1984	1994	2007	
Ghana			1984		2000	2010
Guinea			1983	1996		2014
Kenya	1969	1979	1989	1999	2009	
Lesotho				1996	2006	
Liberia		1974			2008	
Malawi			1987	1998	2008	
Mali			1987	1998	2009	
Mozambique				1997	2007	
Rwanda				1991	2000	2012
Senegal			1988		2002	2013
Sierra Leone					2004	2015
South Africa				1996	2001/07	2011/16
Sudan[1]					2008	
Tanzania			1988		2002	2012
Togo	1960	1970				2010
Uganda				1991	2002	2014
Zambia				1990	2000	2010
Zimbabwe						2012

[1]Sudan stands for both Sudan and South Sudan, as both countries were the same in the baseline period of 2000. The IPUMS data for these countries are available for the same year of 2008.

2000. Finally, I multiply the shares at the importer-exporter-crop level by the importer GDP of G-Econ for the year of 2000.

International migration data. I obtain bilateral gross migration flows between SSA countries from Abel and Cohen (2019)'s database. It is a comprehensive source of data on gross migration flows between about 200 x 200 country pairs during 5-years intervals from 1990 to 2015; I filter it for all SSA country pairs for 1990 to 2000.

Internal (within-country) migration data. I construct a bilateral matrix of internal migration flows using census data obtained from the IPUMS International Project from IPUMS (2020). Table A.3 documents the set o country-census waves available. For each of these, I retrieve individual-level data on migration status and location of origin (within the same country). The whole data set, of about 17 million data points, is then aggregated at the subnational region pair level. I use the "Geography & GIS" supplementary data sources in IPUMS to obtain the time consistent boundaries of the subnational regions (or provinces, depending on the country – see fig. 1). That allows me to calculate long-term changes in potential yields for each of these regions (for fig. 3) or to match them to grid cells (to obtain total internal migration for Section 5.4).

Main populated places. I collect the coordinates of the main populated places of SSA from the Populated Places data set from Natural Earth. It consists of a geo-referenced

dataset with the coordinates of about 90 percent of all cities, towns and settlements in the World. I use it to set coordinates for each of the cells of SSA. If a certain cell contains more than one location, I pick the one with the highest population. If another does not have any location to obtain the coordinates, I set them to be the cell's centroid. If any of the centroids are not located in the mainland (e.g., ocean), I set it to be the closest coordinate to the centroid that is on the mainland.

B Theory Appendix

B.1 The producer problem, shipping prices, trade probabilities, price indexes, and consumption shares

Producers in the economy face a perfect competition. Hence, taking all prices as given, a firm/farmer in i produce variety ω of sector k choosing inputs $L_i^k(\omega)$ and $H_i^k(\omega)$ that, subject to production function Equation (1), maximize profits

$$p_{ij}^k(\omega)q_j^k(\omega) - w_i L_i^k(\omega) - r_i H_i^k(\omega), \tag{B.1}$$

where $p_{ij}^k(\omega)$ is the price at destination/consumption location j. This standard Cobb-Douglas producer problem, solved as a cost minimization problem, yields the following unit cost of producing variety ω in i:

$$p_i^k(\omega) = \frac{\bar{c}^k w_i^{\alpha_k} r_i^{1-\alpha_k}}{z_i^k(\omega)}, \tag{B.2}$$

where $\bar{c}^k = \alpha^{-\alpha}(1-\alpha)^{\alpha-1}$. Hence, scaling Equation (B.2) with the bilateral iceberg trade costs between i and a buyer location j, τ_{ij}, yields the bilateral shipping prices between locations in Equation (3). Moreover, the bilateral sectoral trade shares of Equation (6) are equivent to

$$\lambda_{ij}^k \equiv \mathbb{P}\left(p_{ij}^k \leq \min_{s \neq i}\{p_{sj}^k\}\right), \tag{B.3}$$

that is, the probability that i is the cheapest supplier of sector k goods to destination j.[50] The distributional assumptions on z_i^k that conditional trade probabilities for a

[50]Note that sectoral varieties become symmetric conditional on productivities, which allows us to disregard the ω index and focus on the location pair-sector dimension.

given price p, $\lambda_{ij}^k(p)$, are also distributed extreme value:

$$\lambda_{ij}^k(p) = \mathbb{P}\left(p = p_{ij}^k \leq \min_{s\neq i} p_{sj}^k\right) = \prod_{s\neq i}\mathbb{P}\left(p_{sj}^k \geq p\right) = \prod_{s\neq i}\left[1 - G_{sj}^k(p)\right] = e^{\Phi_j^{k,-i}p^{-\xi_k}}, \text{ where}$$

$$\Phi_j^{k,-i} = \sum_{s\neq i} b_s^k A_s^k \left(\bar{c}^k w_s^{\alpha_k} r_s^{1-\alpha_k}\tau_{sj}\right)^{-\xi_k}$$

Following Eaton and Kortum (2002), integrating over $p \in \mathbb{R}_+$ yields λ_{ij}^k:

$$\begin{aligned}
\lambda_{ij}^k &= \int_0^\infty \lambda_{ij}^k(p) d\mathbb{P}\left(p_{ij}^k \leq p\right) dp \\
&= \int_0^\infty e^{\Phi_j^{k,-i}p^{-\xi_k}} \times e^{b_i^k A_i^k\left(\bar{c}^k w_i^{\alpha_k} r_i^{1-\alpha_k}\tau_{ij}\right)^{-\xi_k} p^{-\xi_k}} \left(-\xi_k\right) p^{\xi_k - 1} b_i^k A_i^k \left(\bar{c}^k w_i^{\alpha_k} r_i^{1-\alpha_k}\tau_{ij}\right)^{-\xi_k} dp \\
&= b_i^k A_i^k \left(\bar{c}^k w_i^{\alpha_k} r_i^{1-\alpha_k}\tau_{ij}\right)^{-\xi_k} / \Phi_j^k, \text{ where} \qquad \text{(B.4)} \\
\Phi_j^k &= \sum_{i\in S} b_i^k A_i^k \left(\bar{c}^k w_i^{\alpha_k} r_i^{1-\alpha_k}\tau_{ij}\right)^{-\xi_k}. \qquad \text{(B.5)}
\end{aligned}$$

Moreover, the CES utility over varieties with elasticity of substitution $\eta_k < 1 + \xi_k \ \forall k$ yields sectoral price indexes at destination j as:

$$\begin{aligned}
P_j^k &= \left(\int_0^1 p_j^k(\omega)^{1-\eta_k} d\omega\right)^{1/1-\eta_k} \\
&= \Gamma^k \left(\Phi_j^k\right)^{1/\xi_k}, \text{ where} \qquad \text{(B.6)} \\
\Gamma^k &= \left[\Gamma\left(\frac{1-\eta_k}{\xi_k} + 1\right)\right]^{1/1-\eta_k}
\end{aligned}$$

is a constant and $\Gamma(a)$ is the Gamma function. Note that Equation (B.6) is equivalent to Equation (7); plugging it into Equation (B.4) yields Equation (6).

Sectoral consumption shares. These follow standard CES properties. Starting with crops, workers at j maximize welfare with respect to crop consumption by solving:

$$\max_{\{C_j^k\}_k} \quad C_j \quad \text{s. to} \sum_{k\neq K} P_j^k C_j^k \leq \mu^a v_j \quad ,$$

where C_j is (implicitly) defined in eq. (11), C_j^k are the sectoral CES composites in eq. (5), and μ^a is j's expenditure share in agriculture (i.e., crops). Then, rearranging the first order conditions yields $C_j^k / C_j^{k'} = \left(P_j^k / P_j^{k'}\right)^{-\gamma_a}$. Then, by defining Ξ_j^k as the share of j's agricultural expenditure on crop $k \neq K$ goods (and making use of the

$C_j^k / C_j^{k'}$ ratio), one obtains:

$$\Xi_j^k = \frac{P_j^k C_j^k}{\sum_{k' \neq K} P_j^{k'} C_j^{k'}} = \left(P_j^k / P_j^a \right)^{1-\gamma_a} \quad \forall i, j,$$

where the last equation takes advatage of the definition of the agricultural price index from eq. (10). Note that, for the upper CES nest (choice between agricultural and non-agricultural consumption bundles), the derivation is analogous but with the additional income effect following Comin et al. (2021).

B.2 Derivation of migration shares

Take the definition of the welfare attained by a worker v living in i and moving to j as $W_{ij}(v) = (w_j / P_j) \bar{m}_{ij}^{-1} \varepsilon_j(v)$, $\varepsilon_i \sim G_j(v) = e^{-v^{-\theta} u_j L_j^{-\alpha}}$. Following Eaton and Kortum (2002), one can obtain the distribution of the welfare from one specific location i as

$$A_{ij}(w) \equiv \mathbb{P}(W_{ij} \leq w) = G_j(w P_j \bar{m}_{ij} / w_j) = e^{-(w P j \bar{m}_{ij} / w_j)^{-\theta} u_j L_j^{-\alpha}}.$$

Thus, the joint distribution of welfare of all destinations s from i can be derived as

$$A_i(w) = \prod_{s \in S} e^{-(w P_s \bar{m}_{is} / w_s)^{-\theta} u_s L_s^{-\alpha}} = e^{-\Phi_i \times w^{-\theta}}, \quad \text{where } \Phi_i = \sum_{s \in S} (P_s \bar{m}_{is} / w_s)^{-\theta} u_s L_s^{-\alpha}.$$

Now, recalling the share of workers moving from i to j is equivalent to the probability that the welfare attained by moving to j, w, is the highest among all other possible s destinations, one writes

$$\Pi_{ij}(w) = \mathbb{P}\left(W_{ij}(v) \equiv w \geq \max\{W_{is}(v)\}_{s \neq j} \right) = \prod_{s \neq j} \mathbb{P}(W_{is} \leq w) = e^{-\Phi^{-j} \times w^{-\theta}}.$$

With that, it is possible to obtain the unconditional probability Π_{ij} by integrating over all possible values of $w \in \mathbb{R}_+$, i.e.

$$\begin{aligned}
\Pi_{ij} &= \int_0^\infty \Pi_{ij}(w) \, d\mathbb{P}(W_{ij} \leq w) \, dw \\
&= \int_0^\infty e^{-\Phi^{-j} \times w^{-\theta}} \times e^{(w P_j \bar{m}_{ij} / w_j)^{-\theta} u_j L_j^{-\alpha}} \times (-\theta) w^{-\theta-1} (P_j \bar{m}_{ij} / w_j)^{-\theta} u_j L_j^{-\alpha} \, dw \\
&= \frac{(w_j / P_j)^\theta \bar{m}_{ij}^{-\theta} u_j L_j^{-\alpha}}{\sum_{s \in S} (w_s / P_s)^\theta \bar{m}_{is}^{-\theta} u_s L_s^{-\alpha}},
\end{aligned}$$

which is the equivalent of eq. (18).

B.3 Spatial equilibrium

Given the geography $\mathcal{G}(S)$ and the parameters $\Theta \equiv \{\Omega_k, \eta_k, \gamma_a, \epsilon_k, \alpha_k, \xi_k, \sigma, \theta, \beta\}$, a spatial equilibrium is a vector of factor prices and labor allocations $\{w_j, r_j, L_j\}_{j \in S}$ such that eqs. (7), (10), (12) to (14) and (19) hold, and markets for goods clear. Formally, market clearing requires trade-balacing, such that each j's income equals total exports to and total imports from all locations $i \in S$, as in Equation (20). In fact, by using eq. (14) on (20), one characterizes the spatial equilibrium with the following system of $7 \times N$ equations and unknowns:

$$v_j L_j = \sum_{i \in S} \sum_{k \neq K} b_i^k A_i^k \left(\Gamma^k \bar{c}^k w_i^{\alpha_k} r_i^{1-\alpha_k} \tau_{ij} / P_j^k \right)^{-\xi_k} \left(\frac{P_j^k}{P_j^a} \right)^{1-\gamma_a} \Omega^a \left(\frac{P_j^a}{P_j} \right)^{1-\sigma} \left(\frac{v_j}{P_j} \right)^{\epsilon_a - (1-\sigma)} v_j L_j +$$
$$+ \sum_{i \in S} b_i^K A_i^K \left(\Gamma^K \bar{c}^K w_i^{\alpha_K} r_i^{1-\alpha_K} \tau_{ij} / P_j^K \right)^{-\xi_K} \Omega^K \left(\frac{P_j^K}{P_j} \right)^{1-\sigma} \left(\frac{v_j}{P_j} \right)^{\epsilon_K - (1-\sigma)} v_j L_j \tag{B.7}$$

$$P_j = \left(\sum_{k \in \{a, K\}} \left(\Omega^k \left(P_j^k \right)^{1-\sigma} \right)^{\frac{1-\sigma}{\epsilon_k}} \left(\mu_j^k v_j^{1-\sigma} \right)^{\frac{\epsilon_k - (1-\sigma)}{\epsilon_k}} \right)^{\frac{1}{1-\sigma}} \tag{B.8}$$

$$P_j^k = \Gamma^k \left(\sum_{i \in \mathcal{S}} b_i^k A_i^k \left(\bar{c}^k w_i^{\alpha_k} r_i^{1-\alpha_k} \tau_{ij} \right)^{-\xi_k} \right)^{-1/\xi_k} \tag{B.9}$$

$$L_j = \sum_{i \in S} \frac{(v_j / P_j)^\theta \bar{m}_{ij}^{-\theta} u_j L_j^{-\alpha}}{\sum_{s \in S} (v_s / P_s)^\theta \bar{m}_{is}^{-\theta} u_s L_s^{-\alpha}} \times L_i^0 \tag{B.10}$$

$$\mu_j^k = \Omega^k \left(P_j^k / P_j \right)^{1-\sigma} \left(v_j / P_j \right)^{\epsilon_k - (1-\sigma)} \tag{B.11}$$

$$P_j^a = \left(\sum_{k \neq K} \left(P_j^k \right)^{1-\gamma_a} \right)^{\frac{1}{1-\gamma_a}} \tag{B.12}$$

$$v_j = w_j + \left(r_j H_j \right) / L_j \tag{B.13}$$

Existence and Uniqueness. My model is not isomorphic to the general set up of Allen and Arkolakis (2014) and, as a consequence, the existence and uniqueness of the equilibrium cannot be guaranteed under their conditions for such. The reason for that is the additional non-linearity introduced by the middle- and upper-level CES structures. I address that by solving my model for several parametric choices, starting from many different initial guesses. The solution is invariant across all cases.

B.4 Numerical algorithm for solving the model

I find $\{w_j, r_j, L_j\}_{j \in S}$ that solves for the spatial equilibrium characterized by the system of equations (B.7) to (B.13) with an algorithm that nests three loops in one another.

Inner loop. I start with a guess for $\{w_j, r_j, L_j\}_j$ and solve for sectoral price indexes in eqs. (B.9) and (B.12). Then, with a guess for $\{P_j\}_j$, I iterate over eqs. (B.8) and (B.11)

to find a simultaneous solution for $\{P_j, \mu_j^k\}_{j,k}$. In particular, with the guess for $\{P_j\}_j$, I solve for $\{\mu_j^k\}_k$ in eq. (B.11), replace it on eq. (B.8) to update solve for $\{P_j\}_j$, and iterate until both solutions converge.

Middle loop. I use the solution for $\{P_j^k, P_j^a, P_j, \mu_j^k\}_{j,k}$ and the guesses for $\{w_j, r_j, L_j\}_j$ in eq. (B.13) and (B.7) to update $\{w_j, r_j\}_j$.[51]

Outer loop. I use the solution of $\{w_j, r_j, P_j\}_j$ and the guess for $\{L_j\}_j$ in eq. (B.10) to obtain an update for $\{L_j\}_j$, iterating it until the solution converges.

I then replace the solutions for $\{w_j, r_j, L_j\}_j$ back in the inner loop and repeat the procedure above until all solutions converge to a fixed point. Importantly, I winsorize both data and fundamentals when (i) bringing the model to the data (Appendix B.6) and (ii) solving the model with the calibrated geography. I do that to remove the role of extreme outliers on the counterfactual results. Appendix B.6.3 provides further details.

B.5 Details of the economy represented as line

The illustration of the model mechanisms in Section 4.2 represents the economy as a line with a discrete number of locations. To make the exposition of these mechanisms the cleanest possible, I make the economy as homogeneous as possible in many fundamentals, like amenities and land endowments. For the latter, I take a further simplification step: I disregard land as a factor, which implies that labor (wages) is the only factor (rent) in the economy.[52] Hence, to make the consumption choices of agents consistent (and more transparent) with new setting, I change the lower CES tier to a pure Armington set-up where the CES for local varieties, η_k, disciplines the trade elasticity of the economy.[53]

The only sources of spatial heterogeneity in this stylized economy are the trade frictions $\mathcal{T}$ and, most importantly, fundamental productivities $\mathcal{A}$. Specifically, I assume the left-most regions (and country) to be less productive in both sectors, as shown in Figure B.1 Panel A. Moreover, as shown in Panel B, when simulating the impact of climate change in this economy, I assume it affects only the left regions, thus making them even less productive in agriculture.

[51] For that, I use the Cobb-Douglas fixed proportion of factor bills. For the case of labor rents, that implies $w_j L_j = \sum_k \alpha_k X_j^k$, which can be solved for w_j (X_j^k is the right-hand side of eq. (B.7)).

[52] In practice, it implies weaker dispersion forces vis-à-vis the full-fledged model.

[53] That is, $\lambda_{ij}^k = (p_{ij}^k / P_j^k)^{\eta_k} = (w_i^k \tau_{ij} / A_i^k P_j^k)^{\eta_k}$, while equations (B.7) to (B.13) remain nearly identical.

Figure B.1: Spatial distribution of productivities $\{A_j^1, A_j^2\}_j$ in the line economy with and without climate change

Panel A: Baseline (no climate change)

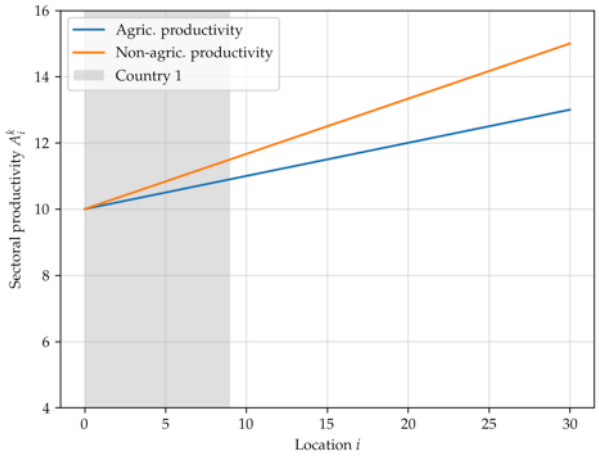

Panel B: Climate change affects agriculture

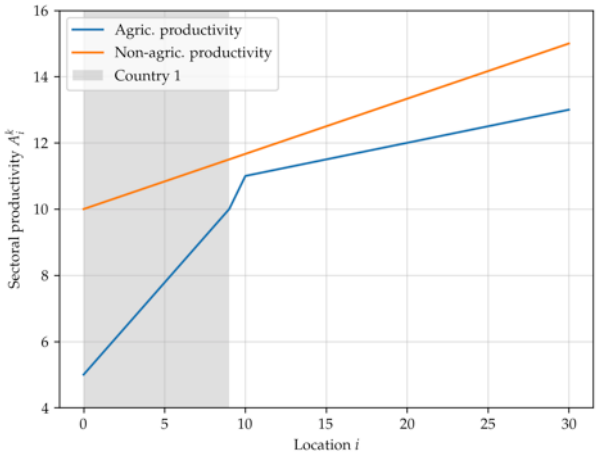

B.6 Model quantification

I quantify the parameters and fundamentals related to technology and location choice in two different steps, each consisting of a two-stage procedure. When doing so, I link the theory to data; Appendix B.6.3 discusses aspects related to data quality and measurement error.

B.6.1 Technology

Conditional on parameters from the literature and fundamentals observed from the data, this step quantifies $\mathbf{t} \equiv \{\tau_{ij}^F, \delta\}$ and $\mathbf{T} \equiv \{\{A_i^K\}_i, \{b_i^k\}_{i,k}, \{\Omega_a, \Omega_K\}\}$ with a two-stage procedure (with the inner stage nested on the outer). Specifically, the first stage (inner loop), guesses values for $\mathbf{t}$ and quantify $\mathbf{T}$ by inverting the general equilibrium conditions of the model. Then, the second stage (outer loop) estimates $\hat{\mathbf{t}}$ with a GMM that targets model-generated moments to their data counterparts conditional on the first stage.

Inner loop. With a guess on $\hat{\mathbf{t}}$, it finds $\mathbf{T} \equiv \{\{A_i^K\}_i, \{b_i^k\}_{i,k}, \{\Omega_a, \Omega_K\}\}$ such that make the model perfectly match, respectively, the spatial distribution of nominal income $\{v_j L_j\}_j$, the spatial-sector distribution of production $\{X_j^k\}_{j,k}$, and the aggregate sec-

toral expenditure ratios X^K/X^a. The model counterpart of these moments are:

$$v_j L_j = \sum_{i \in S} \sum_{k \neq K} \lambda_{ji}^k \Xi_i^k \mu_i^a v_i L_i + \sum_{i \in S} \lambda_{ji}^K \mu_i^K v_i L_i \tag{B.14}$$

$$X_j^k = \sum_{i \in S} \lambda_{ji}^k \Xi_i^k \mu_i^a v_i L_i \quad \forall k \neq K \tag{B.15}$$

$$X_j^K = \sum_{i \in S} \lambda_{ji}^K \mu_j^K v_i L_i \tag{B.16}$$

$$X_K / X_a = \frac{\sum_{j \in S} \sum_{i \in S} \lambda_{ji}^K \mu_i^K v_i L_i}{\sum_{k \neq K} \sum_{j \in S} \sum_{i \in S} \lambda_{ji}^k \Xi_i^k \mu_i^a v_i L_i}. \tag{B.17}$$

Then, one can invert each of the equations above to obtain the expressions for the unobserved fundamentals of interest. For instance, for $\{A_j^K\}_j$, one inverts eq. (B.14) to obtain:

$$\begin{aligned} v_j L_j = \sum_{i \in S} \sum_{k \neq K} \lambda_{ji}^k \Xi_i^k \mu_i^a v_i L_i + \sum_{i \in S} b_j^K A_j^K \left(\Gamma^K \bar{c}^K w_j^{\alpha_K} r_j^{1-\alpha_K} \tau_{ji} / P_i^K \right)^{-\xi_K} \mu_i^K v_i L_i \rightarrow \\ A_j^K = \frac{v_j L_j - \sum_{i \in S} \sum_{k \neq K} \lambda_{ji}^k \Xi_i^k \mu_i^a v_i L_i}{\sum_{i \in S} b_j^K \left(\Gamma^K \bar{c}^K w_j^{\alpha_K} r_j^{1-\alpha_K} \tau_{ji} / P_i^K \right)^{-\xi_K} \mu_i^K v_i L_i}. \end{aligned} \tag{B.18}$$

Importantly, I do not observe factor prices $\{w_i, r_i\}_i$ from the data, but rather nominal incomes $\{v_i\}_i$, sectoral production $\{X_i^k\}_{i,k}$, land endowments $\mathcal{H}$, and sectoral allocation of land $\{H_i^k\}_{i,k}$.[54] With that, I obtain $\{w_i, r_i\}_i$ with:

$$\begin{aligned} X_i^K = r_i H_i^K / (1 - \alpha_K) \rightarrow \\ r_i = X_i^K \times (1 - \alpha_K) / H_i^K, \text{and} \end{aligned} \tag{B.19}$$

$$\begin{aligned} v_i L_i = w_i L_i + r_i H_i \rightarrow \\ w_i = v_i - (r_i H_i) / L_i, \end{aligned} \tag{B.20}$$

where eq. (B.19) comes from the fixed factor proportion from the Cobb-Douglas pro-

[54] I measure sector-cell-level data on land usage $\{H_i^k\}_{i,k}$ also from GAEZ. Specifically, I retrieve harvested land for all crops of my setting by overlaying (and aggregating) my grid into the GAEZ harvested land data. Then, I obtain $H_i^K = H_i - \sum_{k \neq K} H_i^k \; \forall i$.

duction function.[55] Then, analogous to eq. (B.18), I invert eqs. (B.15) to (B.17) with:

$$b_j^k = X_j^k \times \left[\sum_{i \in S} A_j^k \left(\Gamma^k \bar{c}^k w_j^{\alpha_k} r_j^{1-\alpha_k} \tau_{ji} / P_i^k \right)^{-\xi_k} \Xi_i^k \mu_j^a v_i L_i \right]^{-1} \quad \forall k \neq K \tag{B.21}$$

$$b_j^K = X_j^K \times \left[\sum_{i \in S} A_j^K \left(\Gamma^K \bar{c}^K w_j^{\alpha_K} r_j^{1-\alpha_K} \tau_{ji} / P_i^K \right)^{-\xi_k} \mu_j^K v_i L_i \right]^{-1} \tag{B.22}$$

$$\Omega_K / \Omega_a = \frac{X^K}{X^a} \times \frac{\sum_{k \neq K} \sum_{j \in S} \sum_{i \in S} \lambda_{ji}^k \Xi_i^k \left(P_i^a / P_i \right)^{1-\sigma} \left(v_i / P_i \right)^{\varepsilon_a - (1-\sigma)} v_i L_i}{\sum_{j \in S} \sum_{i \in S} \lambda_{ji}^K \left(P_i^K / P_i \right)^{1-\sigma} \left(v_i / P_i \right)^{\varepsilon_K - (1-\sigma)} v_i L_i}. \tag{B.23}$$

The inversion algorithm finds $\{A_j^K, \{b_j^k\}_{j,k}, \Omega_K / \Omega_a\}$ such that eqs. (B.18) and (B.21) to (B.23) hold simultaneously. However, because $\{b_j^K\}_j$ and $\{A_j^K\}_j$ cannot be separated out in levels, I normalize the latter to one and identify their product in eq. (B.22). That also gives me tractability, as then eq. (B.18) is not needed anymore for inverting the spatial equilibrium.[56] To solve this high-dimensional problem, I proceed as follows: with a guess for $\{b_j^k\}_{j,k}$, I solve for Ω_K / Ω_a in eq. (B.23). I then plug the solution in eqs. (B.21) and (B.22) (embedded in $\{\mu_j^k\}_{j,k}$) to solve for $\{b_j^k\}_{j,k}$. I iterate it until all solutions converge; I represent it, conditional on a guess for $\mathbf{t}$, as $z(\mathbf{T}; \mathbf{t}) = 0$.

Outer loop. Conditional on $z(\mathbf{T}; \mathbf{t}) = 0$, I estimate $\mathbf{t} \equiv \{\tau_{ij}^F, \delta\}$ with a GMM. For that, I design moments that provide the identifying variation for the parameters of interest and that are observable in the data. Specifically, these are:

$$m_1 = \sum_c \sum_{c'} \sum_{i \in c} \sum_{j \in c'} \sum_k X_{ij}^k, \text{ and} \tag{B.24}$$

$$m_2 = \left[\frac{\sum_{j,k \in \mathcal{D}} \left(P_j^k - \bar{P} \right)^2}{N(\mathcal{D})} \right]^{1/2}, \tag{B.25}$$

that is, aggregate export flows and the dispersion (standard deviation) of sectoral price indexes.[57] Note that m_1 provides the required variation for identifying due to the (intuitive) decreasing relationship between bilateral trade flows and tariffs τ^F (i.e., larger tariffs, less international trade). Moreover, the identification of δ relies on the positive relationship between trade frictions and price dispersion in m_2. That is, the

[55] Importantly, all monetary values, built from the data in US$ PPP units (see Section 2), are further normalized to the wages of the first location w_1. This is done as I am not able to pin down levels in my quantification, but instead the spatial distribution of fundamentals up to a normalization.

[56] In particular, that equation holds by construction if eqs. (B.21) and (B.22) hold simultaneously.

[57] Note that $\mathcal{D}$ is the set of location-crop combinations for which the WFP-VAM data provide data for. Moreover, $N(\mathcal{D})$ and $\bar{P}$ are the size and mean of this set, respectively. Analogously, m_1 is calculated with the country pair-crop combinations with export data available from the ITPD-E trade data.

lowest δ, the lower the degree of trade frictions in the economy and, as a consequence, the more homogeneous would price indexes be across space (hence, less dispersion). Importantly, the WFP-VAM price data provides time varying data between 2000 and 2018; I discuss how I decompose these location-crop time series so to match the static feature of my model (and thus, sectoral price indexes $\{P_j^k\}_{i,k}$) in Appendix B.7.

I estimate $\mathbf{t}$ by defining $\mathbf{m} = [m_1, m_2]$ and $g(\mathbf{t}) = \left[\mathbf{m}(\mathbf{t}) - \mathbf{m}^{\text{data}}\right]$ and solving for $\hat{\mathbf{t}}$ that, based on $\mathbb{E}[g(\mathbf{t})] = 0$, satisfies:

$$\hat{\mathbf{t}} = \arg \min_{\mathbf{t}} g(\mathbf{t}) W g(\mathbf{t})' \text{ subject to } z(\mathbf{T}; \mathbf{t}) = 0, \tag{B.26}$$

where W is the weighting matrix.[58] I solve for $\hat{\mathbf{t}}$ with a bidimensional grid search over τ^F and δ values and infer standard errors by bootstrapping it ten thousands iterations.[59] Table 2 documents the estimation results.

Figure B.2 Panels A and B plot the grid search results (with the log objective function $g(\mathbf{t}) W g(\mathbf{t})'$ evaluated at different δ and τ^F pairs). They show a non-linear relationship between the two parameters and the objective function, as well as a "valley-looking region" along the diagonal where the solution lies on. Moreover, Panels C documents slices of the objective function evaluated for a fixed τ^F, showing the relevance of the designed moments in terms of providing identifying variation for the parameters of interest. In particular, it shows that, for a given τ^F, the objective function is U-shaped along the δ dimension (and hence that the relationship between δ and price dispersion is monotonic, as expected).

B.6.2 Location choice

I proceed with an analogous two-stage step where $\mathbf{T} \equiv \{u_i, m_c\}_{i,c}$ and $\mathbf{t} \equiv \phi$.

Inner loop. It solves for $\{u_i\}_i$ and $\{m_c\}_c$ conditional on all previsouly quantified parameters and fundamentals, a guess for $\mathbf{t}$, and the observed following endogenous variables: population $\{L_i\}_i$ and country-level total inflow of foreign migrants, $\{L_c\}_c$ (from Abel and Cohen, 2019, between 1990 and 2000, where 1990 is the earliest period available for SSA). In practice, I use eq. (19) to calculate L_c and invert it to obtain an expression for country barriers as a function of L_c and other endogenous variables

[58] I choose W to be the identity matrix due to the high non-linearity of my moments (thus, the complexity of their Jacobian and Hessian matrices).

[59] Grid search methods can easily lead to curse of dimensionality and global-local optima issues. However, my model requires that tariffs and trade costs are both non negative; which restricts the parametric space. I also rule out global-local optima tradeoffs by running a coarse search over large intervals (Panel A) and then narrowing it down around the minimum of the coarse search (Panel B).

Figure B.2: Results of the outer loops that solve for τ^F, δ, and ϕ

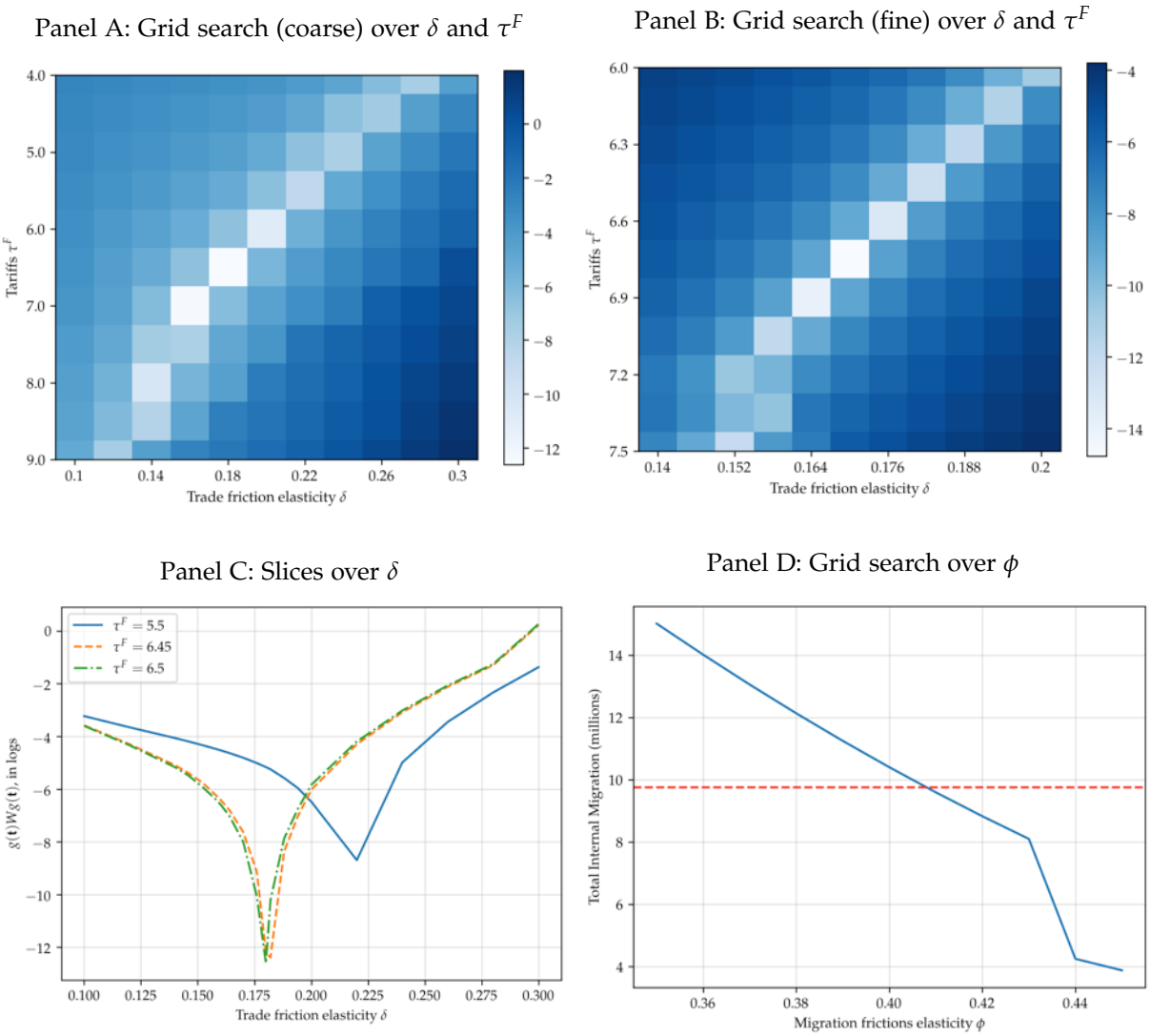

Notes: Panel A and B: Grid searchs over δ (x-axis) and τ^F_{ij} (y-axis) with the colored evaluation of the objective function (in logs) for each of these pairs. Panel C shows slices of A evaluated at fixed values of τ^F. Panel D: analogous grid search over ϕ and the resulting model-generated internal migration flows (the dashed red line stands for observed total internal migration flows from IPUMS data).

and fundamentals as follows:

$$L_c = \sum_{j \in c} \sum_{i \notin c} \frac{\left(v_j / P_j\right)^{\theta} m_{ij}^{-\theta} m_{c(j)}^{-\theta} u_j}{\sum\limits_{s \in c(j)} \left(v_s / P_s\right)^{\theta} m_{is}^{-\theta} u_s + \sum\limits_{s \notin c(j)} \left(v_s / P_s\right)^{\theta} m_{is}^{-\theta} m_{c(s)}^{-\theta} u_s} L_{i0} \rightarrow$$

$$m_c = \left[L_c^{-1} \times \sum_{j \in c} \sum_{i \notin c} \frac{\left(v_j / P_j\right)^{\theta} m_{ij}^{-\theta} u_j}{\sum\limits_{s \in c(j)} \left(v_s / P_s\right)^{\theta} m_{is}^{-\theta} u_s + \sum\limits_{s \notin c(j)} \left(v_s / P_s\right)^{\theta} m_{is}^{-\theta} m_{c(s)}^{-\theta} u_s} L_{i0} \right]^{1/\theta} \tag{B.27}$$

Note that the denominator in the equations above is equivalent to eq. (19)'s – it sepa-

rates the inter/intranational bilateral choices to illustrate the identification of parameters later on. Analogously, I invert eq. (B.10) to pin down amenities $\{u_j\}_j$ as a function of population distribution and other endogenous variables and fundamentals:

$$u_j = L_j \times \left[\sum_{i \in c(j)} \frac{\left(v_j / P_j\right)^{\theta} m_{ij}^{-\theta}}{\sum_{s \in c(j)} \left(v_s / P_s\right)^{\theta} m_{is}^{-\theta} u_s + \sum_{s \notin c(j)} \left(v_s / P_s\right)^{\theta} m_{is}^{-\theta} m_{c(s)}^{-\theta} u_s} L_{i0} + \right.$$
$$\left. \sum_{i \notin c(j)} \frac{\left(v_j / P_j\right)^{\theta} m_{ij}^{-\theta} m_{c(j)}^{-\theta}}{\sum_{s \in c(j)} \left(v_s / P_s\right)^{\theta} m_{is}^{-\theta} u_s + \sum_{s \notin c(j)} \left(v_s / P_s\right)^{\theta} m_{is}^{-\theta} m_{c(s)}^{-\theta} u_s} L_{i0} \right]^{-1} \tag{B.28}$$

I solve eqs. (B.27) and (B.28) as follows: with a guess for $\{u_j\}_j$, I solve for $\{m_c\}_c$ in eq. (B.27), plug it in eq. (B.28) to solve for $\{u_j\}_j$, and iterate it until all solutions converge. Importantly, I am able to separate out $\{u_j\}_j$ from $\{m_c\}_c$ because location pairs can refer to either intra or international migration. That is, conditional on a guess of $\{u_j\}_j$, there are distinct origins s for which a destination j stand for one type of migration of the other (the denominator of eq. (B.27)), and thus where amenities multyplies or not the country migration barriers $\{m_c\}_c$. Considering all possible origins s and destinations j in S, there is at least one pair for which they do and do not multiply one another, which then allows me to separately identify them.

Outer loop. The outer loop estimates $\mathbf{t} \equiv \phi$ similarly to Equation (B.26) but finding $\hat{\phi}$ such that the model-generated internal migration flows, $L^D = \sum_{c \in \mathcal{C}} \sum_{j \in c} \sum_{i \in c} L_{ij}$, matches the observed internal migation flows between 1990 and 2000 from IPUMS.[60] Figure B.2 Panel D shows the results of the grid search, displaying the intutive decreasing relationship between ϕ and internal migration in the economy.

B.6.3 Data issues, measurement error, and trimming data and fundamentals

The calibration of the geography $\mathcal{G}(S)$ for 2000 fits perfectly the observed data for that period. Therefore, the quantified fundamentals incorporate all possible measurement error present in the data. This is particularly important for the dissagregated data on real income, $\{v_j\}_j$, where extreme outliers could map into extraordinary differences in quantified non-agricultural productivities $\{b_j^K\}_j$ and/or amenities $\{u_j\}_j$. To address that, I follow common practice in empirical literature Chen et al. (2023) by winsorizing the income data used in the quantification method of Appendix B.6.

Specifically, as in Desmet et al. (2018) and Conte et al. (2021), the observed real income per capita, $\{v_j\}_j$ is truncated at the 97,5th percentile. However, after visual inspection, that procedure does not eliminte fully the extreme outliers obtained in the

[60] Hence, $\mathcal{C}$ is the set of countries for which migration data is available in IPUMS.

fundamentals, especially with respect to the efficiency shifters $\{b_j^k\}_{j,k}$ and amenities $\{u_j\}_j$. Thus, when solving the model for any simulation using the calibrated model, I also trim $\{b_j^k\}_{j,k}$ and $\{u_j\}_j$ at the 97.5% percentile.

B.7 Mapping the time-varying price data into the static model prices

A challenge to link the sectoral prices $\{P_j^k\}_{j,k}$ to their empirical counterpart from the WFP-VAM data is the "static-dynamic mismatch" between them: while the former is static (due to the static aspect of the model), the latter is time-varying (due to the long location-crop price series available for numerous locations across SSA). The most immediate approach to overcome it is restricting the price data within a time window that is the closest to the baseline period of my quantification, the year of 2000.

This approach implies two drawbacks. First, it restricts the data to a narrow subset with a poor geographical coverage. Second, and most importantly, it incorporates location-crop-time specific shocks at that specific period that could pollute the resulting aggregate price dispersion used in Appendix B.6.1.[61] To avoid that, I propose a time series decomposition approach that, by exploiting the long longitudinal characteristic of each location-crop series, nets them out of these shocks and retrieves a time invariant, location-crop component that maps into $\{P_j^k\}_{j,k}$.

More specifically, I first aggregate the market-crop-level price series at the grid cell-crop level by averaging crop prices across markets that belong to the same grid cell. While in principle this could add noise to the data, in practice the observed prices across markets evolve quite homogeneously in levels and trends within grid cell-crop pairs. Figure B.3 Panels A and B illustrate that for markets located at a common grid cell, one in Mali and another in Malawi, respectively. I define these observed location-crop-time (year-month t) price series as $\tilde{P}_{j,t}^k$ and assume it evolves as:

$$\tilde{P}_{j,t}^k = a_{c(j)} \times t \; + \; b_{c(j)\times m(t)} + \overbrace{c_j^k}^{\equiv P_j^k} + \varepsilon_{j,t}^k, \tag{B.29}$$

where $a_{c(j)} \times t$ is a set of country-specific time trends that account for secular evolution in crop prices that are common for all markets j in the same country $c(j)$. Moreover, $b_{c(j)\times m(t)}$ are country-month of the year (e.g., January or February) fixed effects that account for country-specific ciclicality on crop production and prices. Finally, $c_j^k \equiv P_j^k$ are location-crop fixed effects that absorb the common $j \times k$ component of the price series. Hence, it is the empirical counterpart of the theoretical prices $\{P_j^k\}_{j,k}$: it contains the time invariant, location-crop specific component of prices at each observed

[61] For instance, spatially heterogeneous incidence of droughts by 2000 (or before) could inflate the observed price dispersion, hence underestimating δ.

Figure B.3: WFP-VAM raw data, matching to grid cells, and price decomposition

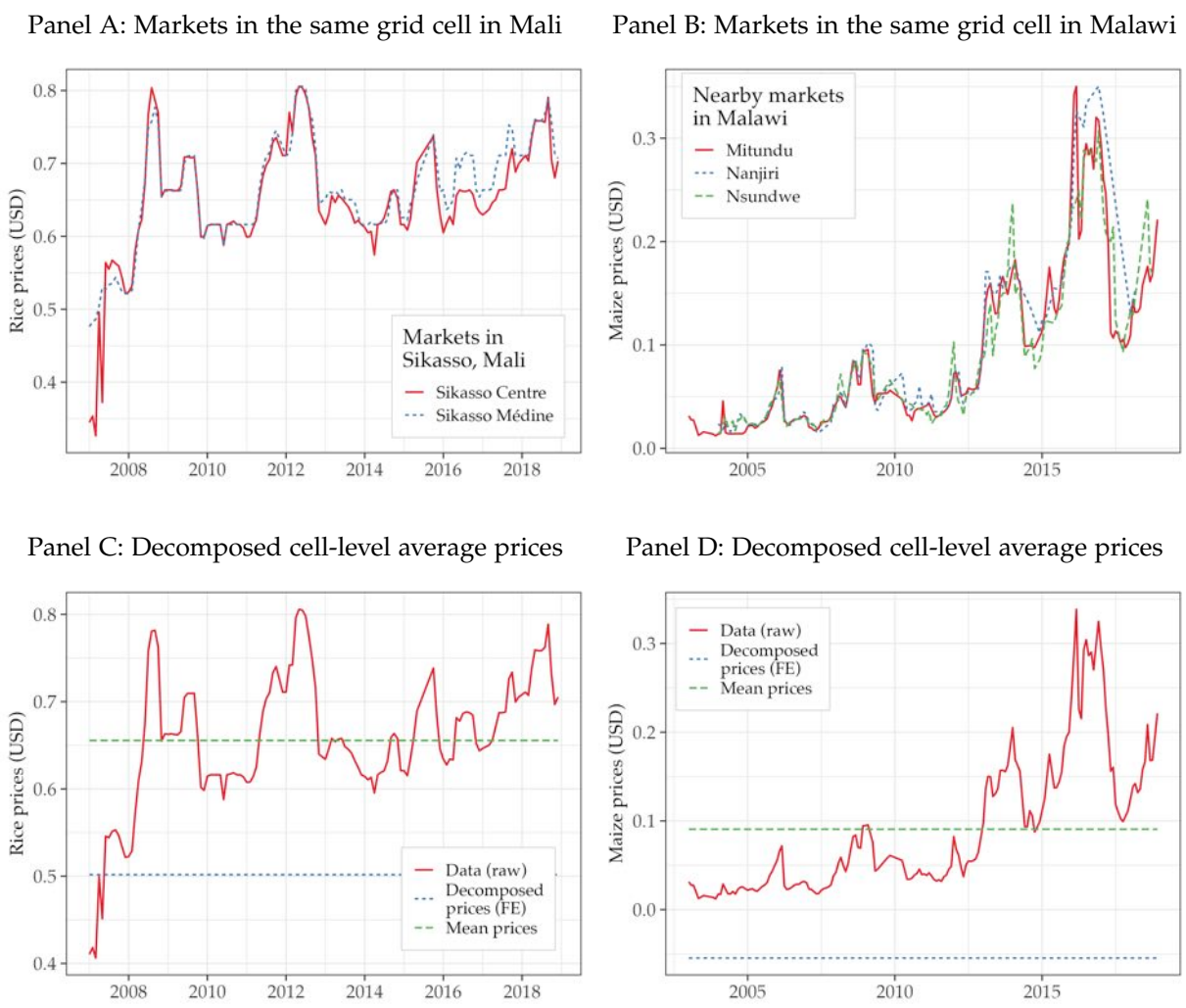

Notes: Panels A and B plot two samples of crop prices in markets within common grid cells (in Mali and Malawi, respectively). Panels C and D show how the grid cell-level average (i.e., across markets within grid cells over time) crop prices are decomposed into a location-crop time invariant component $\bar{c}_j^k \equiv P_j^k$ and contrasts it to the unconditional mean along each $j \times k$ time series ("Mean prices").

$j \times k$ combination (net of the shocks over their time series).[62]

I estimate Equation (B.29) with the WFP-VAM price data and retrieve $\hat{c}_j^k$ as the observed $\{P_j^k\}_{j,k}$. Figure B.3 Panels C and D illustrate the result for the two locations j in Mali and Malawi (from Panels A and B, respectively). They also contrast $\hat{c}_j^k$ to a naive approach of averaging out prices along the grid cell-crop dimension ("Mean prices"). Because of the increasing trend in prices over time, averages are upward biased vis-à-vis $\hat{c}_j^k$ (that account for this secular trends). In fact, some $\hat{c}_j^k$ have negative values – while counterintuitive if thinking of negative prices, this makes sense for the purpose of my exercise (that aims at exploiting (spatial) within-country differences in

[62]Importantly, idiosyncratic shocks to prices – such as weather shocks – are accounted for, but with the underlying assumption that they are normally distributed and have expectation equal to zero (in the error term $\varepsilon_{j,t}^k$) at the $j \times k$ level.

prices). Hence, not accounting for the components in Equation (B.29) overestimates the magnitude of prices. That would, in turn, underestimate the aggregate dispersion of prices across space and, as a consequence, the estimated δ.

B.8 Discussion of the parameters taken from the literature

Lower CES tier. The values taken for $\{\eta_k\}_k$ come from Costinot et al. (2016) and Bernard et al. (2003) for crops and non-agriculture, respectively. These values are widely used in other applications in the literature (e.g. Desmet et al., 2018, for η_K). They nevertheless are estimated in global (or cross-country) settings. Assuming different values for $\{\eta_k\}_k$ (say, substitution of varieties within countries being more intense than across countries) would mainly affect the model-generated trade flows, and consequently the levels of the parameters associated to trade frictions.

Middle CES tier. The value $\gamma_a = 2.5$ comes from Sotelo (2020), who studies rural Peru by early 2000s and focus on intranational trade in that country. Thus, it stands for a context similar to rural SSA as of 2000.

Upper CES tier (and Ω_k shifters). The values for $\{\varepsilon_k\}$ and σ come from the global estimation of Comin et al. (2021) (and are particularly close to Nath (2023)'s estimates). These values therefore reflect preferences between agricultural and non-agricultural goods from a global representative consumer. Thus, the values can underestimate the subsistency aspect of agricultural goods in SSA, where the negative slope of the Engel curve could be steeper vis-à-vis the rest of the world. If so, then, my results would underestimate the welfare losses associated to that mechanism. In fact, the estimated $\{\Omega_k\}_{a,K}$ reflects that: I quantify a relative Ω_a/Ω_K that is about twice the estimates from Nath (2023) for the global economy, reflecting that expenditures in agriculture are much more pronounced in SSA visà-vis the global economy.[63]

B.9 Discussion of the estimated trade and migration frictions

In what follows, I benchmark trade and migration frictions quantified in Section 5 with estimates from related literature. This exercise is relevant due to the different approaches from these studies (in terms of functional format or units of distance), which hinders a direct comparison between their estimates and mine. When comparing them, I also stress the reasons and advantages of my modeling choices.

Trade frictions. Many studies estimate the relationship between distance and trade frictions for developing contexts (e.g. Donaldson, 2018; Sotelo, 2020; Pellegrina and

[63] In particular, I quantify $\Omega_a/\Omega_K = 1/0.19 = 5$, while Nath (2023) estimates a relative agriculture and manufacturing shifters for the global economy of $11.73/3.7 = 3.2$.

Sotelo, 2024; Pellegrina, 2022). Importantly, most of these parametrize trade costs with an exponential format; e.g., $\log(\tau_{ij}) = \delta \times \text{dist}(i,j)$. Moreover, some use different distance metric – such as travel time. Hence, to compare my trade costs estimates to related studies, I use the functional formats and estimates from Donaldson (2018) and Pellegrina (2022) (for India and Brazil, respectively) to calculate and benchmark their resulting τ_{ij} to mine (i.e., with $\text{dist}(i,j)^{0.17}$). Figure B.4 Panel A documents their differences visually. It shows that, for small distances, my estimated τ_{ij} lie between Indian and Brazilian estimates. However, as distances increase, these estimates (exponentially) exceed mine. In fact, for extremely large distances (between, say, the North-South extremes of SSA), the resulting τ_{ij} becomes unreasonably large (which generates numerical problems, such as close-to-infinite prices in the economy). My functional format, instead, is tailored for continental empirical settings like mine, conveying reasonable values τ_{ij} for small (i.e., within country) distances that smoothly increase with (large) distances.

Migration costs. I analogously benchmark my estimated $m_{ij} = \text{dist}(i,j)^{0.41}$ to values from Indonesia, Brazil, and the US (from Bryan and Morten, 2019; Morten and Oliveira, 2024; Allen and Donaldson, 2022, respectively). Figure B.4 Panel B shows the results: my median SSA estimates are about 20 percent larger than the median estimates for Indonesia, and about three to four times larger than those for Brazil and the US, respectively. Moreover, the (exponential) increase in the migration costs for larger distances is also visible, though not as pronounced as for trade costs (however, these patterns hold for continental distances between geographical extremes of SSA).

B.10 Discussion of the inversion results

Figure B.5 illustrates the spatial distribution of some of the quantified fundamentals. Panel A and B show that more productive locations (which have higher real wages) have higher fundamental productivities in the K^{th} sector. Thus, the model rationalizes that, net of the variation in the $K-1$ sectors, locations with a high level of economic activity must be very productive in non-agriculture. This pattern stands out in some capitals and in high-GDP countries, such as South Africa. Panel C illustrates an analogous aspect of the quantified sectoral shifters of cassava. There are high $\{b_i^k\}_i$ values for locations in countries that are large cassava producers, such as Nigeria.

Moreover, Panel D and E show that high-amenity locations have relatively high population density and very low real wages. DR Congo and Zimbabwe are two examples. Their higher amenities are utility compensations that explain why individuals are not living somewhere else in SSA. Intuitively, this captures local cultural or institutional characteristics that work as pull factors (which will be kept constant in

Figure B.4: Equivalence between the quantified (trade and migration) frictions and related estimates from the literature.

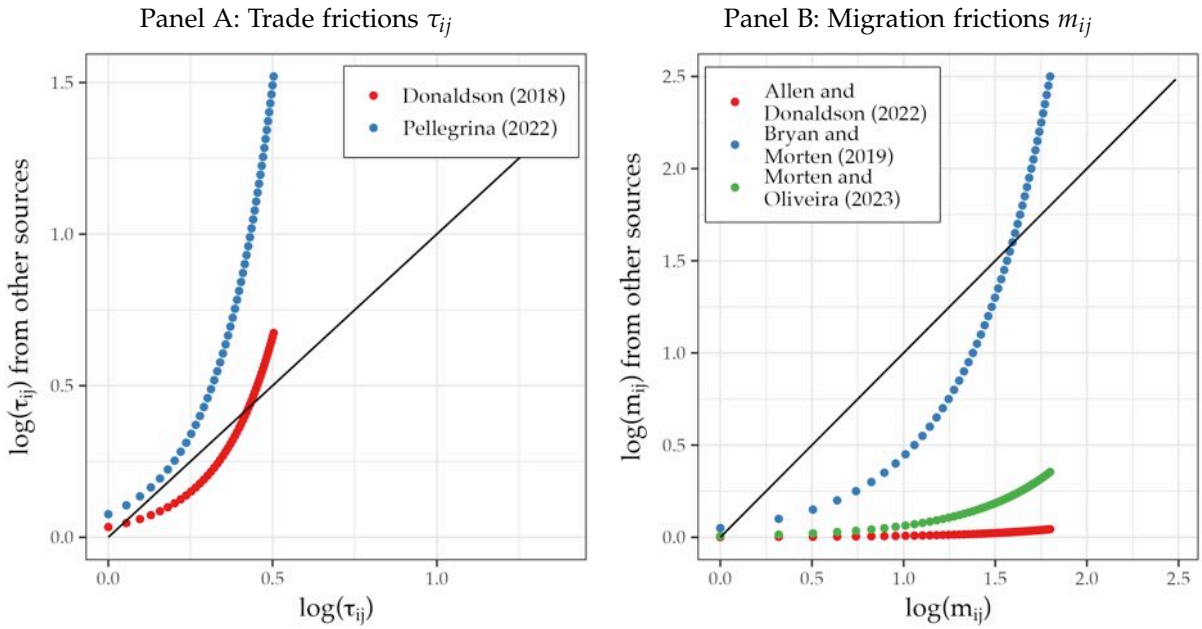

Notes: Scatter plots of the estimated trade (Panel A) and migration (Panel B) costs from Section 5 against estimates from the literature.

the counterfactuals).

However, these characteristics do not include migration frictions, since they are accounted for separately in my framework. To illustrate, Panel F plots the distribution of the quantified country-level migration barriers, i.e. $\{m_c\}_c$. High-barrier countries display two characteristics: higher income differentials relative to neighboring countries and relatively low inflows of migrants. Sudan and South Africa (which are geographically close to DR Congo and Zimbabwe, respectively) illustrate this. Their relative income differences (with respect to their surrounding countries) are disproportionally larger than the observed total flow of immigrants, which implies higher migration barriers.[64]

B.11 Details on the backcasting exercise for 1975

The backcasting exercise consists of solving for the spatial equilibrium of the SSA in 1975. In particular, it uses the calibrated model for 2000 and replaces two fundamentals that reflect the reality of the economy in 1975:

[64] A second mechanism explaining the variation in country barriers is the absolute variation in migration flows. Countries with low migration flows, even if at the left of the real wage distribution, must have, at least to some extent, relatively high migration barriers. The reason for this is the idiosyncratic component of workers' preferences, which generates some migration that must somehow be rationalized.

Figure B.5: Comparison between the calibrated fundamentals and the observed endogenous variables

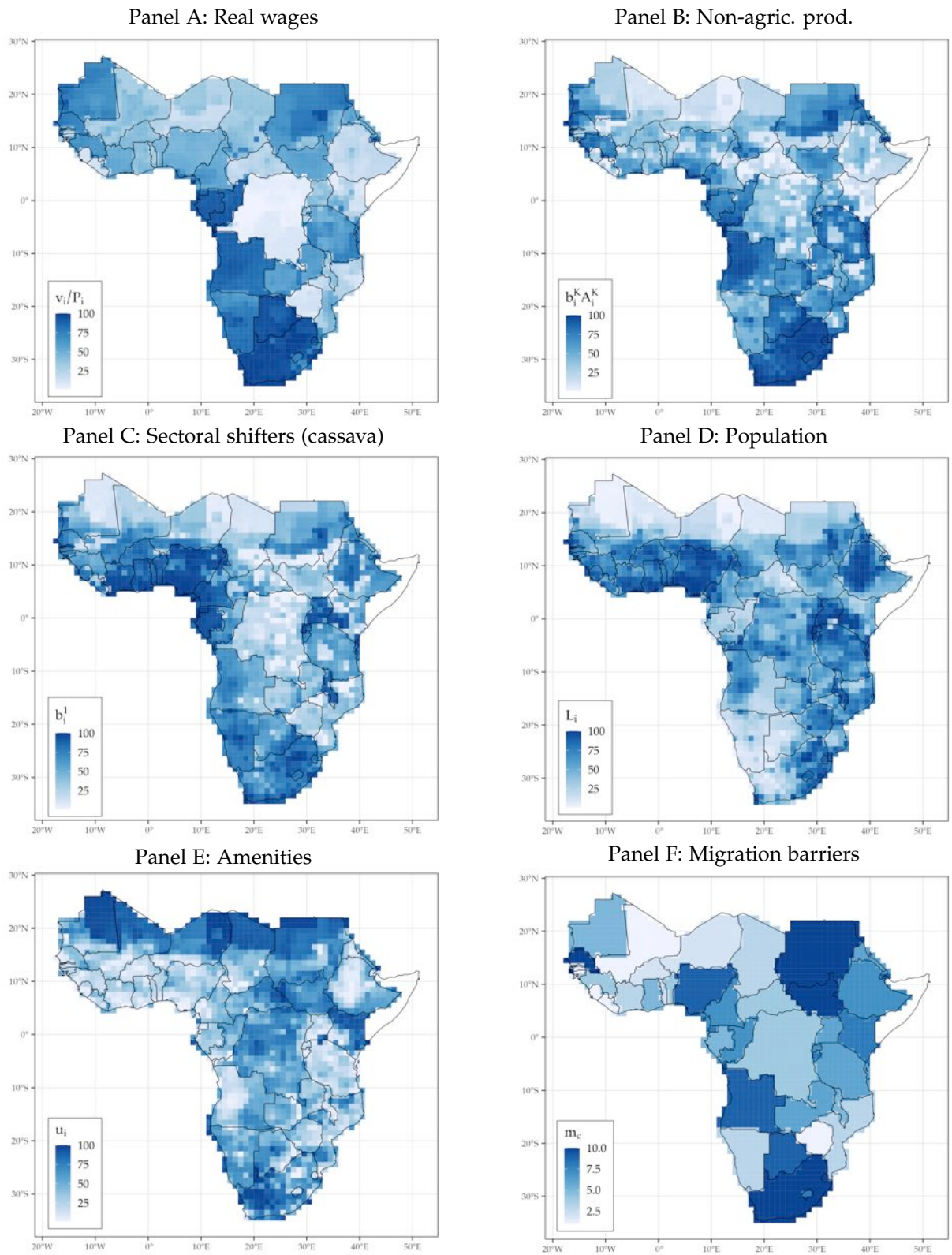

Notes: Each panel plots the spatial distribution of the quantified fundamentals as explained in sections 5.3 and 5.4 in percentiles (or deciles for F), where 100 (or 10) stands top percentile.

Figure B.6: Percentual changes in average crop potential yields within locations in the past and estimates for the future

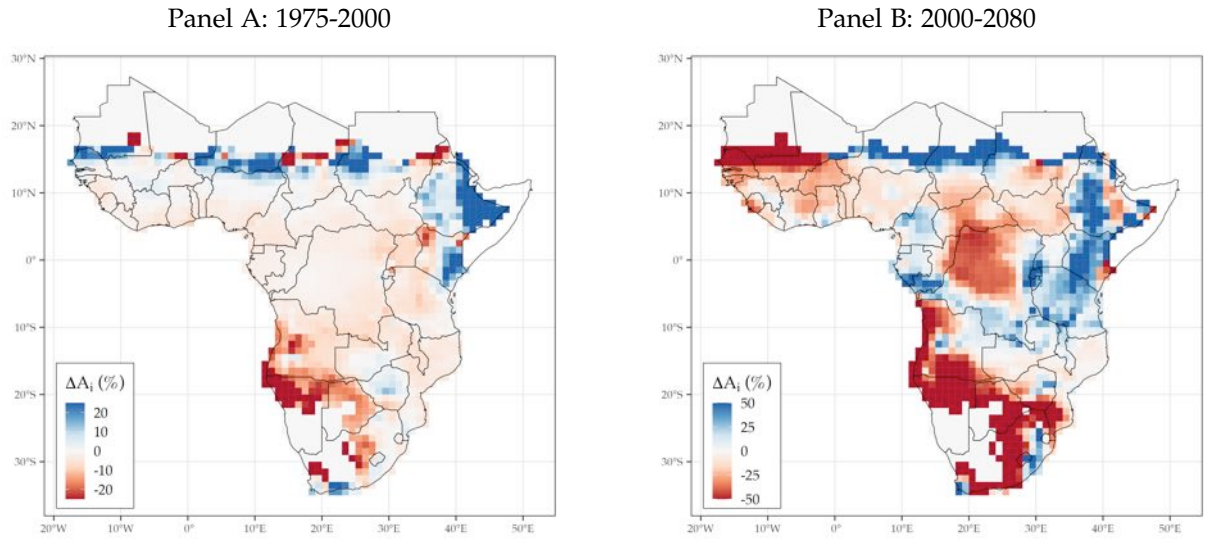

Notes: Panel A: Within grid cell changes (%) in crop suitabilities between 1975 and 2000. Panel B: Analogous changes between 2000 and 2080 (under climate change). Note that the scale between Panels A and B are different to facilitate visualization (they imply that the effects between 1975 and 2000 are much less pronounced than the expected future effects).

Population. I calculate and estimate of the initial population in 1975 by projecting the distribution of the observed population in 2000 into the levels of the SSA population in 1975. The reversibility of the spatial equilibrium follows Desmet et al. (2018), who characterize the possibility of backcasting exercises such as mine (i.e. validating spatial models calibrated in a cross section).

Crop yields. I replace the fundamental productivities $\{A_j^k\}_{k \neq K}$ used in the calibration with the values of 1975. Importantly, during the period there was already climate-driven changes in these productivities so that the model can generate climate migration (Figure B.6 illustrates that). Finally, the validating exercises consists of comparing the model outcomes with observed population data for 1975. Because the data source of the latter (GHSP, Florczyk et al., 2019) differs from the source of population data used in the calibration (G-Econ, Nordhaus et al., 2006), I check the consistency of these two datasets for the period of 2000 (for which data in both sources is available) in terms of grid cell- and country-level population correlation in Figure B.7.

B.12 Details on the calibration with EU data

I take the model to EU data so to retrieve the levels of the tariffs and country barriers paramters τ_{ij}^F and $\{m_c\}_c$. To do that, I build a likewise rich spatial dataset for the EU. I use the same sources described in Section 2, as all of them have a global coverage. Subsequently, I link that data to my model with the procedure described in Section 5.

Figure B.7: Correlations between G–Econ and GHSP datasets for the year of 2000

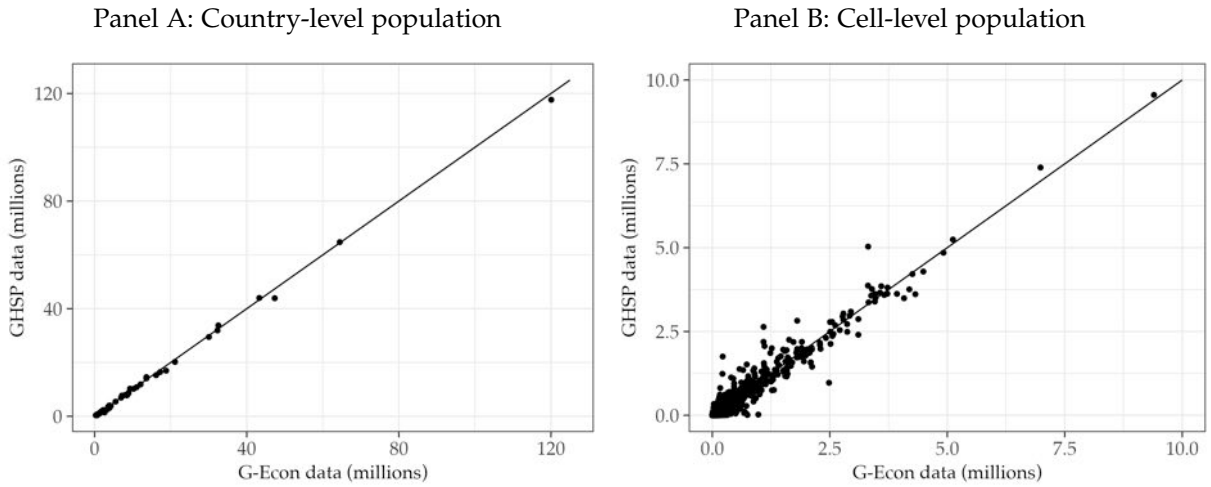

Notes: Panel A (B): Country (grid cell)-level population counts in SSA from G-Econ and GHSP.

Importantly, when doing so, I use the same preference parameters and elasticities to bilateral distance, δ and ϕ. Thus, my quantification for the EU embeds the differences between cross country trade (or migration) in EU and SSA in the policy parameters τ_{ij}^{F} (or $\{m_c\}_c$).

Finally, when replacing the EU policy parameters into the SSA counterfactual, I must match the country level EU parameters $\{m_c\}_c$ to SSA countries. I do that by quantiles. That is, I assign the country barrier value for the bottom decile of the EU sample to the countries in the bottom decile of the SSA county barrier distribution, as so forth for the other deciles. Importantly, to make the levels of $\{m_c\}_c$ comparable across EU and SSA, I normalize the former as a ratio with the minimum. Thus, I in practice simply scale SSA's country barriers in relatives (e.g. the ratio between the least and most strict country) so to reflect the relative ratios of the EU barriers.

C Alternative models

C.1 Extension with the rest of the World

I allow for trade and migration between SSA and the ROW by modeling the latter as a single, representative location R. As such, I use the same data sources and methods in Sections 2 and 5 to link this extended model to global data and perform counterfactuals as in Section 6, but assuming that the ROW is unaffected by the climate.[65,66]

[65] In terms of data, the process is simple. For instance, land endowments (or population) for R are simply the sum of the land area (or population from G-Econ) in all locations but the SSA grid cells.

[66] The reasoning behind this assumption is that, over the course of the decades until the end of the century, the ROW could be able to adapt to the agricultural productivity shocks from GAEZ such that, on average, its productivity would be unaffected.

Table C.1: Aggregate and disaggregate results of the climate change counterfactuals accounting for trade and migration with the rest of the world (ROW)

	(1) Baseline	(2) Baseline + ROW	(3) ROW + no barriers m_R	(4) ROW + no tariffs τ^R	(5) ROW + no tariffs/barriers
Panel A - Aggregate CΔ effects:					
Climate migration[1]	22.32	123.48	111.08	87.80	89.30
(of which to the ROW)[1]		5.35	99.59	58.45	73.23
Δ GDP pc (%)	-1.76	-19.05	-4.76	-1.37	-0.78
ΔL_i^K (non–agric. employment, %)	-0.82	-0.09	-0.14	2.46	2.53
Panel B - Country–level CΔ effects:					
Median Δ population[1]	0.06	0.31	0.22	-1.13	-0.1
Bottom/top deciles	[-2.8; 2.76]	[-15.04; 12.98]	[-6.95; 3.12]	[-8.35; 2.42]	[-6.31; 2.29]
Median Δ GDP pc (%)	-2.15	-18.49	-1.91	-3.75	-1.19
Bottom/top deciles	[-14.62; 3.27]	[-29.7; -8.73]	[-3.91; 1.3]	[-17.5; 6.74]	[-3.64; 2.66]
Median ΔL_i^K (%)	-1.42	-0.01	0.45	-0.01	0.38
Bottom/top deciles	[-5.36; 1.55]	[-0.19; 0.03]	[-8.02; 10.31]	[-0.6; 0.03]	[-8.55; 11.21]
Panel C - Welfare effects:[2]					
Δ Aggregate Welfare (%)	1.16	-2.71	-3.62	-1.17	-1.21
Median Δ Welfare (%)	-1.27	0.06	-0.81	-0.51	-0.66
5th/95th deciles	[-9.89; 0.95]	[-3.93; 6.2]	[-4.73; 3.76]	[-1.76; 2.49]	[-2.43; 2]

Notes: Column 1 presents the baseline results, while columns 2 to 5 present the results of extensions with the ROW: column 2 is analogous to the baseline but where trade and migration also take place between SSA and the ROW, column 3 eliminates migration barriers into the ROW ($m_r = 1$), column 4 eliminates tariffs for trading between SSA and the ROW ($\tau^R = 1$), and column 5 eliminates both barriers. [1]Climate migration in million individuals.

Assuming so facilitates remarkably the quantification of this extended setting. The reason is that it rules out the necessity of separating shifters $\{b_R^k\}_k$ and fundamental productivities $\{A_R^k\}_k$ for the ROW (as they will be all kept fixed in the counterfactuals). Hence, the quantification normalizes $b_R^k A_R^k = 1$ for all k and pins down $\{b_j^k\}_{j \neq R,k}$ in relative terms to the ROW. In terms of trade frictions, I assume $\text{dist}(i, R)$ as the distance to the nearest port and, for simplicity, $\delta = 0.17$ and $\tau_{iR}^F = \tau^F = 6.5$.[67] For migration costs, I also use the port distances and the quantified ϕ. However, to keep a consistent quantification of country migration barriers $\{m_c\}_c$, I aggregate all gross migration flows from SSA to the ROW to pin down m_R.[68]

[67]I set trade barriers with R as the quantified τ^F in the baseline for tractability in my quantification. In principle, one could allow $\tau^F \neq \tau_{iR}^F$, and quantify them separately in the outerloop of Section 5.3 by matching cross-country trade between SSA countries and between SSA and R, respectively. However, that would add another dimension to the grid search (τ_{iR}^F), increasing remarkably its computational requirement (the current grid search requires more than a week of high performance cluster power).

[68]The quantified $\{m_c\}_c$ with the ROW illustrates the degree of real income spatial disparities between SSA and the global economy. Specifically, the quantified m_R is thousands of times larger than the maximum of $\{m_c\}_{c \neq R}$, reflecting that, through the lens of the model, these barriers must be substantial to explain the observed migration choices conditional on real income differences.

C.2 Homothetic preferences

I simulate the climate change effects in SSA with homothetic preferences by setting $\sigma = 4$ (as in Bernard et al., 2003) and $\epsilon_k = 1 - \sigma$ for all $k \in \{a, K\}$. As such, the income effect on Equation (13) cancels out and only relative sectoral prices matters for sectoral expenditures. That is, Equation (13) becomes isomorphic to (9). I link this model to the data with the same procedure as in Section 5 and, with the quantified model in hand, perform a counterfactual as in the baseline of Section 6.

C.3 Endogenous fertility

I endogenize fertility, with respect to climate change, with a simple damage function that assumes that the projected grid-cell-level initial population for 2080 is affected by the average change in local crop yields. Formally:

$$\hat{L}_j^0 = \left(\iota \times \Delta A_j\right) \times L_j^0,$$

where ΔA_j is the average crop yield change in j (as in Section 3) and ι a shitfer that maps the latter into fertility changes. When doing so, the initial population of SSA $\mathcal{L}$ reduces if compared to the baseline case. In particular, it decreases more in the locations and countries that are most affected by climate change. Thus, in distributional terms, the initial population of SSA starts sligthly better distributed, which leads to lower climate migration flows. However, these level differences are not too strike; hence, the aggregate effects of climate change are not stark vis-à-vis the baseline. The fertility robustness results of Table 5 use $\hat{L}_j^0$ and $\iota = .5$ in the climate change simulations. As of completeness, Table C.2 below document how these results are sensitive to the choice of ι.

Table C.2: Robustness of the endogenous fertility exercise with respect to ι

	(1) Climate migration (million individuals)	(2) Δ GDP per capita (%)	(3) Δ Non-agricultural employment (%)
Endogenous fertility $\iota = 0.1$	21.94	-1.76	-0.82
Endogenous fertility $\iota = 0.25$	21.84	-1.76	-0.82
Endogenous fertility $\iota = 0.5$	21.60	-1.75	-0.82

C.4 Economic growth

I account for economic growth in my simulations by scaling up the non-agricultural productivities $\{b_j^K A_j^K\}_j$ with country-level projections of GDP growth. For that, I first

retrieve the GDP growth rates at the country level between 1980 and 2020 from the World Bank Development Indicators. Next, I calculate the country-level cummulative rate in this 40-years interval and use its square as the 80-years projected rate for each country. Figure C.1 Panel A shows the results. Most countries experience a two- to fourfold increase in productivity (and some up to a tenfold increase).

Importantly, Figure C.1 Panel B shows that the $\{b_j^K A_j^K\}_j$ distribution in the two cases barely changes. This is due to the large spatial level differences in the quantified $\{b_j^K A_j^K\}_j$, some in the order of millions.[69] Hence, even if accounting for tenfold growth in some countries, the $\{b_j^K A_j^K\}_j$ distribution, as well as the climate change simulation results in Section 6.4, remain little affected.

C.5 Climate damage on non-agriculture

I consider climate change productivity effects on non-agriculture by scaling $\{b_j^K A_j^K\}_j$ with a damage function that maps climate conditions to the latter. For that, I borrow the non-agricultural $g^K(T_j)$ damage function from Conte et al. (2021). It is a bell-shaped function, quantified at a global scale, that maps local temperature, in Celsius, into a shifter between zero and one. I collect temperatures by the early 2000s and estimates for the end of the century, also from Conte et al. (2021), to calculate a $\Delta g^K(T_j)$. I use the latter as the non-agriculture damage function that scales $\{b_j^K A_j^K\}_j$. Figure C.1 shows the result: there are large spatial differences in the expected changes in non-agricultural productivities (Panel C) but, for the same reason as in Appendix C.4, that does not affect drastically the relative productivities across space (Panel D) and, likewise, the climate change results.

C.6 Climate damage on amenities

I allow for climate change impacts in life quality through a damage function that affects amenities $\{u_j\}_j$. For that, I borrow the amenity damage function $\Lambda^b(T_j)$ from Cruz and Rossi-Hansberg (2024). It provides a non-linear relationship between temperature changes and amenities, quantified for the global economy. I combined it with the expected temperature changes previously calculated (appendix C.5) to retrieve theses changes, illustrated in Figure C.1 Panel F. Similarly to Appendices C.4 and C.5, that barely affects the distribution of amenities across SSA, and hence the result of the simulations in this setting.

[69] That is so due to the likewise large differences in real income per capita across SSA, that my quantification method (conditional on crop productivities and production) interprets as large differences in fundamental non-agricultural productivities $\{b_j^K A_j^K\}_j$.

Figure C.1: Changes in the fundamentals for robustness checks

Panel A: Country-level GDP growth

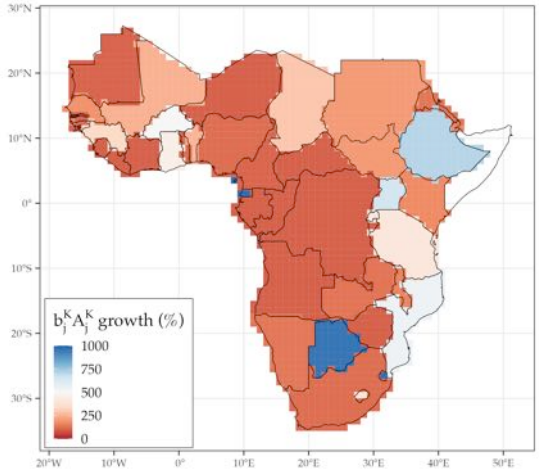

Panel B: $\log(b_j^K A_j^K)$ distribution, in logs

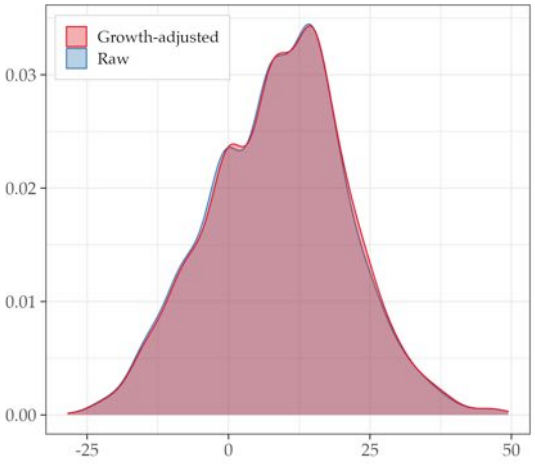

Panel C: Non-agric. damage function $\Delta g^K(T_i)$

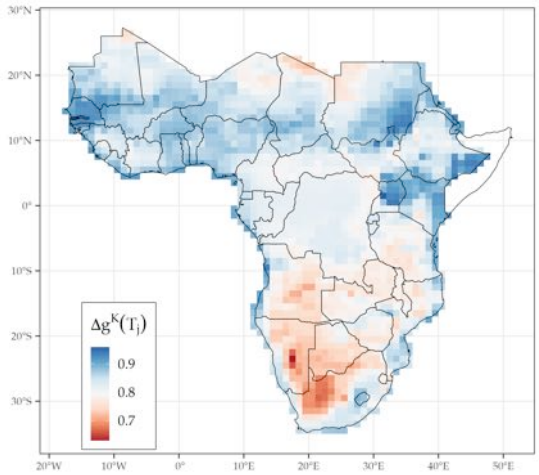

Panel D: $\log(b_j^K A_j^K)$ distribution, in logs

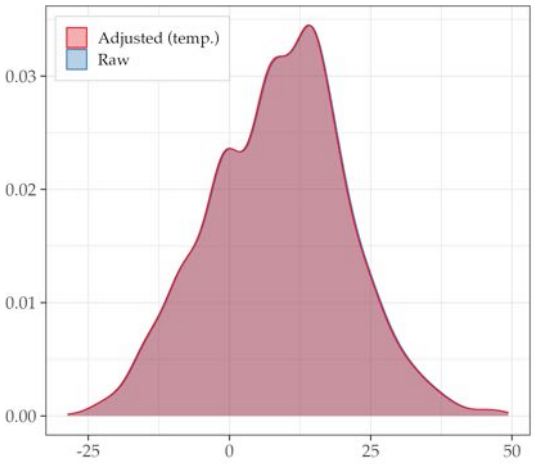

Panel E: Amenity damage function $\Lambda^b(T_i)$

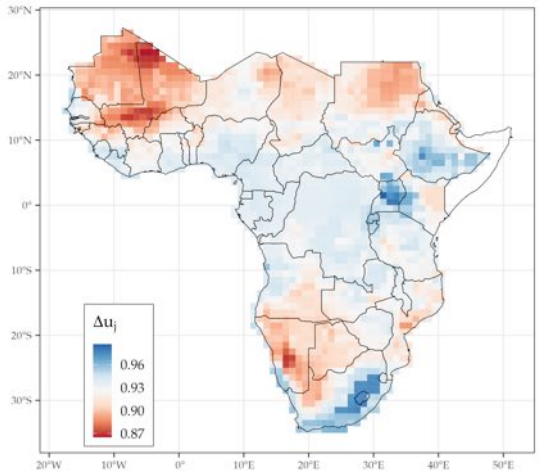

Panel F: $\log(u_j)$ distribution, in logs

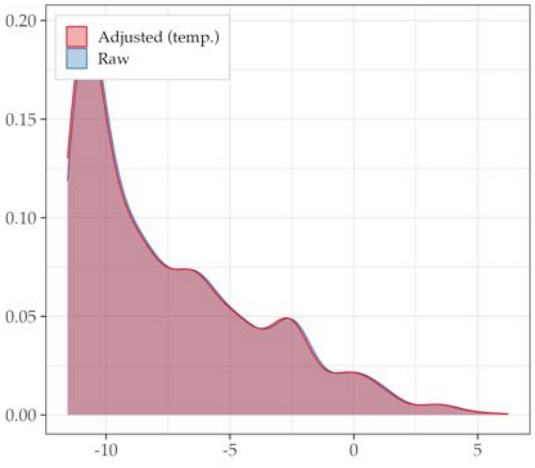

D Additional results

D.1 Motivating facts: additional results and details

The following provides formal support for the Facts 2 and 3 of Section 3 on the correlations between potential crop yields and production, trade, and migration.

Country-level production. I investigate the relationship between country-level crop production and crop yields estimated with:

$$\log(\text{crop production}_i^k) = \alpha \times \log(A_i^k) + a_i + b^k + \varepsilon_i^k, \tag{D.1}$$

where A_i^k is the country i average yields of crop k. Including country a_i and crop b^k fixed effects implies that the variation that identifies α, the parameter of interest, is at the country-crop level. Hence, a positive $\hat{\alpha}$ is evidence of specialization in production across countries, i.e., countries producing the crops that they are, on average, more suitable for, according to the GAEZ potential estimates. Table D.1 Column 1 shows that this is the case, as in Figure 3 Panel A: a 10 percent increase in average country-crop potential yields is associated with a 7 percent larger production of that crop.[70]

Within-country specialization. Table D.1 Column 2 provides additional evidence of specialization in production, but within countries. That is, it shows the regression results of Equation (D.1) on grid cell-level crop production and potential yields. Important, this setting allows for country-crop fixed effects. As a consequence, the variation that identifies α is within-countries: grid cells producing the crops that they are more productive at vis-à-vis other locations within the same country. The results in Column 2 corroborate this hypothesis, with an estimated within country elasticity of production of about 4.5 percent.

Bilateral crop trade. I verify the hypothesis of specialization in trade by estimating:

$$\log(X_{cc'}^k) = \alpha \times \log(A_c^k / A_{c'}^k) + a_{cc'} + b^k + \varepsilon_{cc'}^k, \tag{D.2}$$

where $X_{cc'}^k$ is the bilateral crop k trade flows from country c to c' from the ITPD-E trade data by the early 21st century. Moreover, $A_c^k / A_{c'}^k$ are the exporter-importer relative crop k potential yields calculated from the GAEZ estimates in 2000. By introducing importer-exporter fixed effects, I absorb all fixed characteristics at this dimension – including bilateral trade resistence elements such as bilateral tariffs – and exploit variation at the country pair-crop level. The positive α (Table D.1 Column 3) implies

[70] Importantly, the effective production data is retrieved from national statistics (FAOSTAT). Hence, I exclude an eventual mechanical correlation between production and potential yields that could arrise if building country-level production data by aggregating cell-level data from GAEZ.

Table D.1: Correlational results between potential crop yields (changes) and production, trade, and migration

	log(production$_i^k$)		log(bilateral trade$_{cc'}^k$)			Internal mig$_{ij}$		International mig$_{cc'}$	
	(1)	(2)	(3)	(4)	(5)	(6)	(7)	(8)	(9)
log(potential yields$_i^k$)	0.735**	0.044**							
	(0.339)	(0.019)							
log(relative yields$_{cc'}^k$)			0.433**	0.300*	0.317*				
			(0.183)	(0.154)	(0.166)				
Δ relative yields (%)						1.859	2.562	3.664	6.151
						(6.550)	(6.537)	(47.624)	(83.191)
Bilateral distance					−0.001***		−0.012***		−0.805**
					(0.0001)		(0.004)		(0.336)
Country FE	Yes	No	No	No	No	Yes	Yes	No	No
Crop FE	Yes	No	Yes	Yes	Yes	No	No	No	No
Country-crop FE	No	Yes	No	No	No	No	No	No	No
Origin-destination FE	No	No	Yes	No	No	No	No	No	No
Origin FE	No	No	No	Yes	Yes	No	No	No	No
Destination FE	No	No	No	Yes	Yes	No	No	Yes	Yes
Observations	194	8,136	352	352	352	4,913	4,913	324	324
R^2	0.521	0.876	0.840	0.538	0.589	0.361	0.367	0.074	0.236

Notes: *p<0.1; **p<0.05; ***p<0.01.

that, conditional on a importer-exporter pair, a 10 percent increase in the relative (exporter over importer) average yields of a specific crop is associated with four percent higher exports of that crop. Consistent with Figure 3 Panel A, this elasticity is about 40 percent lower than the one of specialization of production (Column 1).

Subsequently, I use this framework to investigate the role of geographical distance as a bilateral trade resistence. Specifically, I replace the $a_{cc'}$ fixed effects with a set of separate importer and exporter fixed effects in Equation (D.2). The resuls (Table D.1 Column 4) are much less precise, but close to the former estimate in magnitude. I then add to this model (column 5) covariates at the importer-exporter level: bilateral distances (between capitals). The α estimate remains considerably stable, suggesting that non-tariffs trade barriers, such as distances, might not be as strict, as bilateral resistence between countries, if compared to tariffs.

Internal migration flows. I then verify whether changes in crop potential yields, over time, associate with observed internal migration flows. For that, I estimate

$$L_{ij} = \alpha \times \ \Delta\text{relative yields}_{ij} + a_{c(i,j)} + \text{population}_i + \varepsilon_{ij}, \tag{D.3}$$

where L_{ij} is the total number of migrants between subnational region i to j observed in the IPUMS data (that is, from the early 1970s to early 2010s). Along the same lines, $\Delta\text{relative yields}_{ij}$ is the percentual change in the relative (destination over origin) average yields between 1975 and 2000 from GAEZ. Equation (D.3) also controls for

population at origin and country fixed effects.[71]

The results in Table D.1 Column 6 provide evidence of relative potential yields as a push factor of migration (i.e., $\hat{\alpha} > 0$). The point estimate has little power and small magnitude.[72] However, adding origin-destination bilateral distances as a covariate (Column 7) improves that and delivers an economically meaningful message. The $\hat{\alpha}$ estimate increases in magnitude by about 40 percent, suggesting that geographical distances are an important aspect underlying migration choices within countries. Moreover, the precisely estimated negative coefficient of distance aligns with the idea that internal migration becomes more costly for destinations that are further away.

International migration flows. I conclude with an analogous investigation for international migration with:

$$L_{cc'} = \alpha \times \Delta\text{relative yields}_{cc'} + a'_c + \text{population}_c + \varepsilon_{cc'}, \tag{D.4}$$

where $L_{cc'}$ stand for thousands of migrants from country c to country c'. The results (Columns 8 and 9) convey a similar message: international migration in SSA did respond to changes in crop yields in the past decades, and more so for the countries that are geographically close by.

[71] Ultimately, I control for population at origin by using migration flows per thousand inhabitants at origin in the regressions.

[72] This is not surprising given the high urbanization rates experienced in SSA (which does not need to be necessarily driven by changes in relative yields at destination but rather other forces driving structural change).

D.2 Additional figures and tables

Table D.2: Share of grain crop production (in tonnes) over total production of the main staple and cash crops in SSA.

Grain crop	Share	Cash crop	Share
Cassava	56.65%	Coffee	1.13%
Maize	11.75%	Cotton	1.14%
Millet	4.59%	Groundnut	2.72%
Rice	2.18%	Palm oil	4.93%
Sorghum	6.15%	Soybean	0.33%
Wheat	1.13%	Sugarcane	7.31%
Total:	82.45%	*Total:*	17,55%

Source: GAEZ production data for 2000 aggregated in over all countries of my empirical setup. SSA includes all sub-Saharan African countries but Somalia.

Table D.3: Climate migration results for country capitals

Country	Capital	ΔL_i (K)	Country	Capital	ΔL_i (K)
Angola	Luanda	-374.56	Lesotho	Maseru	-4.75
Burundi	Bujumbura	1,388.74	Mali	Bamako	50.94
Benin	Cotonou	10.30	Mozambique	Maputo	-446.89
Burkina Faso	Ouagadougou	26.21	Mauritania	Nouakchott	81.99
Botswana	Gaborone	-660.51	Malawi	Lilongwe	6.14
Central African Republic	Bangui	15.83	Namibia	Windhoek	-160.07
Ivory Coast	Abidjan	26.47	Niger	Niamey	10.96
Cameroon	Yaounde	19.38	Nigeria	Abuja	65.81
Congo (Kinshasa)	Kinshasa	718.65	Rwanda	Kigali	473.70
Congo (Brazzaville)	Pointe-Noire	154.15	Sudan	Khartoum	51.10
Djibouti	Djibouti	11.42	Senegal	Dakar	534.41
Eritrea	Asmara	16.74	Sierra Leone	Freetown	-88.24
Ethiopia	Addis Ababa	45.67	Swaziland	Mbabane	23.18
Gabon	Libreville	298.14	Chad	Ndjamena	-8.33
Ghana	Accra	52.20	Togo	Lome	26.04
Guinea	Conakry	-61.65	Tanzania	Dar es Salaam	44.76
The Gambia	Banjul	31.07	Uganda	Kampala	-3.45
Guinea Bissau	Bissau	6.89	South Africa	Johannesburg	26.67
Equatorial Guinea	Malabo	43.02	Zambia	Lusaka	-32.69
Kenya	Nairobi	-26.75	Zimbabwe	Harare	-29.06
Liberia	Monrovia	111.40			